Massachusetts Institute of Technology
Woods Hole Oceanographic Institution

Joint Program
in Oceanography/
Applied Ocean Science
and Engineering

1930

DOCTORAL DISSERTATION

The Marine Biogeochemistry of Zinc Isotopes

by

Seth G. John

June 2007

MIT/WHOI
2007-08

The Marine Biogeochemistry of Zinc Isotopes

by

Seth G. John

Massachusetts Institute of Technology
Cambridge, Massachusetts 02139

and

Woods Hole Oceanographic Institution
Woods Hole, Massachusetts 02543

June 2007

DOCTORAL DISSERTATION

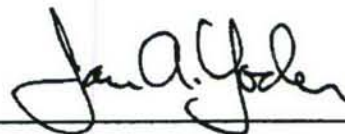Approved for Distribution:

_____

Ken O. Buesseler, Chair
Department of Marine Chemistry and Geochemistry

_____

Paola Malanotte-Rizzoli
MIT Director of Joint Program

_____

James A. Yoder
WHOI Dean of Graduate Studies

THE MARINE BIOGEOCHEMISTRY OF ZINC ISOTOPES

By

Seth Greeley John

B.A., Carleton College, 1999

Submitted in partial fulfillment of the requirements for the degree of

Doctor of Philosophy

at the

MASSACHUSETTS INSTITUTE OF TECHNOLOGY

and the

WOODS HOLE OCEANOGRAPHIC INSTITUTION

June 2007
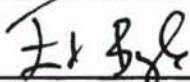
The author hereby grants to MIT and WHOI permission to reproduce paper and electronic copies of this thesis in whole or in part and to distribute them publicly.

_____

Seth G. John
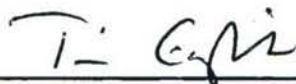Joint Program in Chemical Oceanography
Massachusetts Institute of Technology and Woods Hole Oceanographic Institution

_____

Edward A. Boyle
Professor of Ocean Geochemistry, MIT
Thesis supervisor

_____

Tim Eglinton
Chair, Joint Committee for Chemical Oceanography

The Marine Biogeochemistry of Zinc Isotopes

By

Seth G. John

Submitted to the WHOI/MIT Joint Program in Oceanography in
February, 2007, in partial fulfillment of the requirements for the
degree of Doctor of Philosophy in Chemical Oceanography

Abstract

Zinc (Zn) stable isotopes can record information about important oceanographic processes. This thesis presents data on Zn isotopes in anthropogenic materials, hydrothermal fluids and minerals, cultured marine phytoplankton, natural plankton, and seawater. By measuring Zn isotopes in a diverse array of marine samples, we hope to understand how Zn isotopes are fractionated in the oceans and how Zn isotopes may be used as tracers of marine biogeochemical processes. Common forms of anthropogenic Zn had $\delta^{66}Zn$ from +0.08 ‰ to +0.32 ‰, a range similar to Zn ores and terrigenous materials. Larger variations were discovered in hydrothermal fluids and minerals, with hydrothermal fluids ranging in $\delta^{66}Zn$ from 0.02 ‰ to +0.93 ‰, and chimney minerals ranging from -0.09 ‰ to +1.17 ‰. Lower-temperature vent systems had higher $\delta^{66}Zn$ values, suggesting that precipitation of isotopically light Zn sulfides drives much of the Zn isotope fractionation in hydrothermal systems. In cultured diatoms, a relationship was discovered between Zn transport by either high-affinity or low-affinity uptake pathways, and the magnitude of Zn isotope fractionation. We established isotope effects of $\delta^{66}Zn = -0.2$ ‰ for high-affinity uptake and $\delta^{66}Zn = -0.8$ ‰ for low-affinity uptake. This work is the first to describe the molecular basis for biological fractionation of transition metals. Biological fractionation of Zn isotopes under natural conditions was investigated by measuring Zn isotopes in plankton collected in the Peru Upwelling Region and around the world. Seawater dissolved Zn isotopes also reflect the chemical and biological cycling of Zn. The $\delta^{66}Zn$ of deep seawater in the North Pacific and North Atlantic is about 0.5‰, and the dissolved $\delta^{66}Zn$ gets lighter in the upper water column. This is unexpected based our observations of a biological preference for uptake of light Zn isotopes, and suggests that Zn transport to deep waters may occur by Zn adsorption to sinking particles rather than as primary biological Zn. The thesis, by presenting data on several important aspects of Zn isotope cycling in the oceans, lays the groundwork for further use of Zn isotopes as a marine biogeochemical tracer.

Thesis supervisor: Edward A. Boyle

Title: Professor of Ocean Geochemistry

Mak Saito's excitement about his research and interest in rigorously interpreting his data has been inspiring since I first met him when he was finishing his thesis and I was a prospective Joint Program student. Meeting him then was a major influence in my decision to become a JP student and thus an oceanographer. Mak encouraged me to use culture experiments to understand biological processes and provided valuable advice in developing the experimental methods to do this.

Bernhard Peucker-Ehrenbrink was always able to get to the heart of a matter with a simple question. His guidance was invaluable in developing the methods for isotopic analysis. Even before I showed him anything, his influence was valuable as I tried to anticipate his questions by thinking clearly and comprehensively about my data.

Ariel Anbar gave a seminar that I attended as a beginning isotope geochemist that forever changed my perspective on how isotopes could be used. My interest in the biological fractionation of metal isotopes dates back to his talk.

Ed Boyle, my most important mentor as a graduate student, has been a wonderful advisor. Ed gave me freedom to choose for myself what I wanted to explore, and guidance to help me make progress. When I first met Ed to decide on a thesis project, he pulled out a copy of the periodic table and a table of element profiles in the ocean. This focus on the data taught me to be a good scientist. Ed taught me that if you pick your samples carefully, and make accurate measurements, the world will speak to you.

Thanks to my parents for raising me right. Thanks to my wife Andrea for making my years as a graduate student a wonderful time.

Table of contents

List of Figures

Chapter 4

Zinc isotope fractionation associated with two separate

uptake pathways in a marine diatom

Chapter 5

Zinc isotopes in seawater and natural marine plankton

Chapter 6

Conclusions

Chapter 1

Introduction

Zinc (Zn) atoms, regardless of isotope, have thirty protons in the nucleus and therefore have a similar configuration of electrons orbiting the nucleus. The chemistry of Zn is determined mostly by the interactions of these protons and electrons with each other and with charged particles of other atoms. The difference between Zn isotopes lies in the number of neutrons in the nucleus. Slight differences in nuclear mass will have a small effect on the strength of the bonds that the atoms forms. Slight differences in the bonding strength of difference isotopes can lead to a preferential accumulation of heavy or light Zn isotopes in certain bonding environments. Zn isotope ratios therefore contain information about the chemical processes that have acted upon Zn atoms. The growth of phytoplankton in the oceans, chemical adsorption to sinking particles, the circulation of

seawater through hydrothermal vents, and other oceanographic processes involve changes in the chemical bonding of Zn. Zn isotopes therefore contain information about the chemical history of samples and may be valuable tracers of chemical oceanographic processes.

1.1 Historical overview

1.1.1 The development of MC-ICP-MS

The development of multi-collector inductively-coupled plasma mass spectrometry (MC-ICP-MS) has increased the ease and accuracy of isotope measurement for trace elements. Isotopic analysis by thermal ionization mass spectrometry (TIMS) is, in comparison, more time-consuming, less effective at ionizing transition metals such as Zn, and subject to errors based on the time-dependent fractionation of isotopes during evaporation from a filament. The accuracy of single-collector ICP-MS, in which different isotopes are measured in rapid succession, is limited by plasma instability, rapid variations in ionization efficiency on timescales less than the timescale of measurement. Multi-collector measurements correct for this by simultaneously collecting data on all masses of interest.

The development of MC-ICP-MS has led to an explosion in the study of "non-traditional" stable isotopes. Natural variations have been discovered in the stable isotopes of Cr, Fe, Cu, Zn, Mo, Cd, Hg, and many other elements (Anbar and Rouxel, In revision; Johnson et al., 2004).

1.1.2 Natural Zn isotopes in environmental and marine systems

Figure 1 presents the natural Zn isotope measurements that had been reported at the time I proposed to undertake this thesis. Data on Zn isotopes in the ocean included measurements on manganese nodules and marine sediment trap material (Maréchal et al., 2000). Manganese nodules had generally higher Zn isotope ratios in polar regions than in low latitudes, an effect that was suggested to correlate with biological Zn uptake in the upper ocean (Fig. 2). Sediment trap data showed a remarkable seasonal signal in the Zn isotope composition of sinking particles (Chapter 6). Data showing large variations in the $\delta^{66}Zn$ leached from bulk sedimentary carbonates over the last 175 ka suggested that Zn isotopes might have uses as a paleotracer for surface productivity (Pichat et al., 2003).

Several notable papers on Zn isotopes in marine and environmental systems have been published in the past few years. Zinc isotopes have been measured in ancient hydrothermal deposits (Mason et al., 2005; Wilkinson et al., 2005), air and lichen samples influenced by anthropogenic Zn (Cloquet et al., 2006; Dolgopolova et al., 2006), cultured phytoplankton (Gélabert et al., 2006), and seawater (Bermin et al., 2006).

1.2 Zinc stable isotope analysis

Zinc has five stable isotopes: ^{64}Zn (49.2%), ^{66}Zn (27.8%), ^{67}Zn (4.0%), ^{68}Zn (18.4%), and ^{70}Zn (0.6%) (Tanimizu et al., 2002). MC-ICP-MS can be used to measure the ratio of Zn isotopes in a sample. We measure ^{64}Zn, ^{66}Zn, and ^{68}Zn, the three most dominant Zn isotopes. All isotopic measurements were made on an IsoProbe MC-ICP-MS. Typical
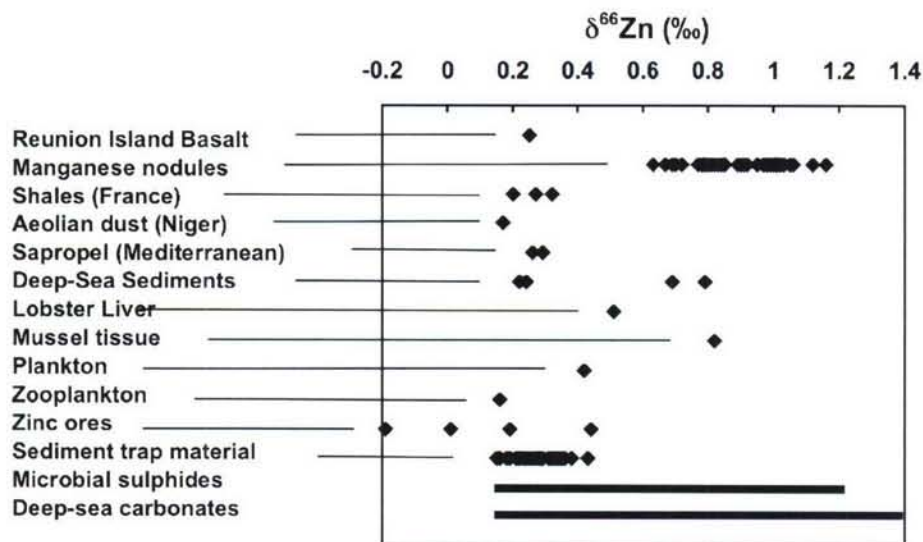
Figure 1.1. Published measurements of Zn isotopes in natural samples when this thesis began. Data is from (Maréchal et al., 2000), except for data on microbial sulfides (Archer and Vance, 2002), and deep-sea carbonates (Pichat et al., 2003).
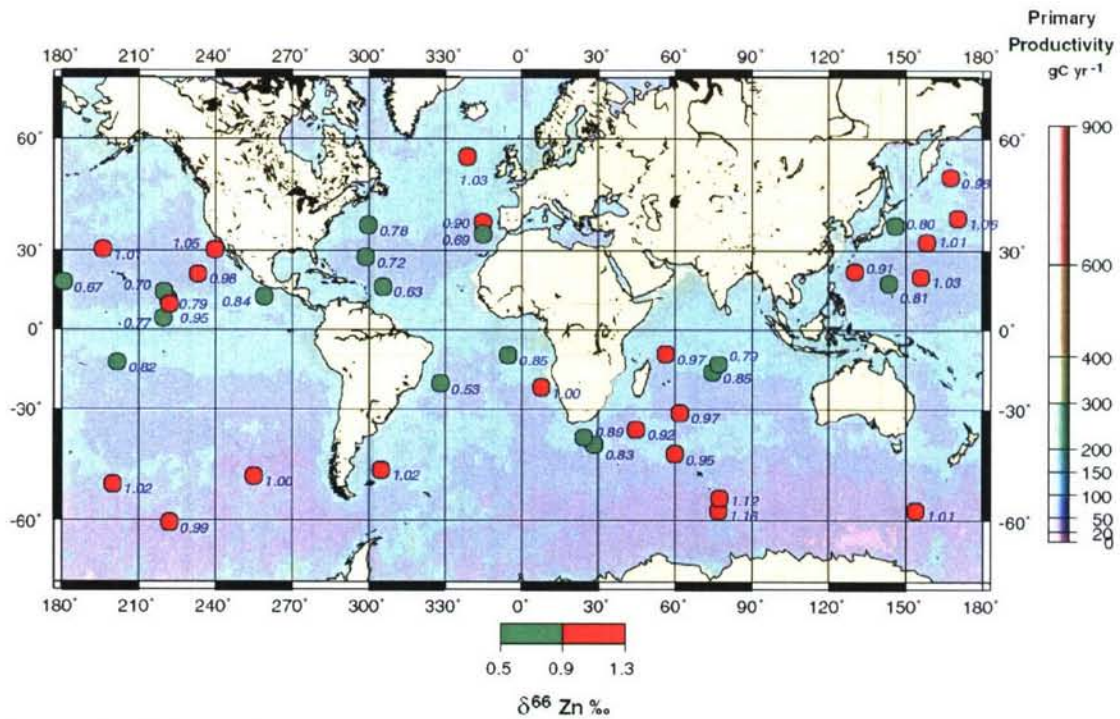
Figure 1.2. The Zn isotope composition of manganese nodules from around the world. From Maréchal et. al. (2000).

analytical conditions are shown in Table 1.

1.2.1 Conventions for reporting Zn isotope ratios

Zinc isotope data is typically reported in terms of the $^{64}Zn/^{66}Zn$ ratio of the sample in relation to the "Lyon – JMC standard" from the lab of Francis Albarède (Maréchal et al., 1999) according to the equation:

$$\delta^{66}Zn = \left(\frac{(^{66}Zn/^{64}Zn)_{sample}}{(^{66}Zn/^{64}Zn)_{JMC\ standard}} - 1 \right) \bullet 1000$$

Similarly, the ratio of $^{68}Zn/^{64}Zn$ is reported as:

$$\delta^{68}Zn = \left(\frac{(^{68}Zn/^{64}Zn)_{sample}}{(^{68}Zn/^{64}Zn)_{JMC\ standard}} - 1 \right) \bullet 1000$$

In this thesis, isotope effects (or any offset between the $\delta^{66}Zn$ of two samples) are reported as:

$$\Delta^{66}Zn = \delta^{66}Zn_A - \delta^{66}Zn_B$$

where A and B are the two samples. This terminology is potentially confusing because Δ terminology is also used to describe non-mass dependant mass fractionation of O, S, and Hg isotopes. ε notation, often used to describe biological isotope effects in measurements

19

Typical IsoProbe operating conditions:

Sample cone: Aluminum
Skimmer cone: Ni "X-cone"

Nebulizer: MicroMist glass nebulizer
Aspiration rate: 75 μL/min, free draw

Desolvator: APEX Q
Desolvating membrane: none

Cool gas flow:	13-14	L/min
Intermediate gas flow:	0.9-1.0	L/min
Neb gas 1:	0.2-0.3	L/min
Neb gas 2:	0.7-0.9	L/min

Sample matrix: 2% (vol.) HNO_3

Sample uptake time before measurement:	3 min
Data acquisition time:	3 min
Rinsing time between measurements:	6 min

Collector	Mass	Predominant isotopes
L1	60	^{60}Ni
Ax	63	^{63}Cu
H1	64	^{64}Zn, ^{64}Ni
H3	65	^{65}Cu
H4	66	^{66}Zn
H5	67	^{67}Zn
H7	68	^{68}Zn

Table 1.1. Typical analytical conditions for Zn isotope analysis on the IsoProbe.

of $\delta^{13}C$, is inappropriate because ε is also used in reporting Nd isotope measurements to signify that result is in parts-per-ten thousand. '$\Delta\delta$' notation, where:

$$\Delta\delta^{66}Zn = \delta^{66}Zn_A - \delta^{66}Zn_B$$

was first used for C isotopes, and is attractive because it's meaning is intuitively clear (Shackleton and Pisias, 1984). Unfortuantely, this terminology is not currently used within the trace-metal community and changing common notation is difficult. Issues of terminology will undoubdetly become more complicated if mass independent isotope effects are discovered in more trace metals such as Fe.

1.2.3 Mass-dependant fractionation

For mass-dependent fractionation processes, the magnitude of $\delta^{68}Zn$ should be approximately twice the magnitude of $\delta^{66}Zn$ (see Chapter 5 for further discussion). The exact relationship between these two quantities depends on the law that is used to describe isotope fractionation. The commonly used "exponential law" takes the form:

$$R_f = R_i \bullet \left(\frac{m_1}{m_2}\right)^\beta$$

where the ratio of two isotopes after fractionation (R_f) is related to the initial ratio of the two isotopes (R_i) as a function of the isotopic masses (m_1 and m_2) and a fractionation factor (β). According to the exponential fractionation law, the ratio of $\delta^{68}Zn$ to $\delta^{66}Zn$ will be 1.985.

1.2.4 Correcting for instrumental mass bias

1.2.4.1 Using Cu or a Zn double-spike to correct for mass bias

During the analysis of Zn isotopes by MC-ICP-MS, large isotopic fractionations are induced in the spectrometer between sample induction and isotope signal measurement. Several different schemes are available to correct for this mass bias. The simplest involves sample-standard bracketing. Assuming that the magnitude of instrumental mass bias is constant between samples and standards, the measured difference in the isotope ratios will be equal to the actual difference in the isotope ratios.

In practice, small differences in the matrix between samples and standards often leads to changes in instrumental mass bias. Instrumental mass bias must be continuously monitored in order to correct for this effect. For Zn, both Cu normalization and a double-spike method can be used. Cu has only two stable isotopes, ^{63}Cu (69.2%) and ^{65}Cu (30.8%). By spiking both samples and standards with Cu, changes in instrumental mass bias can be monitored by looking at changes in the measured $^{65}Cu/^{63}Cu$ ratio. The exponential mass bias fractionation factor (β) calculated for Cu cannot, however, be directly applied to correct for Zn fractionation (Fig. 3). Instead an empirical relationship between the values of β must be established (Maréchal et al., 1999).

A double-spike can also be used to correct for instrumental mass bias. To do this, all samples are spiked with a known mixture of non-natural Zn isotopes, typically ^{64}Zn and ^{67}Zn. By simultaneously collecting data on the abundances of ^{64}Zn, ^{66}Zn, ^{67}Zn, and ^{68}Zn it is possible to calculate both the concentration ratio of spike to sample and the

22

mass bias of the instrument. It is then possible to calculate the isotope composition of the original sample.

1.2.4.2 The comparative advantages of Cu and Zn double-spike correction

Correction with a Cu spike and a Zn double-spike each have their own advantages and disadvantages. A drawback of the Cu correction scheme is that Cu and Zn behave differently during ICP-MS analysis. This is apparent from the fact that values of β are different for these two elements. While the Cu-correction scheme outlined above has been rigorously tested and demonstrated to work well for standards under many conditions (Archer and Vance, 2004; Maréchal et al., 1999), it cannot be proved that this correction scheme always works for real samples.

Another difference is that the Cu correction scheme requires complete recovery of Zn from the sample. Conversely, a Zn double-spike can be added to the sample before processing to account for fractionation of the isotopes during sample processing. This simplifies sample processing, especially in cases such as the analysis of Zn isotopes in seawater where achieving complete recovery of Zn can be difficult.

Finally, the correction schemes differ in that only Cu-correction allows a check for the presence of isobaric interferences by simultaneously measuring δ^{68}Zn and δ^{66}Zn. Isobaric interferences will interfere differently with the measured values of δ^{66}Zn and δ^{68}Zn, causing them to fall off the expected linear relationship governed by mass-dependant fractionation. In double-spike analysis, δ^{66}Zn and δ^{68}Zn cannot be measured simultaneously, so isobaric interferences cannot be distinguished from changes in sample
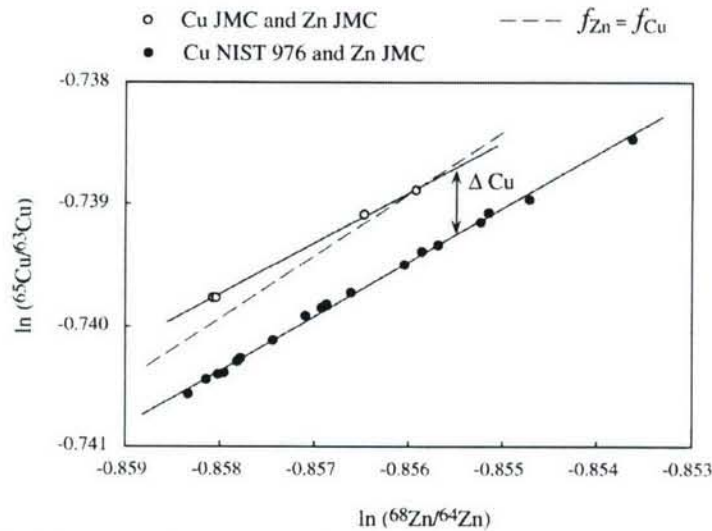
Figure 1.3. During the course of a day, the measured isotope ratios change as instrumental mass bias (β, or f in this figure)changes. However, the extent of fractionation of these two elements is not the same for the two elements as predicted by the exponential fractionation law. In the case shown here, for example, the exponential mass bias factor for Zn varies by more than the exponential mass bias factor for Cu ($f_{Zn} > f_{Cu}$). An empirically determined relationship between f_{Zn} and f_{Cu} allows one to make a proper correction for varying instrumental mass bias. (Maréchal et al., 1999).

fractionation or instrumental mass bias. Polyatomic isobaric interferences may occur when sample matrix is not completely eliminated. Polyatomic interferences are of special concern on the IsoProbe where an Al sampling cone (rather than Ni) is required for proper heat dissipation. An $^{27}Al^{40}Ar^{+}$ interference on mass 67 is present with typical signals of several mV.

During data collection for this thesis, a Cu-correction scheme was most often used. A double-spike was used to measure Zn isotopes in six hydrothermal samples (Chapter 3) and several standards. Both correction schemes produced the same results, though the internal error for the Zn double-spike analysis was larger. The origin of this

error is not known, but may result from variations in the magnitude of $^{27}Al^{40}Ar$ interferences.

It might be possible to achieve the advantages of the double-spike method, without introducing susceptibility to isobaric interferences, by making measurements in medium or high-resolution mode where interferences can be separated from Zn by mass. This requires a significantly larger samples size in order to produce the same signal intensity.

1.3 Thesis chapters

Chapter 2 presents data on the Zn isotope ratios found in many anthropogenic materials. Laboratory standards were found to be very fractionated (up to several permil) from typical continental material. The more common types of anthropogenic Zn, such as pennies and health products, were found to have similar values of $\delta^{66}Zn$ to continental materials. I discuss how this data can be used to estimate the $\delta^{66}Zn$ of many anthropogenic Zn sources into the environment and oceans.

Chapter 3 discusses Zn isotope data for hydrothermal vent fluids and chimneys. Fluids $\delta^{66}Zn$ values were measured on samples from several different hydrothermal fields in both the Pacific and Atlantic. A relationship was discovered between the temperature of hydrothermal fluids and their Zn isotope composition. Cooler fluids (<250°C) had $\delta^{66}Zn$ values that were significantly heavier than basalt or high-temperature fluids leading us to hypothesize that the subsurface precipitation of light Zn sulfides was associated

with fluid cooling. Measurements from fluids and chimney sulfides taken from the same vent allow us to measure the isotope effect for hydrothermal precipitation *in situ*.

In Chapter 4 we present the results from diatom cultures grown at a range of Zn concentrations and analyzed for Zn isotopes. By carefully distinguishing between extracellular Zn and intracellular Zn, we have been able to measure the isotope effects associated with separate high-affinity ($\Delta^{66}Zn = -0.2‰$) and low-affinity ($\Delta^{66}Zn = -0.8‰$) transport pathways. These are the first experiments to explain transition metal isotope fractionation in terms of the molecular biology of uptake mechanisms. This data provides a means of relating the $\delta^{66}Zn$ of seawater to the biological cycling of Zn in the oceans.

Chapter 5 details efforts to measure Zn isotopes in natural seawater and phytoplankton samples. I have developed new methods for the analysis of Zn concentration in seawater, and a new method for the $Mg(OH)_2$ co-precipitation of Zn from seawater for isotopic analysis. Analytical problems with seawater isotope analysis are discussed. $\delta^{66}Zn$ values for marine plankton tows range from about 0.0‰ to +0.6‰. Analysis of five separate samples of seawater from the deep Pacific yielded an average $\delta^{66}Zn$ of $+0.50 \pm 0.08‰$. There appears to be a trend towards lighter Zn values of $\delta^{66}Zn$ in surface seawater. This suggests the preferential removal of isotopically heavy Zn from the surface ocean. I hypothesize that adsorption of Zn onto sinking particles is a major pathway for the removal of Zn from the surface oceans.

Chapter 6 briefly explores some fundamental questions about Zn cycling in the ocean, and the factors that control Zn isotope distribution in the oceans.

References for Chapter 1:

Anbar, A.D. and Rouxel, O.J., In revision. Metal Isotopes in Paleoceanography. Annual Review of Earth and Planetary Sciences.

Archer, C. and Vance, D., 2002. Large fractionations in Fe, Cu and Zn isotopes associated with Archean microbially-mediated sulphides. Geochimica et Cosmochimica Acta, 66(15A): A26-A26.

Archer, C. and Vance, D., 2004. Mass discrimination correction in multiple-collector plasma source mass spectrometry: an example using Cu and Zn isotopes. Journal of Analytical Atomic Spectrometry, 19: 656-665.

Bermin, J., Vance, D., Archer, C. and Statham, P.J., 2006. The determination of the isotopic composition of Cu and Zn in seawater. Chemical Geology, 226(3-4): 280-297.

Cloquet, C., Carignan, J. and Libourel, G., 2006. Isotopic composition of Zn and Pb atmospheric depositions in an urban/periurban area of northeastern France. Environmental Science & Technology, 40(21): 6594-6600.

Dolgopolova, A. et al., 2006. Use of isotope ratios to assess sources of Pb and Zn dispersed in the environment during mining and ore processing within the Orlovka-Spokoinoe mining site (Russia). Applied Geochemistry, 21: 563-579.

Gélabert, A. et al., 2006. Interaction between zinc and freshwater and marine diatom species: Surface complexation and Zn isotope fractionation. Geochimica et Cosmochimica Acta, 70(4): 839-857.

Johnson, C., Beard, B. and Albarède, F. (Editors), 2004. Geochemistry of non-traditional stable isotopes. Reviews in Mineralogy and Geochemistry, 55.

Maréchal, C.N., Nicolas, E., Douchet, C. and Albarède, F., 2000. Abundance of zinc isotopes as a marine biogeochemical tracer. Geochemistry Geophysics and Geosystems, 1: 1999GC000029.

Maréchal, C.N., Telouk, P. and Albarède, F., 1999. Precise analysis of copper and zinc isotopic compositions by plasma-source mass spectrometry. Chemical Geology, 156(1-4): 251-273.

Mason, T.F.D. et al., 2005. Zn and Cu isotopic variability in the Alexandrinka volcanic-hosted massive sulphide (VHMS) ore deposit, Urals, Russia. Chemical Geology, 221(3-4): 170-187.

Pichat, S., Douchet, C. and Albarède, F., 2003. Zinc isotope variations in deep-sea carbonates from the eastern equatorial Pacific over the last 175 ka. Earth and Planetary Science Letters, 210(1-2): 167-178.

Shackleton, N.J. and Pisias, N.G., 1984. Atmospheric carbon dioxide, orbital forcing, and climate. In: E.T. Sundquist and W.S. Broeker (Editors), The Carbon Cycle and Atmospheric CO2: Natural Variations Archean to Present. Am. Geophys. Union Mon., pp. 313-318.

Tanimizu, M., Asada, Y. and Hirata, T., 2002. Absolute isotopic composition and atomic weight of commercial zinc using inductively coupled plasma mass spectrometry. Analytical Chemistry, 74(22): 5814-5819.

Wilkinson, J.J., Weiss, D.J., Mason, T.F.D. and Coles, B.J., 2005. Zinc isotope variation in hydrothermal systems: Preliminary evidence from the Irish Midlands ore field. Economic Geology, 100(3): 583-590.

Chapter 2

The isotopic composition of some common forms of anthropogenic zinc

Anthropogenic sources account for much of the zinc (Zn) in the environment. Constraining the isotopic composition of anthropogenic Zn is therefore essential to understanding the environmental biogeochemical cycling of Zn isotopes. This study examines the isotopic variability in several different kinds of anthropogenic Zn. Laboratory standards are highly purified and can be significantly fractionated from natural Zn. Industrial Zn dust and U.S. pennies, which are made from the most common grade of Zn metal (Special High Grade), were studied to represent common Zn metal. Vitamins were studied because they are more highly purified than typical Zn metals and are made from chemical compounds such as Zn oxide or Zn gluconate. The isotopic composition of laboratory standards ranged in δ^{66}Zn from -9.15‰ to +0.17‰ compared to Lyon-JMC Zn. Zn dust and pennies ranged from +0.09‰ to +0.31‰, and vitamins ranged from +0.09‰ to +0.27‰. External

reproducibity was 0.052‰ (2σ s.d.) based on several standards, and was similar to internal error. The isotopic range for non-laboratory standards is much smaller than the total range seen in Zn ore deposits, but has a similar average Zn isotope ratio. This data presents a first look at the range of $\delta^{66}Zn$ values that is typical of common anthropogenic Zn products.

2.1 Introduction

Zinc (Zn) is commonly used in many man-made items and over 3 million metric tons are estimated to be released into the environment every year (Graedel et al., 2005). It is used in the manufacture of galvanized steel, in alloys with other metals in many objects, in the manufacture of rubber to neutralize acidity, and in agriculture as a crop nutrient (Gordon et al., 2003). Zn is also used in many health products and is a common component in vitamins, sunscreen, cold medicine, and skin creams. The purification of Zn from ores as described by (Gordon et al., 2003) is a multi-step process. The first step is a high temperature roast to convert Zn sulfides into oxides. The resulting calcine is then dissolved in sulfuric acid and impurities may be removed by precipitation. The final purification step is electrowinning, in which high-purity Zn is electroplated from solution onto aluminum cathodes. Zn may then be manually removed from the cathodes and melted for processing into ingots, shot, dust, and other forms. A less common method of Zn refining uses high-temperature distillation of metallic Zn in place of electrowinning. Zn oxide is typically made by evaporation and oxidation of Zn and Zn oxide is a precursor to many other Zn compounds (FDA, 2002).

Anthropogenic sources are a major contributor to the Zn found in natural environments. Approximately half of total Zn emissions to the atmosphere are thought to have anthropogenic sources (Pacyna and Pacyna, 2001) and as much as half of the global fluvial flux of Zn to the oceans may be

anthropogenic (Shiller and Boyle, 1985). The influence of anthropogenic Zn is seen even in remote locations far from the major sources of Zn pollution. For example, one third of the Zn dry deposition to the ocean near Bermuda is thought to be anthropogenic (Arimoto et al., 2003), and anthropogenic Zn has been measured in ice from both Greenland (Candelone et al., 1995) and Antarctica (Planchon et al., 2002). In order to model the global cycling of Zn isotopes, we need to characterize the isotopic composition of anthropogenic Zn.

Previous studies have found large variations in the Zn isotope composition of anthropogenic Zn standards (Mason et al., 2004; Tanimizu et al., 2002). The standards measured by Tanimizu et al. ranged from $\delta^{66}Zn_{JMC} = -2.41‰$ to $+0.13‰$. This suggests that isotopic fractionation may be common during the purification of laboratory standards. Tanimizu et al. found that the sample with the greatest deviation from continental material was NIST-SRM 682, which was also the purest Zn standard tested. They suggest that this large fractionation resulted from the distillation, zone refining, and gasification employed in the final purification of this sample. Metal reduction during electroplating may also have a significant kinetic isotope effect (Kavner et al., 2005), suggesting that electrolytically-purified Zn could also have a unique anthropogenic signature.

Non-electrolytic processes may also fractionate Zn isotopes. Analysis of Zn isotopes samples from a Pb-Zn refinery and a steel mill show variations in $\delta^{66}Zn$ from -0.63‰ to +0.58‰. In the Pb-Zn refinery, there was a trend towards lighter isotope values near the end of the refining process, with the lightest value found in the chimneystack (Mattielli et al., 2005). Zn isotopes from lichens collected near an ore-processing and mining site are heavier than minerals collected from the mining site or the typical mineralogical spread of Zn isotope values (Dolgopolova et al., 2006). The authors suggest that such isotopic signals may be used to trace anthropogenic or natural Zn in aerosols. Zn isotopes in

31

rainwater in France varied by about 0.3‰, and differences were seen between anthropogenically

influenced and marine-source rain (Luck et al., 1999).

Mineral ores may also be a source of variability in anthropogenic Zn. Samples collected at

ancient hydrothermal sites, the source of modern Zn ores, range from $\delta^{66}Zn = -0.43‰$ to $+1.33‰$

(Mason et al., 2005; Wilkinson et al., 2005). Wilkinson et al. compiled Zn isotope data for all

terrestrial samples measured to date to show that they span the entire range between the heaviest and

lightest hydrothermal sample. Three homogenized ore samples have a smaller isotopic range, between

$\delta^{66}Zn = -0.06‰$ and $+0.33‰$ (Chapman et al., 2006). Zn isotopes are variable on spatial scales of

centimeters and millimeters (Mason et al., 2005), so the lesser variability found in ores may represent

the effects of homogenization.

While the total variability in anthropogenic Zn isotopes including laboratory standards and

aerosols may be several permil, the variability of Zn isotopes in the most common forms of

anthropogenic Zn has not previously been investigated. Several grades of Zn are manufactured and

used in the US including Special High Grade (SHG), High Grade (HG), Prime Western (PW) with

minimum purities of 99.99%, 99.95% and 98.50%, respectively. Together, these three grades account

for 94% of the reported Zn use in the US during 2004 and SHG Zn alone accounted for 63% of Zn use

during this time (Jorgenson, 2004). U.S. pennies, which have been made from Zn with a thin coating of

Cu since 1982, are made with SHG Zn and are therefore representative of the majority of Zn used in

the US (Jasinski, 1994). If there is isotopic fractionation associated with industrial Zn refining and

production processes, we expect this to be most apparent in SHG Zn compared to less purified HG and

PW grade Zn. We have also measured some health and medical products; although they represent only

a small portion of Zn use, they require the most highly purified Zn used in common anthropogenic

products and are made from Zn compounds such as Zn oxide and Zn gluconate rather than Zn metal (FDA, 2002).

2.2 Materials and methods

2.2.1 Zinc samples

Dissolved Zn standards were NIST-SRM 682 and a 1000 ppm Zn standard (AccuTrace, AccuStandard Inc., Lot#B2075078). Laboratory-grade Zn metal samples were 10 mesh (#1: B&A, Lot D355Z077R) and 30 mesh (#2: J.T. Baker, Lot G42701). Laboratory Zn acetate standards were from Mallinckrodt (#1: Lot WALP, and #2: Lot KDSJ) and Baker Scientific (#3: Lot H20157). Industrial Zn metal dust samples of 98.5% purity were obtained from the US Zinc (Austin, TX) as regular (USZ # 1), regular superfine (USZ # 5), and low Pb Zn (USZ #1 XL). Industrial high purity Zn shot (99.995%) was obtained from the Canadian Electrolytic Zinc (CEZ) refinery (Salaberry-de-Valleyfield, Québec) through Falconbridge Limited. U.S. pennies were obtained from circulation and are noted by the year in which they were minted. Health and medical products were obtained from local commercial sources and include Benadryl Itch Stopping Cream (Pfizer Consumer Healthcare, Lot #23454L), Centrum Silver multivitamins (Wyeth Consumer Healthcare, Control #A98404), Dr. Zinc lozenges (McKesson, Lot #3KVO305), Nature's Bounty zinc tablets (Nature's Bounty, Inc., Lot #20515101), and ColdEeze zinc lozenges (The Quigley Corporation).

2.2.2 Sample preparation

Samples were handled under Class-100 clean air flow conditions. Water was deionized and distilled in a borosilicate glass still (Corning MegaPure), and all acids were triply-distilled in Vycor

glass to remove contaminants. All labware was acid cleaned PFA (Savillex), polypropylene or polyethylene. Metal samples were prepared by dissolving directly in 2% HNO_3 for analysis, or by dissolving in 2N HCl prior to purification by anion exchange chromatography. Zn acetate samples were twice dissolved in 2% HNO_3 and evaporated to drive off acetic acid before redissolution in 2% HNO_3. Pennies were washed with 2% Citranox detergent, rinsed with distilled water, and dissolved in 2N HCl prior to anion exchange purification. Health and medical products were dissolved in 2% nitric acid and small aliquots were removed and evaporated to dryness. These subsamples were then combusted for 8 hours at 450°C to remove all organic material and the remaining material was dissolved in 2N HCl prior to anion exchange purification.

Between 10 to 200 µg of each sample was purified by anion exchange chromatography on AG-MP1 resin (BioRad) according to a method previously used for the purification of Fe, Cu, and Zn for isotopic analysis (Maréchal et al., 1999). Because samples were not being processed for Fe and Cu isotope analysis, samples were loaded in 2N HCl. The sample was rinsed with 15 mL of 2N HCl to elute other elements, and then the Zn fraction was eluted in 12 mL 0.5N HNO_3. The eluent was evaporated and reacted with 200 µL of 14N HNO_3 and 100 µL of H_2O_2 (Ultrex II, J.T. Baker), to oxidize organics that may have leached from the resin. With every group of samples processed by column chromatography, two process blanks and one or two isotope standards were processed and analyzed to assess the magnitude of contamination and matrix effects during measurement.

2.2.3 Isotope analysis

All samples were diluted to 200 ppb Zn in 2% HNO_3 for isotope analysis and spiked with 100 ppb Cu (Ultra Scientific, Lot #D00204) to monitor instrumental mass bias. Data was collected on an

IsoProbe multi-collector ICP-MS (Thermo Electron, formerly Micromass), using Faraday collectors to monitor signals on masses 60, 63, 64, 65, 66, 67, and 68. Samples were introduced into the plasma by an Apex Q inlet system with a desolvating membrane (ESI) using a 75 µL/min MicroMist® (Glass Expansion) nebulizer. On-peak acid blank subtraction was applied to all samples by monitoring the signal from 2% HNO_3 during one 60 second block, three minutes before sample analysis. Sample and standard data was collected in fifteen cycles of ten seconds, and up to two cycles more than two standard deviations from the mean were discarded.

The only spectral interference for which we apply a correction is ^{64}Ni (overlapping with ^{64}Zn). This correction is made by monitoring the abundance of ^{60}Ni, assuming natural isotopic abundances, and correcting for instrumental mass bias with an internal Cu spike (see below). Ni corrections were insignificant at our analytical precision. We first determine Zn isotope ratios by sample-standard bracketing alone and then correct these data for sample matrix effects on instrumental mass bias using an internal Cu spike. The relationship between Zn and Cu mass bias can differ from that expected based on the exponential mass bias law alone (Albarède and Beard, 2004; Maréchal et al., 1999). Following their suggestion, we determine the linear relationship between the natural log of measured $^{66}Zn/^{64}Zn$ versus measured $^{65}Cu/^{63}Cu$ for all standards analyzed during a single session, a procedure termed empirical external normalization (EEN) (Clayton et al., 2002; Mason et al., 2004). We apply this correction to both samples and standards, for a 'modified' EEN sample-standard bracketing technique. All samples were measured in triplicate and $^{68}Zn/^{64}Zn$ ratios were measured to verify mass-dependent fractionation and the absence of Zn spectral interferences.

NIST-SRM 682 has been measured repeatedly against the Lyon-JMC Zn (Maréchal et al., 1999) and is lighter by $\delta^{66}Zn_{JMC} = -2.45$ ‰. All measurements are corrected with this offset so that isotope ratios may be reported compared to Lyon-JMC Zn.

2.3 Results and Discussion

2.3.1 Error analysis

The measured isotope ratio of samples compared to unprocessed bracketing standards can be affected by Zn contamination of the samples, isotopic fractionation during the purification procedure, or analytical changes resulting from matrix residues. We discount the effect of Zn contamination because process blank concentrations were low (consistently between 0 and 10 ng and never more than 0.1% of the sample concentrations). Assuming that contamination sources have an isotopic ratio similar to other continental and anthropogenic samples, this amount of contaminant Zn is too small to have a measurable effect on the isotope ratio of samples. Zn recoveries were always greater than 98%, so there should be no isotopic fractionation associated with column purification and other processing steps. NIST-SRM 682 process standards were treated by the same purification protocol as samples in order to gauge the accuracy and precision of our analytical methods (Figure 1). Most of the Cu-corrected ratios are higher than the raw data corrected by sample-standard bracketing alone. Although the magnitude of this correction is small (the average $\Delta\delta^{66}Zn = +0.02$‰ for the five standards), it may reflect a genuine systematic matrix effect on the Cu isotope ratio in samples.

In our experience, though, the main source of analytical error is occasional appearance of a systematic offset between pre-column and post-column standards, as has also been observed in other
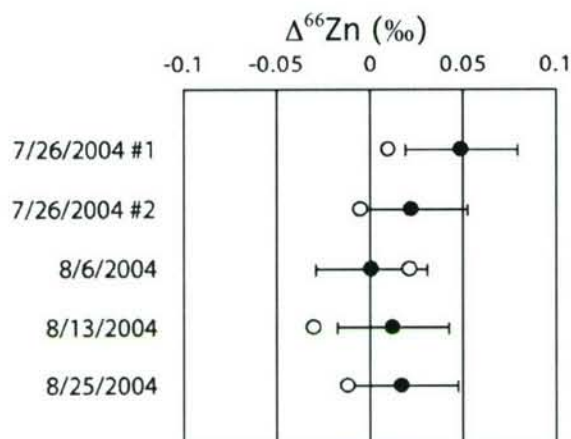
Figure 2.1. Sample-standard bracketing corrected (O) and sample corrected (●) Zn isotope ratios of standards processed alongside samples on several different dates.

studies (Archer and Vance, 2004). In some analytical sessions, use of the desolvating membrane attached to the APEX resulted in systematic offsets in all post-column samples of as much as +0.2‰. In this study, careful post-column treatment of the samples with HNO_3/H_2O_2 to remove organics seems to have largely prevented this problem. In other experiments, we found that removing the desolvating membrane appears to eliminate this problem.

Reproducibility for triplicate analysis of individual samples was between 0.00‰ and 0.06‰ (2σ s.d.) (Table 1). The difference in measured isotope ratio (Δ) between standards used for sample-standard bracketing and standards run through the full sample purification protocol was used to estimate external reproducibility. The standard deviation of $\Delta^{66}Zn$ for the five process standards was 0.052‰ (2σ), greater than the internal reproducibility within triplicate analyses for nearly all of our
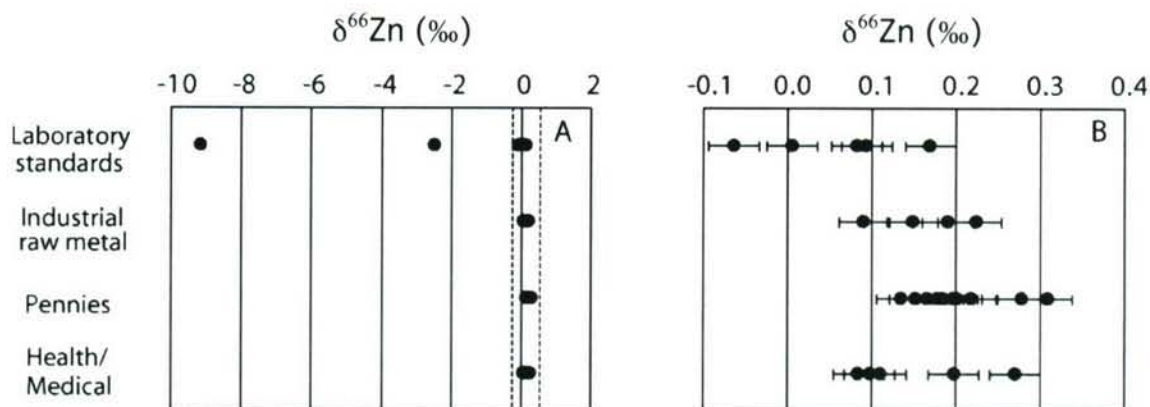
Figure 2.2. Zn isotopic composition of anthropogenic samples showing A) the entire measured range and B) the smaller range in which all non-laboratory standards fall.

samples. We are wary of applying the error calculated for post-column standards to samples with a potentially more complicated matrix, but we believe that this error is more appropriate than the smaller errors calculated from internal reproducibility. A standard deviation of 0.052‰ is equivalent to a standard error of 0.030‰ (2σ) for triplicate analysis. Several samples were run in different analytical sessions months apart, these replicate analyses give the same δ^{66}Zn values within the analytical error.

2.3.2 Zn isotopes in anthropogenic samples

Zn isotope ratios were measured for twenty-two anthropogenic Zn samples (Figure 2). The isotopic compositions of the laboratory standards ranged from δ^{66}Zn$_{JMC}$ = -9.15‰ to +0.17‰. The AccuTrace standard has the lightest Zn isotope ratio reported to date. NIST-SRM 682 and two of the

Sample name	Sample-Standard Bracketing (SSB) corrected data			Sample-Standard Bracketing/ Cu Empirical External Normalization (EEN) corrected data		
	$\delta^{66}Zn_{NIST-SRM\ 682}$	$\delta^{66}Zn_{JMC}$	s.d. (2σ)	$\delta^{66}Zn_{NIST-SRM\ 682}$	$\delta^{66}Zn_{JMC}$	s.d. (2σ)
NIST SRM-682				0.00	-2.45	
AccuTrace Std				-6.70	-9.15	
Metal (10 mesh	2.61	0.16	0.03	2.62	0.17	0.00
Metal (30 mesh	2.53	0.08	0.03	2.54	0.09	0.03
Acetate #1	2.61	0.16	0.24	2.46	0.01	0.04
Acetate #2	2.61	0.16	0.10	2.53	0.08	0.05
Acetate #3	2.51	0.06	0.06	2.39	-0.06	0.04
Std Dust	2.41	-0.04	0.09	2.60	0.15	0.02
Fine Dust	2.46	0.01	0.02	2.64	0.19	0.04
Low Pb dust	2.48	0.03	0.08	2.54	0.09	0.03
CEZ shot	2.66	0.21	0.02	2.67	0.22	0.03
1983 Penny	2.51	0.06	0.07	2.60	0.15	0.02
1983 Penny #2	2.56	0.11	0.03	2.59	0.14	0.04
1985 Penny	2.54	0.09	0.07	2.65	0.20	0.04
1985 Penny #2	2.56	0.11	0.03	2.63	0.18	0.03
1991 penny	2.49	0.04	0.11	2.67	0.22	0.06
1991 Penny #2	2.59	0.14	0.03	2.64	0.19	0.05
1999 Penny	2.55	0.10	0.06	2.62	0.17	0.01
2000 Penny	2.69	0.24	0.07	2.76	0.31	0.05
2000 Penny #2	2.69	0.24	0.02	2.73	0.28	0.02
2002 Penny	2.61	0.16	0.06	2.65	0.20	0.05
Benadryl	2.54	0.09	0.01	2.56	0.11	0.02
Centrum	2.53	0.08	0.05	2.54	0.09	0.02
Dr Zn	2.63	0.18	0.03	2.65	0.20	0.02
Nature's Bounty	2.59	0.14	0.24	2.55	0.10	0.03
ColdEeze	2.61	0.16	0.07	2.72	0.27	0.04

Table 2.1. Zn isotopic composition of anthropogenic samples compared to NIST SRM-682 and Lyon-JMC Zn. Standard deviations are reported for triplicate analysis of individual samples.

Zn acetate samples (#1 and #3) were lighter than any of the non-laboratory Zn samples measured. The δ^{66}Zn of Zn dust ranged from +0.09‰ to +0.22‰, δ^{66}Zn for pennies ranged from 0.14‰ to 0.31‰, and the health and medical products δ^{66}Zn ranged from 0.09‰ to 0.27‰.

All common types of anthropogenic Zn (excluding laboratory standards) fell within a small range of isotope compositions. The total range in δ^{66}Zn that we measured for common Zn is +0.09‰ to +0.28‰, more than an order of magnitude smaller than the range seen in hydrothermal samples discussed in Section 1. Interestingly, the average isotopic composition of our "common" Zn is δ^{66}Zn = +0.18‰, quite similar to the +0.15‰ average isotope composition of samples measured in two Zn ore fields (Mason et al., 2005; Wilkinson et al., 2005). Based on this, we suggest that the δ^{66}Zn variability we see in different anthropogenic samples represents isotopic differences between ores, modified by homogenization during processing. We do not find evidence of a large isotope effect associated with the purification of Zn ore into metal.

2.4 Conclusions

When studying Zn isotopes in the environment (for example, in seawater (Bermin et al., 2006), marine materials (Maréchal et al., 2000), or plants (Weiss et al., 2005), there may be both natural and anthropogenic sources of Zn. We believe that the samples analyzed here are broadly representative of both the average isotopic composition and the variability that will be found in common forms of anthropogenic Zn.

References for chapter 2:

Albarède, F. and Beard, B., 2004. Analytical methods for non-traditional isotopes, Geochemistry of Non-Traditional Stable Isotopes, pp. 113-152.

Archer, C. and Vance, D., 2004. Mass discrimination correction in multiple-collector plasma source mass spectrometry: an example using Cu and Zn isotopes. Journal of Analytical Atomic Spectrometry, 19: 656-665.

Arimoto, R., Duce, R.A., Ray, B.J. and Tomza, U., 2003. Dry deposition of trace elements to the western North Atlantic. Global Biogeochemical Cycles, 17(1): Art. No. 1010.

Bermin, J., Vance, D., Archer, C. and Statham, P.J., 2006. The determination of the isotopic composition of Cu and Zn in seawater. Chemical Geology, 226(3-4): 280-297.

Candelone, J.P., Hong, S.M., Pellone, C. and Boutron, C.F., 1995. Postindustrial Revolution Changes in Large-Scale Atmospheric-Pollution of the Northern-Hemisphere by Heavy-Metals as Documented in Central Greenland Snow and Ice. Journal of Geophysical Research-Atmospheres, 100(D8): 16605-16616.

Chapman, J.B., Mason, T.F.D., Weiss, D.J., Coles, B.J. and Wilkinson, J.J., 2006. Chemical separation and isotopic variations of Cu and Zn from five geological reference materials. Geostandards and Geoanalytical Research, 30(1): 5-16.

Clayton, R., Andersson, P., Gale, N.H., Gillis, C. and Whitehouse, M.J., 2002. Precise determination of the isotopic composition of Sn using MC-ICP-MS. Journal of Analytical Atomic Spectrometry, 17(10): 1248-1256.

Dolgopolova, A. et al., 2006. Use of isotope ratios to assess sources of Pb and Zn dispersed in the environment during mining and ore processing within the Orlovka-Spokoinoe mining site (Russia). Applied Geochemistry, 21: 563-579.

FDA, 2002. Code of Federal Regulations, Title 21, 73.1991 Zinc oxide.

Gordon, R.B. et al., 2003. The characterization of technological zinc cycles. Resources Conservation and Recycling, 39(2): 107-135.

Graedel, T.E. et al., 2005. The multilevel cycle of anthropogenic zinc. Journal of Industrial Ecology, 9(3): 67-90.

Jasinski, S.M., 1994. Zinc, Minerals Yearbook. The Bureau of Mines, Washington, D.C.

Jorgenson, J.D., 2004. Zinc, Minerals Yearbook. The Bureau of Mines, Washington, D.C.

Kavner, A., Bonet, F., Shahar, A., Simon, J. and Young, E., 2005. The isotopic effects of electron transfer: An explanation for Fe isotope fractionation in nature. Geochimica et Cosmochimica Acta, 69(12): 2971-2979.

Luck, J.M., Ben Othman, D., Albarède, F. and Telouk, P., 1999. Pb, Zn, and Cu isotopic variations and trace elements in rain. Geochemistry of the Earth's Surface. Balkema, Rotterdam.

Maréchal, C.N., Nicolas, E., Douchet, C. and Albarède, F., 2000. Abundance of zinc isotopes as a marine biogeochemical tracer. Geochemistry Geophysics and Geosystems, 1: 1999GC000029.

Maréchal, C.N., Telouk, P. and Albarède, F., 1999. Precise analysis of copper and zinc isotopic compositions by plasma-source mass spectrometry. Chemical Geology, 156(1-4): 251-273.

Mason, T.F.D. et al., 2005. Zn and Cu isotopic variability in the Alexandrinka volcanic-hosted massive sulphide (VHMS) ore deposit, Urals, Russia. Chemical Geology, 221(3-4): 170-187.

Mason, T.F.D. et al., 2004. High-precision Cu and Zn isotope analysis by plasma source mas spectrometry - Part 2. Correcting for mass discrimination effects. Journal of Analytical Atomic Spectrometry, 19(2): 218-226.

Mattielli, N. et al., 2005. Isotopic study of two biolimiting metals (Zn and Cu) in industrial aerosols. Geophysical Research Abstracts, 7: 10030.

Pacyna, J.M. and Pacyna, E.G., 2001. An assessment of global and regional emissions of trace metals to the atmosphere from anthropogenic sources worldwide. Environmental Reviews, 9: 269-298.

Planchon, F.A.M. et al., 2002. Changes in heavy metals in Antarctic snow from Coats Land since the mid-19th to the late-20th century. Earth and Planetary Science Letters, 200(1-2): 207-222.

Shiller, A.M. and Boyle, E., 1985. Dissolved Zinc in Rivers. Nature, 317(6032): 49-52.

Tanimizu, M., Asada, Y. and Hirata, T., 2002. Absolute isotopic composition and atomic weight of commercial zinc using inductively coupled plasma mass spectrometry. Analytical Chemistry, 74(22): 5814-5819.

Weiss, D.J. et al., 2005. Isotopic discrimination of zinc in higher plants. New Phytologist, 165(3): 703-710.

Wilkinson, J.J., Weiss, D.J., Mason, T.F.D. and Coles, B.J., 2005. Zinc isotope variation in hydrothermal systems: Preliminary evidence from the Irish Midlands ore field. Economic Geology, 100(3): 583-590.

Chapter 3

Zn isotopes in hydrothermal vent fluids and chimneys

Many of the heaviest and lightest natural zinc (Zn) isotope ratios have been discovered in hydrothermal ore deposits. However, the processes responsible for fractionating Zn isotopes in hydrothermal systems are poorly understood. We have studied Zn isotopes in seafloor hydrothermal chimneys and vent fluids from several vent fields along the East Pacific Rise (EPR) and Mid-Atlantic Ridge in order to better assess the total range of Zn isotopes in hydrothermal systems and to understand the factors which are responsible for this isotopic fractionation. Zn isotopes may then be used to better understand hydrothermal processes. Of all the physical and chemical parameters examined such as pH and concentrations of many trace elements, only temperature was found to correlate with fluid δ^{66}Zn values. Lower temperature fluids (<250C) had both

heavier and more variable δ^{66}Zn values compared to higher temperature fluids from the same hydrothermal field. Similarly, chimney sulfides from a low-temperature vent at EPR 9°N were found to be heavier and more variable in δ^{66}Zn values than sulfides sampled from a high-temperature vent. We hypothesize that subsurface cooling of hydrothermal fluids leads to the precipitation of isotopically light Zn in sulfides, and that this process is the primary cause of Zn isotope variation in hydrothermal fluids.

3.1 Introduction

With multi-collector inductively coupled plasma mass spectrometry (ICPMS), stable isotope variability of transition metals has been seen in many natural samples. Metal isotopes studied in active hydrothermal systems include Fe isotopes (Rouxel et al., 2004b; Severmann et al., 2004; Sharma et al., 2001), Cu isotopes (Rouxel et al., 2004a; Zhu et al., 2000), Mo isotopes (McManus et al., 2002), Se isotopes (Rouxel et al., 2004b), and Sb isotopes (Rouxel et al., 2003).

Zn isotopes have been studied in rocks (Chapman et al., 2006; Maréchal et al., 2000), marine sediments (Pichat et al., 2003), biological materials (Maréchal et al., 2000; Weiss et al., 2005), seawater (Bermin et al., 2006), and ore deposits (Mason et al., 2005; Wilkinson et al., 2005). It is possible that Zn isotopes may help contribute to understanding ore formations and hydrothermal processes. Economic deposits of Zn ore originate mainly as hydrothermal vent fields (Herzig, 1999), and Zn isotopes have been proposed as a tool for distinguishing between Zn-rich areas in mining deposits and distal regions where Zn is less concentrated (Wilkinson et al., 2005).

The fractionation of Zn isotopes in hydrothermal systems may influence the Zn isotope ratios seen in the environment. The deposits from hydrothermal systems contain both the heaviest and lightest Zn isotope samples reported to date ($\delta^{66}Zn$ = -0.43‰ and $\delta^{66}Zn$ = +1.33‰) (Wilkinson et al., 2005). Zn isotope signals may be transported throughout the environment by the weathering of ancient hydrothermal deposits and contemporary hydrothermal fluid discharge.

Thorough studies of Zn isotopes have been carried out in the Alexandrika volcanic-hosted massive sulfide ore deposit in Urals, Russia (Wilkinson et al., 2005) and the Irish Midlands ore field (Mason et al., 2005). The Alexandrika ore deposit formed as a seafloor hydrothermal system similar to modern systems studied here. Samples were analyzed from the hydrothermal-metasomatic stockwork believed to be the feeder zone to the hydrothermal deposit, a seafloor chimney, and some clastic sediments. $\delta^{66}Zn$ values from the deposit ranged from -0.43‰ to +0.23‰. A systematic increase in $\delta^{66}Zn$ values from the chimney core to the chimney rim was attributed to either a temperature dependence in the fractionation factor for precipitation or Rayleigh distillation as fluids diffuse through the chimney wall. Zn isotopes in the Irish Midlands ore field show a general trend of lighter Zn isotopes precipitated in the deep feeder veins and heavier Zn isotopes near the top of the hydrothermal system. This data is consistent with Rayleigh distillation of Zn with isotopically light Zn partitioning into Zn sulfides. Other studies have investigated Zn isotopes in sulfides from various ore deposits (Maréchal et al., 1999) and Archean shales (Archer and Vance, 2002).

Despite these initial studies, the cause of Zn isotope fractionation in hydrothermal systems remains poorly constrained. It is hoped that the study of active hydrothermal vents will permit to provide a better understanding of how factors such as fluid temperature, temperature of sulfide precipitation, and the mineralogy of hydrothermal precipitates will affect Zn isotope fractionation.

3.1.1 Geologic settings

The 21°N site on the East Pacific Rise (EPR) was among the first ridge-crest hydrothermal systems to be studied (Von Damm et al., 1985). Three of the vent sites (Ocean Bottom Seismometer (OBS), South West (SW), and Hanging Gardens (HG)) were typical high temperature black smokers and their chemical composition remained quite stable over the three years between 1979 and 1981 (Campbell et al., 1988). The fourth (National Geographic Society (NGS)) was a black smoker when originally sampled in 1979. The vent had become sealed off when revisited in 1981, and it emitted low-temperature white smoker fluids when broken open. The 9°N site is one of the youngest hydrothermal sites on the EPR as determined by volcanic activity and $^{210}Po/^{210}Pb$ dating (Von Damm, 2000). The site was first sampled in 1991 and with only fifteen years between the first hydrothermal activity and sampling, we expected less hydrothermal alteration here than at other sites. The Guaymas basin lies in the Gulf of California, also on the East Pacific Rise but, in contrast to the 9°N and 21°N sites, it is covered by a thick layer of sediments through which hydrothermal fluids pass before venting on the seafloor. The TAG hydrothermal field lies on the more slowly spreading

Mid-Atlantic Ridge. This site is distinguished by the large extent of subsurface Zn sulfide redissolution, particularly in the numerous white smokers.

3.2 Methods

3.2.1 Sample collection

Most hydrothermal vent fluids were obtained from the collection of John Edmond stored at the Massachusetts Institute of Technology (MIT). All these samples were collected using a titanium syringe with a snorkel that could reach directly into the vent chimney for sampling (Von Damm et al., 1985). It was believed at the time that this sampling method prevented the precipitation of sulfides from the samples, and that when sulfides did form they could be quickly redissolved by the addition of 6N HCl to a pH of about 1.6. In fact, these early sampling methods may have left some particles behind in the syringes ("dregs"). All samples were visually inspected to ensure that no visible precipitates remained. Precipitates that formed since sample collection were analyzed to ensure that they contained very little Zn.

For fluids from the MIT hydrothermal vent collection, the highest recorded temperature from the vent field was used instead of the temperature recorded for any individual sample. Individual temperature measurements were quite difficult with the ALVIN temperature probe (Campbell et al., 1988). For samples collected at the 21°N site, only sample 1160-7 had a recorded temperature (224°C) that was more than a few degrees different from the field end-member temperature (350°C). This particular sample most likely represents an inaccurate temperature measurement (K. Von Damm, personal

communication). Trace-metal concentrations in this sample (including Cu) support our assumption that this is a high-temperature vent.

Samples from the Pacific were collected from ALVIN dives during 1981-2 cruise to the hydrothermal fields at 21°N on the East Pacific Rise and the Guaymas basin. Numerous geochemical parameters were reported in previous studies, including temperature, pH, alkalinity, and the concentrations of Mg, SiO_2, Li, Na, K, Rb, Se, Ca, Sr, Ba, Cl, SiO_4, H_2S, NH_4, NO_2, PO_4, and the trace metals Mn, Fe, Co, Cu, Zn, Ag, Cd, Pb, As, Se, and Al (Von Damm, 1984).

Samples from the Mid-Atlantic Ridge were collected at the TAG and Snake Pit hydrothermal sites in 1990. Vents sampled on this cruise included both high temperature "black smokers" and lower temperature "white smokers". White smoker and black smoker end-member concentrations (Edmond et al., 1991) and data on dissolved trace-element fluxes have been previously reported (German et al., 1991). Chemical and physical data on individual samples was provided by Andy Campbell (personal communication).

Samples from the hydrothermal field at 9-10°N on the East Pacific Rise were collected in 2004 in the ALVIN submersible dives 4053 and 4057 during the cruise AT11-2 (Rouxel et al., in prep). The high-temperature vent Bio9'' is located at 9°50′N within an area where dramatic changes in the hydrothermal systems have taken place. Prior to 1994, Bio9 was the only high temperature vent sampled in the Bio9 area. By 1994, the Bio9' vent was a distinct individual black smoker. By 1999, the number of smokers around Bio9 had begun to increase, replacing some of the areas that had

48

previously been characterized by diffuse flow. Bio9" is the third distinct smoker in the Bio9 area which has been initially sampled in 2002. K-vent at 9'29.8°N is the most southerly active vent, before encountering a zone of extinct vents (Von Damm, 2000). K-vent has a distinctly lower temperature than other vents (203°C), which is even lower than the temperature reported in 1991 (263°C) (Von Damm, 2000).

3.2.2 Sample Processing

3.2.2.1 Chimney sulfides

Hydrothermal vent fluids and chimney minerals were sampled at both a high temperature vent (Bio 9" vent) and a low temperature vent (K-vent). In both cases, the chimney was removed and hydrothermal fluids were sampled from the remaining base of the chimney.

Hydrothermal sulfide samples were crushed between two plexiglass discs inside a Teflon bag using a hydraulic press. Sulfide grains were collected between 500 μm and 1.0 mm sieves and mono-mineral sulfide phases were isolated by hand picking under a microscope. For each sample, between 15 and 50 mg of mineral grains were picked in order to obtain a representative sample. Care was taken to select pure sulfide grains without other mineral inclusions but, in some cases, inclusions were unavoidable especially for sphalerite (ZnS) which includes other phases such as pyrite and chalcopyrite. Representative splits of mineral separates were saved for Fe and S-isotope analysis and trace element concentrations (Rouxel et al., in prep). Samples were weighted in 15 mL Teflon beakers and dissolved using 5 mL of concentrated HNO_3. After

evaporation on a hot plate at 60°C, complete dissolution was achieved by a second

evaporation step using 5mL of aqua regia. Dry residue was dissolved in 5 mL of 6N HCl

with trace H_2O_2 by heating at 40°C in a closed vessel.

When the fluids from these sites were brought on board the ship they were

acidified with concentrated HCl to pH ~ 1. The "dregs" (insoluble or precipitated

particles remaining in the Ti-samplers) are recovered when the samplers are disassembled

by rinsing with Milli-Q water and acetone on 0.45 μm filters and saved for chemical

analysis. Class-100 clean airflow conditions were maintained during further manipulation

of all samples.

3.2.2.2 Hydrothermal fluids

Vent fluids from the MIT collection were mixed with 6N HCl to a concentration

of 2 M Cl⁻ for purification by anion exchange chromatography. Because vent fluids from

the 9°N site contained some precipitate, 12 mL of the homogenized fluid-particle mixture

was reacted overnight in a closed PFA capsule with 3 mL 14N HNO_3 and 3 mL 6N HCl

in order to oxidize and dissolve precipitates. The solution was diluted to 20 mL with a Cl⁻

concentration of 2 M for column purification.

3.2.2.3 Purification by anion exchange chromatography

Samples were purified by anion exchange chromatography using a procedure

modified from that of Maréchal et al. (Maréchal et al., 1999). Samples were loaded in 2N

HCl in order to minimize the amount of acid used and decrease the chance of premature

elution, as the affinity of Zn for the resin is highest at 2N HCl (Kraus and Moore, 1953).

Zn was eluted in 0.06N HCl, which may help avoid elution of other elements (Chapman

et al., 2006). Samples were evaporated to dryness in 5mL PFA capsules, and reacted at

high heat overnight with 200 μL concentrated HNO_3 and 100 μL concentrated HF to

remove residual silicates from the sample and residual organics that may have leached

from the column.

3.2.3 Isotopic analysis

Samples were redissolved in 2% HNO_3 at a Zn concentration of 50, 100, or

200 ppb for isotopic analysis. All samples were analyzed with 100 ppb Cu (Ultra

Scientific, Lot #D00204) for instrumental mass fractionation correction. Isotope ratio

measurements were made on an IsoProbe multi-collector ICP-MS (Thermo Electron

Corporation, formerly Micromass) using an APEX Q inlet system (ESI) with a 75 μL

min^{-1} MicroMist nebulizer (Glass Expansion). The optional desolvating membrane was

not used as we have sometimes observed large instrumental mass bias when using it.

Signal intensity was measured on masses 60, 63, 64, 66, 67, and 68 using Faraday

collectors in fifteen blocks of ten seconds. $^{64}Ni^+$ was subtracted from the $^{64}Zn^+$ signal by

monitoring the signal from $^{60}Ni^+$. Because we used Al sampling cones, the corrections for

Ni were insignificant. All peaks were corrected for acid blanks using an on-peak zero

immediately prior to measurement. All Zn isotope data is reported in terms of deviation

from the "Lyon JMC" Zn standard.

Data was corrected for instrumental mass bias using the Cu internal spike. The relationship between Cu and Zn instrumental fractionation has been shown to differ from predictions of the exponential mass bias law (Albarède and Beard, 2004; Maréchal et al., 1999). A linear relationship between the natural log of $^{65}Cu/^{63}Cu$ and $^{66}Zn/^{64}Zn$ in standards was used instead to determine the mass bias relationship. Because natural changes in instrumental mass fractionation are greatly reduced with the removal of the desolvator from the APEX, modified standards containing H_2SO_4, Sr, or organics leached from polyelthylene bottles after many months of storage were sometimes used to artificially increase mass bias (Archer and Vance, 2004). All samples were measured in triplicate and were corrected for mass bias using Cu. Sample standard bracketing with Cu-corrected samples and standards was used to obtain the final values.

Mass bias was also corrected on several samples using a Zn double spike. A spike mixed predominately from ^{64}Zn and ^{67}Zn was used added to samples for a final $^{64}Zn:^{66}Zn:^{67}Zn:^{68}Zn$ ratio of 4.2 : 1.3 : 1.6 : 1. Isotope ratios were calculated using a Newton Raphson iteration (Albarède and Beard, 2004).

Many of the MIT samples had a small amount (less than a gram) of a clear crystalline precipitate in the bottom. These samples had been filtered upon collection, so the precipitate must have formed during sample storage. The composition of the precipitate is unknown, but it could be amorphous silica or elemental sulfur. This precipitate was separated from 10mL of homogenized fluid by centrifugation and redissolved in 2% HNO_3 for elemental analysis. Measurements were performed on a PlasmaQuad 2+ quadrupole ICP-MS (VG Elemental, now Thermo Electron) using an In

spike to correct for sensitivity changes. In all fluids the amount of Zn in the precipitate was less than 0.1% of the dissolved concentration.

3.3 Results and discussion

3.3.1 Analytical accuracy and precision

Error was estimated by calculating the pooled standard deviation of seven samples each run on two different days, combined with the analytical error for five process standards. The calculated error was 0.069‰ (2σ s.d.). The internal error averaged over hundreds of samples was 0.067‰ (2σ s.d.), indicating similar error for samples and standards after the chemical purification process. There was no apparent difference in the magnitude of internal error of triplicate analysis between hundreds of samples run at 50, 100, and 200 ppb.

Data was checked for polyatomic or doubly charged interferences by comparing $\delta^{66}Zn$ values to $\delta^{68}Zn$ values (Fig. 1). With two exceptions, the data showed the expected trend in mass bias within error. These two samples were run twice and the discrepancy lies in the $\delta^{68}Zn$ values, indicating that the $\delta^{66}Zn$ values are accurate. The values obtained by correcting for instrumental mass bias using a double spike matched those corrected for mass bias using Cu, indicating that both mass bias corrections are robust (Fig. 2). Duplicate samples taken with two different pistons on the Ti-sampler were analyzed for both Bio9 and K-vent at EPR 9°N and their isotopic composition agrees within our analytical precision.
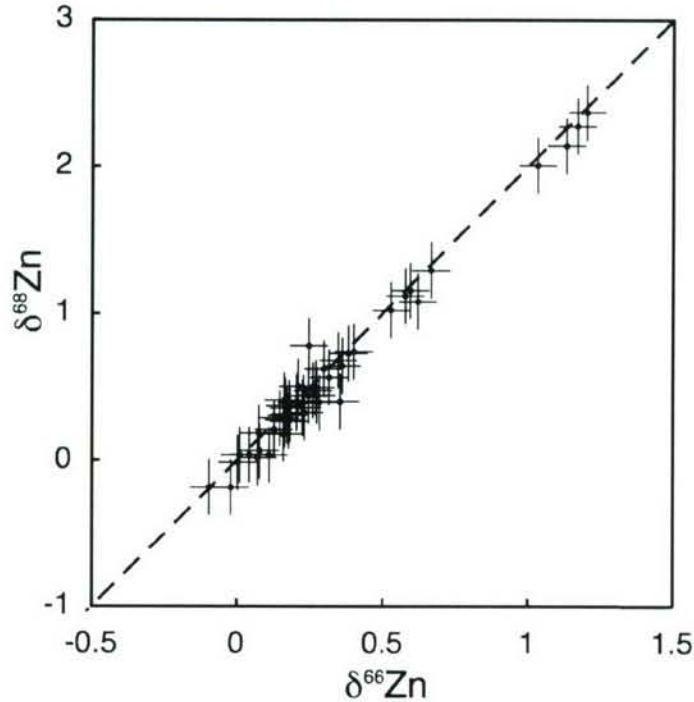
Figure 3.1. Comparison of $\delta^{68}Zn$ and $\delta^{66}Zn$ values for all samples in this study demonstrate the absence of isobaric interferences. The two outliers (circled) were measured twice with matching $\delta^{66}Zn$ values. There appears to be a small unexplained bias towards heavy $\delta^{66}Zn$ compared to the values predicted by $\delta^{68}Zn$.

3.3.2 Bio 9'' high-temperature vent

Mineral samples at this vent range from $\delta^{66}Zn$ = -0.09‰ to +0.32‰. These values represent real differences in Zn isotopes, since the range is much larger than our analytical uncertainty. Yet, there is no clear relationship between $\delta^{66}Zn$ and location in the chimney that would allow us to determine what process is responsible for the observed differences. Changes in the fluid $\delta^{66}Zn$ values across the chimney wall, or
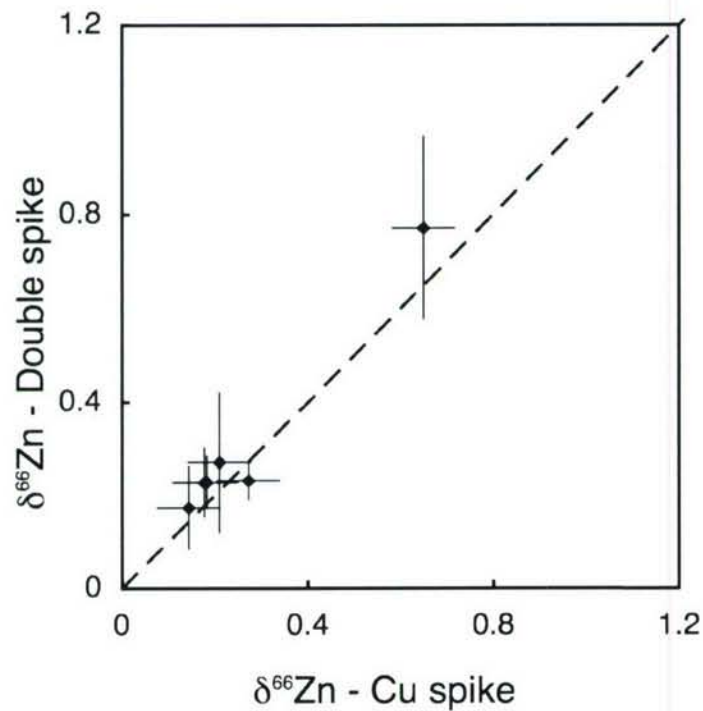
Figure 3.2. Comparison of $\delta^{66}Zn$ values measured using either a double spike method or an internal Cu spike to correct for instrumental mass bias. Within the analytical error, values provided by both methods are in agreement.

isotope fractionations during sulfide precipitation (equilibrium or kinetic) could be responsible. Our data does not show the same relationship between Zn isotopes in co-existing sphalerite and chalcopyrite samples as observed in previous studies: chalcopyrite $\delta^{66}Zn$ samples were around 0.4‰ lighter than nearby sphalerite in samples from the Alexandrika deposit in Russia (Mason et al., 2005). Although we find that chalcopyrite is lighter in three of the four locations sampled, the maximum difference of $\Delta^{66}Zn$ is only 0.18‰. At one location in the chimney the sphalerite was heavier than the chalcopyrite.

Site	Vent area	Sample ID	n=	$\delta^{66}Zn$	± 2σ s.d.	T (°C)	pH	[Cl] (mM)	[Zn] (µM)	[Cu] (µM)	[Fe]/ [Mn]
EPR 21°N	SW	1149-1	2	0.14	0.12	355	3.6	498	99	11	1.0
EPR 21°N	NGS	1151-14	1	0.25	0.04	273	3.8	559	56	0	1.3
EPR 21°N	NGS	1151-6	2	0.65	0.09	273	3.8	575	41	0	0.9
EPR 21°N	OBS	1152-16	1	0.18	0.08	350	3.4	502	93	45	1.9
EPR 21°N	SW	1153-9	1	0.27	0.03	355	3.6	500	98	11	1.2
EPR 21°N	NGS	1155-1	1	0.55	0.06	273	3.8	577	41	0	0.9
EPR 21°N	OBS	1158-16	1	0.21	0.15	350	3.4	491	114	43	1.8
EPR 21°N	HG	1160-7	2	0.18	0.07	351	3.3	500	107	40	2.9
Guaymas Basin	7	1175-9	1	0.33	0.07	285	5.9	548	24		4.2
TAG		2179-3C	1	0.20	0.08	363	3.4		46	135	8.2
TAG		2187-1C	2	0.38	0.11	287	3.0	636	350	3	5.1
TAG		2187-4C	1	0.13	0.08	287	3.0	636	350	3	5.1
TAG		2187-6C	2	0.31	0.16	287	3.0	636	350	3	5.1
TAG		2194-4C	2	0.02	0.02	363	3.4		46	135	8.2
TAG		2194-6C	1	0.25	0.14	363	3.4		46	135	8.2
EPR 9°N	K-vent	4053 W1	1	0.90	0.03	203		550	2	1	1.3
EPR 9°N	K-vent	4053 W2	1	0.93	0.06	203		550	3	2	1.2
EPR 9°N	Bio 9"	4057 W1	2	0.18	0.05	380		290	64	29	78.3
EPR 9°N	Bio 9"	4057 W2	2	0.22	0.07	380		290	339	79	93.7

Table 3.1. Data on all individual fluid and mineral samples measured. Sample ID is the information written on the sample bottle. n is the number of triplicate analyses performed on different days. Error is the internal standard deviation for triplicate analysis or the pooled standard deviation from two separate triplicate analyses. Temperature and pH are given as the end-member values for the vent area (Von Damm, 1984). Elemental concentrations are calculated for pure hydrothermal fluid assuming that all the Mg in samples comes from seawater entrained during sampling, data taken from Von Damm, 1984 (EPR 21°N and Guayamas) from data provided by Andy Campbell (TAG) and data provided by Olivier Rouxel (EPR 9°N).

This disparity may result from differences in the conditions under which the minerals precipitated. While the minerals studied by Mason et al. were formed deep within the hydrothermal stockwork, our samples were taken from a chimney where minerals most likely precipitated much more quickly as vent fluids mixed with seawater. Precipitation might have occurred too quickly for isotopic equilibrium to be established between Zn in sphalerite and chalcopyrite, or might quantitatively precipitate Zn within the chimney wall overwhelming any kinetic or equilibrium fractionations that did occur.

Hydrothermal fluids sampled from the Bio9'' chimney have an isotopic composition similar to the chimney minerals. The average Zn isotope composition of the fluids was $\delta^{66}Zn$ = +0.20‰, compared to +0.13‰ for the minerals sampled. Zn isotope ratios for particulate and fluid fractions in the water samplers was the same within analytical error. The values are also similar to existing measurements for the $\delta^{66}Zn$ of basalt. The similarity between the $\delta^{66}Zn$ of vent fluids and basalt suggests that chemical cycling of Zn at the site is minimal. The range for all reported measurements of Zn isotopes in basalt is +0.19‰ to +0.30‰ (Archer and Vance, 2002; Chapman et al., 2006; Dolgopolova et al., 2006; Maréchal et al., 2000). Because of the isotopic similarity between the basalt Zn source rock and the hydrothermal fluids, we hypothesize that subsurface precipitation of Zn sulfides at this site is minimal.

3.3.3 K-vent low-temperature vent

There was a large isotopic offset between the fluids ($\delta^{66}Zn$ = +1.29‰) and dregs ($\delta^{66}Zn$ = +0.33‰) in the samplers from this site. Because the fluids were observed to be
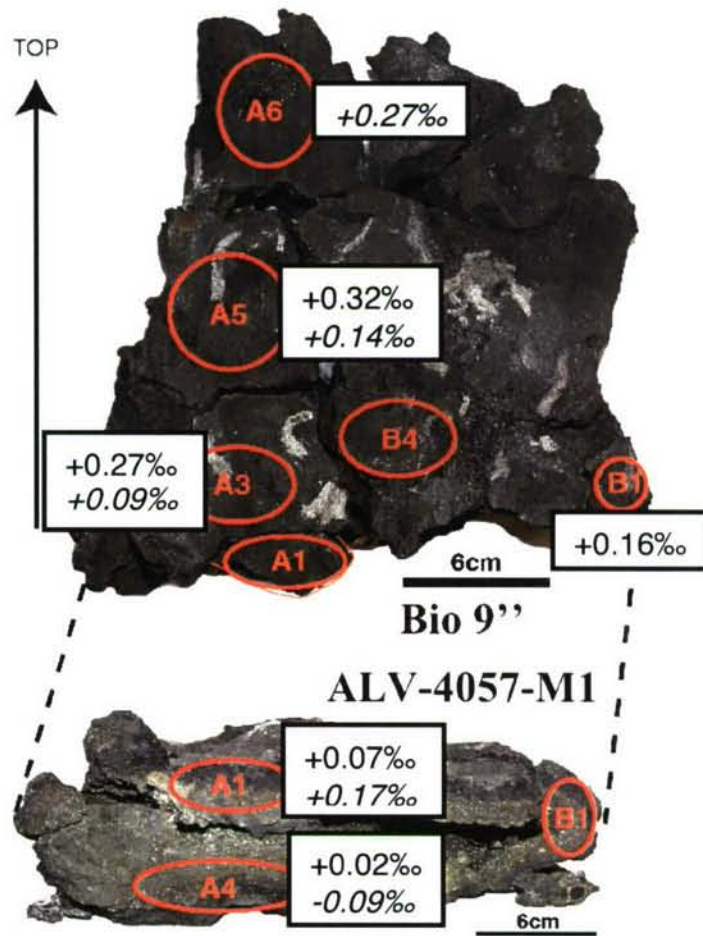
Figure 3.3A. Sample locations and $\delta^{66}Zn$ values of sphalerite (regular) and chalcopyrite (italic) samples taken from a chimney at the Bio 9'' vent site at 9°N on the East Pacific Rise. (Modified from Rouxel et al., in prep.)
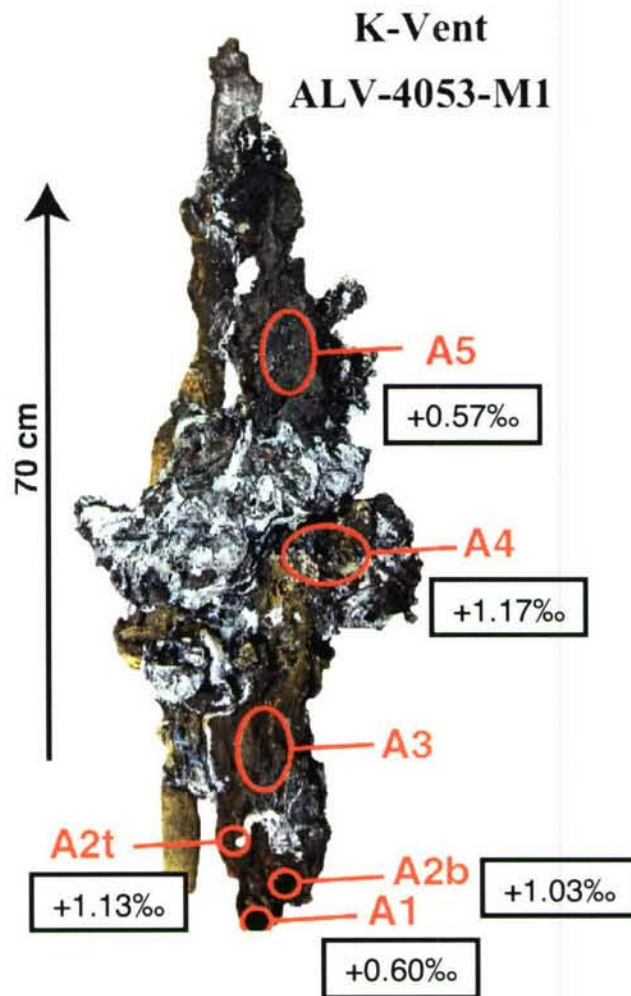
Figure 3.3B. Sample locations and $\delta^{66}Zn$ values for sphalerite samples taken from a chimney at K-vent at 9°N on the East Pacific Rise. (Modified from Rouxel et al., in prep.)
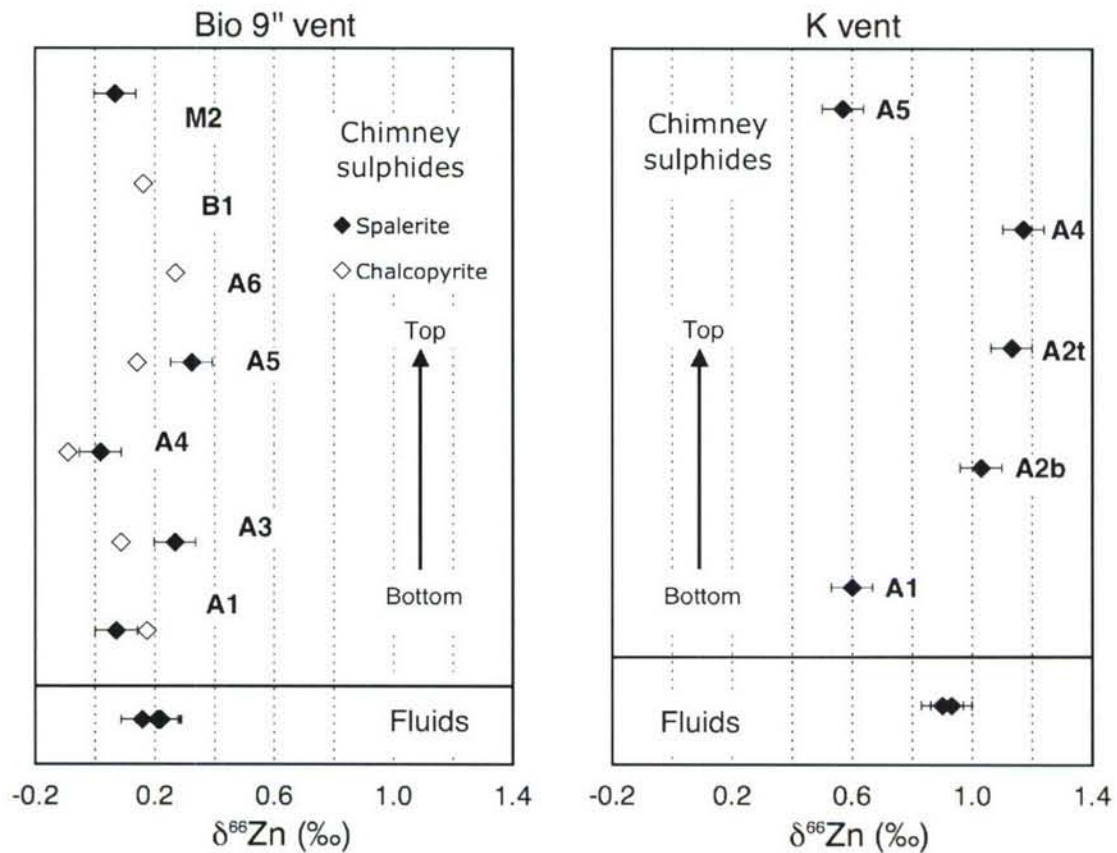
Figure 3.3C. $\delta^{66}Zn$ values of chimney sulfides and fluids from the high-temperature (380°C) Bio9'' vent and the low-temperature (203°C) K vent from the hydrothermal fields at 9°N on the East Pacific Rise. Mineral samples are aligned roughly from top to bottom.

60

clear when they exited the vent, we presume that the particulates formed in the sampler rather than the subsurface fluids. Assuming that the particles precipitated after sampling, the δ^{66}Zn of the original fluids are calculated by isotope mass balance as δ^{66}Zn = +0.90‰ and +0.93‰ for the duplicate samples. The fractionation factors (Δ^{66}Zn) calculated from the Rayleigh equations calculated here are -0.79‰ and -0.73‰.

The chimney minerals at this vent site range from δ^{66}Zn = +0.57‰ to +1.17‰, a greater range than at the high-temperature vent Bio 9" and significantly heavier than the predicted δ^{66}Zn in the basalt source rock. Based on our evidence that sulfides are lighter than the fluids from which they precipitate, we believe that the presence of isotopically heavy chimney minerals reflects their precipitation from isotopically heavy vent fluids. The variation in δ^{66}Zn values observed in these chimney minerals may result from temporal variations in the fluid δ^{66}Zn, or variations in the precipitation isotope effect.

3.3.4 Worldwide hydrothermal fluids

No significant trend in fluid δ^{66}Zn was observed as a function of concentrations of Zn, 1/Zn, Cu, Fe, H_2S, HS⁻, fluid pH, or [Fe]/[Mn], but a negative correlation with temperature was observed ($p < 0.0001$) (Fig. 4). All four of the highest δ^{66}Zn values occurred in fluids with relatively low Cu concentrations (≤ 1 µM) and Fe/Mn ratios (≤ 1.3).

Several factors may be responsible for differences in fluid δ^{66}Zn, including fractionation during phase separation, kinetic or equilibrium fractionation during subsurface precipitation of Zn sulfides, and subsurface redissolution of Zn sulfides.

61

Because the total range of fluid $\delta^{66}Zn$ is an order of magnitude greater than variations in basalt (Archer and Vance, 2002; Chapman et al., 2006; Maréchal et al., 2000), we suspect that source rocks are not the source of isotopic variability. Phase separation also seems unlikely to fractionate Zn isotopes because we do not observe any relationship between chlorinity and $\delta^{66}Zn$.

We hypothesize that the subsurface precipitation of light Zn sulfides in lower-temperature vents is the main cause of isotopic variation in hydrothermal fluids. Sulfide precipitation in the laboratory was accompanied by an isotope effect of $\Delta^{66}Zn = -0.36‰$ (Archer et al., 2004). While the magnitude of this fractionation may vary under different hydrothermal conditions, we assume that sulfides are lighter than the fluid from which the precipitate under hydrothermal conditions as well. Temperature can have a large impact on sphalerite solubility in hydrothermal fluids. Sphalerite solubility in modeled hydrothermal fluids increases by as much as three orders of magnitude between 200°C and 350°C (Tivey et al., 1999). Cooling may therefore be an important factor in governing the extent of Zn sulfide precipitation.

Fe/Mn ratios and Cu and Zn concentration data are consistent with our hypothesis that Zn sulfide precipitation causes hydrothermal fluid $\delta^{66}Zn$ to rise. Fe is more rapidly precipitated when hydrothermal fluids cool whereas Mn is conservative during fluid cooling, so low Fe/Mn ratios are a good indicator of subsurface metal sulfide precipitation (Seewald and Seyfried, 1990). The heaviest $\delta^{66}Zn$ fluids also have low concentrations of Cu and Zn. This may be due to differences in metal leaching from the

source rock, or to the precipitation of sulfides. Cu and Zn sulfides precipitate from hydrothermal fluids under similar conditions.

Either conductive cooling or mixing with seawater could cause the fluid cooling that we observe. The low concentrations of Mg in fluid samples from K-vent and Bio9'' suggest that mixing with seawater was not a factor at these sites. In fluid samples from the MIT collection, Mg in the samples could come from either subsurface mixing of hydrothermal fluids with seawater or mixing during sampling.

3.3.5 The hydrothermal Zn isotope budget

Zn in hydrothermal vent fluids may impact on the δ^{66}Zn of seawater. The mid-ocean ridge hydrothermal Zn flux has been estimated to be 1300% of the natural riverine flux (Wheat et al., 2002). Much of the Zn in hydrothermal vent fluids precipitates quickly as metal sulfides in the region near the vent, but some may remain in hydrothermal plumes either as particles or dissolved Zn (German et al., 1991). Estimates of ocean cycling time through hydrothermal plumes are several thousand years (Elderfield and Schultz, 1996), on the order of the residence time of the deep ocean. Isotopic exchange between hydrothermal and deep-water Zn in hydrothermal plumes could affect seawater Zn isotopes. We estimate the riverine and atmospheric input of Zn to the ocean to have a δ^{66}Zn isotopic composition between 0.09 and 0.29‰. This range encompasses measurements of Zn isotopes in basalts, Niger dust (Maréchal et al., 2000), an average of four reference ores (Chapman et al., 2006), and measurements of common anthropogenic Zn products (S. John et. al., submitted). We see vent fluids as heavy as 1.29‰ in our

63
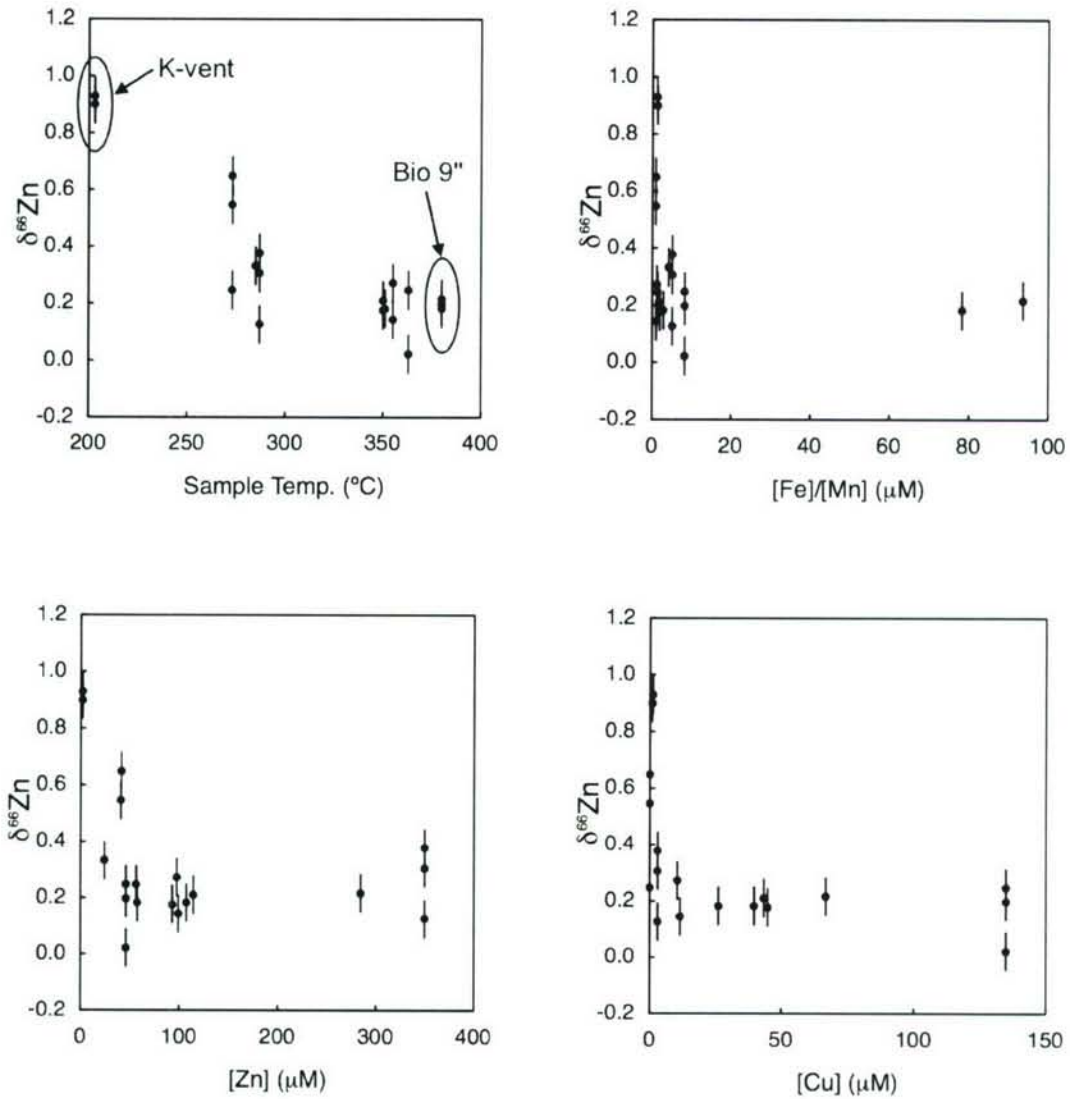
Figure 3.4. δ^{66}Zn as a function of fluid temperature and dissolved elemental concentrations. Temperature is the highest recorded for that vent during the research cruise, elemental concentrations were measured for each individual sample (Von Damm, 1984) and extrapolated to the hydrothermal endmember based on the assumption of zero Mg concentration in the hydrothermal fluids.

study. When hydrothermal fluids mix with seawater, even more light Zn may be lost into sulfide precipitates, so Zn in hydrothermal plumes could be even heavier. We have measured the isotopic composition of deep Pacific seawater to be $\delta^{66}Zn = +0.46‰$ (John et al., 2005), heavier than our estimated riverine and atmospheric input. Hydrothermal processes may be responsible for this difference.

3.4 Conclusions

We present the first data on Zn isotopes in modern hydrothermal systems and the first data on Zn isotopes in hydrothermal vent fluids. There is a strong negative correlation between the temperature of the vent fluids and their $\delta^{66}Zn$. We hypothesize that this results from the precipitation of isotopically light Zn sulfides from low-temperature fluids. Cu concentration data and Fe/Mn data in the fluids is consistent with this hypothesis. Zn isotopes may be a tool to help us understand the plumbing and chemistry of hydrothermal systems. Hydrothermal systems may also be an important factor in setting the $\delta^{66}Zn$ of the deep ocean.

References for chapter 3:

Albarède, F. and Beard, B., 2004. Analytical methods for non-traditional isotopes, Geochemistry of Non-Traditional Stable Isotopes, pp. 113-152.

Archer, C. and Vance, D., 2002. Large fractionations in Fe, Cu and Zn isotopes associated with Archean microbially-mediated sulphides. Geochimica et Cosmochimica Acta, 66(15A): A26-A26.

Archer, C. and Vance, D., 2004. Mass discrimination correction in multiple-collector plasma source mass spectrometry: an example using Cu and Zn isotopes. Journal of Analytical Atomic Spectrometry, 19: 656-665.

Archer, C., Vance, D. and Butler, I., 2004. Abiotic Zn isotope fractionations associated with ZnS precipitation. Geochimica et Cosmochimica Acta, 68(11): A325-A325.

Bermin, J., Vance, D., Archer, C. and Statham, P.J., 2006. The determination of the isotopic composition of Cu and Zn in seawater. Chemical Geology, 226(3-4): 280-297.

Campbell, A.C. et al., 1988. A Time-Series of Vent Fluid Compositions from 21-Degrees-N, East Pacific Rise (1979, 1981, 1985), and the Guaymas Basin, Gulf of California (1982, 1985). Journal of Geophysical Research-Solid Earth and Planets, 93(B5): 4537-4549.

Chapman, J.B., Mason, T.F.D., Weiss, D.J., Coles, B.J. and Wilkinson, J.J., 2006. Chemical separation and isotopic variations of Cu and Zn from five geological reference materials. Geostandards and Geoanalytical Research, 30(1): 5-16.

Dolgopolova, A. et al., 2006. Use of isotope ratios to assess sources of Pb and Zn dispersed in the environment during mining and ore processing within the Orlovka-Spokoinoe mining site (Russia). Applied Geochemistry, 21: 563-579.

Edmond, J.M. et al., 1991. Time series studies of vent fluids from the TAG and MARK sites (1986,1990) Mid-Atlantic Ridge: a new solution chemistry model and a mechanism for Cu/Zn zonation in massive sulphide ore bodies. In: L.M. Parson, C.L. Walker and D.R. Dixon (Editors), Hydrothermal Vents and Processes. Geological Society Special Publication, pp. 77-86.

Elderfield, H. and Schultz, A., 1996. Mid-ocean ridge hydrothermal fluxes and the chemical composition of the ocean. Annual Review of Earth and Planetary Sciences, 24: 191-224.

German, C.R., Campbell, A.C. and Edmond, J.M., 1991. Hydrothermal Scavenging at the Mid-Atlantic Ridge - Modification of Trace-Element Dissolved Fluxes. Earth and Planetary Science Letters, 107(1): 101-114.

Herzig, P.M., 1999. Economic potential of sea-floor massive sulphide deposits: ancient and modern. Philosophical Transactions of the Royal Society of London Series a-Mathematical Physical and Engineering Sciences, 357(1753): 861-873.

John, S.G., Bergquist, B.A., Saito, M.A. and Boyle, E.A., 2005. Zinc isotope variations in phytoplankton and seawater. Geochimica et Cosmochimica Acta, 69(10): A546-A546.

Kraus, K.A. and Moore, G., E., 1953. Anion exchange studies. VI. The dIvalent transition elements manganese to zinc in hydrochloric acid. Journal of the American Chemical Society, 75: 1457-60.

Maréchal, C.N., Nicolas, E., Douchet, C. and Albarède, F., 2000. Abundance of zinc isotopes as a marine biogeochemical tracer. Geochemistry Geophysics and Geosystems, 1: 1999GC000029.

Maréchal, C.N., Telouk, P. and Albarède, F., 1999. Precise analysis of copper and zinc isotopic compositions by plasma-source mass spectrometry. Chemical Geology, 156(1-4): 251-273.

Mason, T.F.D. et al., 2005. Zn and Cu isotopic variability in the Alexandrinka volcanic-hosted massive sulphide (VHMS) ore deposit, Urals, Russia. Chemical Geology, 221(3-4): 170-187.

McManus, J., Nagler, T.F., Siebert, C., Wheat, C.G. and Hammond, D.E., 2002. Oceanic molybdenum isotope fractionation: Diagenesis and hydrothermal ridge-flank alteration. Geochemistry Geophysics Geosystems, 3: Art. No. 1078.

Pichat, S., Douchet, C. and Albarède, F., 2003. Zinc isotope variations in deep-sea carbonates from the eastern equatorial Pacific over the last 175 ka. Earth and Planetary Science Letters, 210(1-2): 167-178.

Rouxel, O., Fouquet, Y. and Ludden, J.N., 2004a. Copper isotope systematics of the Lucky Strike, Rainbow, and Logatchev sea-floor hydrothermal fields on the Mid-Atlantic Ridge. Economic Geology and the Bulletin of the Society of Economic Geologists, 99(3): 585-600.

Rouxel, O., Fouquet, Y. and Ludden, J.N., 2004b. Subsurface processes at the Lucky Strike hydrothermal field, Mid-Atlantic Ridge: Evidence from sulfur, selenium, and iron isotopes. Geochimica et Cosmochimica Acta, 68(10): 2295-2311.

Rouxel, O., Ludden, J. and Fouquet, Y., 2003. Antimony isotope variations in natural systems and implications for their use as geochemical tracers. Chemical Geology, 200(1-2): 25-40.

Seewald, J.S. and Seyfried, W.E., 1990. The Effect of Temperature on Metal Mobility in Subseafloor Hydrothermal Systems - Constraints from Basalt Alteration Experiments. Earth and Planetary Science Letters, 101(2-4): 388-403.

Severmann, S. et al., 2004. The effect of plume processes on the Fe isotope composition of hydrothermally derived Fe in the deep ocean as inferred from the Rainbow vent site, Mid-Atlantic Ridge, 36 degrees 14' N. Earth and Planetary Science Letters, 225(1-2): 63-76.

Sharma, M., Polizzotto, M. and Anbar, A.D., 2001. Iron isotopes in hot springs along the Juan de Fuca Ridge. Earth and Planetary Science Letters, 194(1-2): 39-51.

Tivey, M.K., Stakes, D.S., Cook, T.L., Hannington, M.D. and Petersen, S., 1999. A model for growth of steep-sided vent structures on the Endeavour Segment of the Juan de Fuca Ridge: Results of a petrologic and geochemical study. Journal of Geophysical Research-Solid Earth, 104(B10): 22859-22883.

Von Damm, K.L., 1984. Chemistry of submarine hydrothermal solutions at 21° north, East Pacific Rise and Guaymas Basin, Gulf of California, Massachusetts Institute of Technology, Cambridge, Massachusetts, 240 pp.

Von Damm, K.L., 2000. Chemistry of hydrothermal vent fluids from 9 degrees-10 degrees N, East Pacific Rise: "Time zero," the immediate posteruptive period. Journal of Geophysical Research-Solid Earth, 105(B5): 11203-11222.

Von Damm, K.L., Edmond, J.M., Grant, B. and Measures, C.I., 1985. Chemistry of Submarine Hydrothermal Solutions at 21-Degrees-N, East Pacific Rise. Geochimica et Cosmochimica Acta, 49(11): 2197-2220.

Weiss, D.J. et al., 2005. Isotopic discrimination of zinc in higher plants. New Phytologist, 165(3): 703-710.

Wheat, C.G., Mottl, M.J. and Rudnicki, M., 2002. Trace element and REE composition of a low-temperature ridge-flank hydrothermal spring. Geochimica et Cosmochimica Acta, 66(21): 3693-3705.

Wilkinson, J.J., Weiss, D.J., Mason, T.F.D. and Coles, B.J., 2005. Zinc isotope variation in hydrothermal systems: Preliminary evidence from the Irish Midlands ore field. Economic Geology, 100(3): 583-590.

Zhu, X.K., O'Nions, R.K., Guo, Y., Belshaw, N.S. and Rickard, D., 2000. Determination of natural Cu-isotope variation by plasma-source mass spectrometry: implications for use as geochemical tracers. Chemical Geology, 163(1-4): 139-149.

Chapter 4

Zinc isotope fractionation associated with two separate uptake pathways in a marine diatom

When micronutrients such as zinc are transported across a cell membrane, some

isotopes may be taken up more quickly than others. This biological fractionation is

recorded as deviations in the ratio of $^{66}Zn/^{64}Zn$ in environmental samples such as

seawater (Bermin et al., 2006), marine sediments (Pichat et al., 2003), and marine life

(Maréchal et al., 2000). Measuring the magnitude of zinc isotope fractionation by marine

phtoplankton is crucial to interpreting these natural signals. Here we distinguish between

cellular Zn acquired through separate high-affinity and low-affinity Zn transport systems,

and calculate the isotopic fractionation associated with each pathway. We have calculated the biological isotope effect for high- and low-affinity transport to be $\Delta^{66}Zn = -0.2‰$ and $-0.8‰$, respectively, in the ecologically important marine diatom *Thalassiosira oceanica*. We have discovered these transport-related isotope effects by growing cultures at a range of Zn concentrations, and distinguishing between isotopically light intracellular Zn and the isotopically heavy Zn which adsorbs to the cell exterior. Consequently, this study is the first to describe a molecular basis for metal isotope fractionation during transport. A switch in the predominance of high-affinity and low-affinity transport occurs in many species of phytoplankton over an oceanographically relevant range of Zn concentrations (Sunda and Huntsman, 1992; Sunda and Huntsman, 1998), suggesting that the isotope fractionations seen here may be common in the ocean. By demonstrating that fractionation values can be tied to specific transporters, we show that natural variations in transition metal isotope ratios can be interpreted in terms of the underlying molecular biological processes from which they arise. By studying the transport-associated fractionation of other metals and in other organisms, transition metal isotopes have the potential to address many questions of oceanographic, environmental, and medical importance.

4.1 Introduction

Zinc is an essential biological nutrient in the oceans where the concentration distribution of Zn is controlled largely by phytoplankton Zn uptake and remineralization (Bruland and Lohan, 2003). Biological Zn isotope effects of up to 0.5‰ in $\delta^{66}Zn$ have been observed in land plants (Weiss et al., 2005) and phytoplankton (Gélabert et al., 2006) and are substantial compared to a total reported range for natural $\delta^{66}Zn$ values of about 1.5‰ (Wilkinson et al., 2005), where:

$$\delta^{66}Zn = \left(\frac{(^{66}Zn/^{64}Zn)_{sample}}{(^{66}Zn/^{64}Zn)_{standard}} - 1 \right) \cdot 1000. \tag{1}$$

The biological fractionation of Zn isotopes has been invoked to interpret natural Zn isotope signals in seawater (Bermin et al., 2006), seafloor sediments (Pichat et al., 2003), marine particles, and manganese nodules (Maréchal et al., 2000). By accurately measuring the magnitude of biological Zn isotope fractionation, changes in the isotopic composition of Zn in seawater or ancient sediments can be directly related to the extent of biological Zn uptake in surface waters. The stable isotopes of C and N have been used for many years to study environmental and biological processes; Zn isotopes may have a similar potential to help us understand present and ancient oceans.

4.1.1 The kinetics of high-affinity and low-affinity transport

We have grown the marine diatom *Thalassiosira oceanica* in EDTA-buffered
seawater media at free-Zn concentrations spanning the natural range of the marine
environment, from 10^{-12} M in the nutrient-poor central ocean gyres (Bruland, 1989) up to
10^{-8} M in anthropogenically impacted coastal waters such as Narragansett Bay (Kozelka
and Bruland, 1998). In order to distinguish between extracellularly adsorbed Zn and Zn
that has been transported to the cell interior, filtered cells from each culture were split
into two fractions and washed either with Zn-free seawater or with an EDTA-oxalate
wash that removes adsorbed metals (Tang and Morel, 2006; Tovar-Sanchez et al., 2003;
Tovar-Sanchez et al., 2004). By removing extracellular metals, we can isolate the
fractionation of Zn associated with transport across the cell membrane. The internalized
specific Zn uptake rate measured in our experiments shows a sigmoidal relationship to Zn
concentration, consistent with the shift between low-affinity and high affinity zinc
transporters that has been observed to occur in marine diatoms (Sunda and Huntsman,
1992) (Fig. 2). This sigmoidal uptake curve has been described by the cumulative uptake
of high and low affinity transporters governed by the equation:

$$V = \frac{V_{max}[Zn^{2+}]}{[Zn^{2+}]+K_M} + A[Zn^{2+}]. \tag{2}$$

The uptake rate (V) is the cumulative effect of two terms representing the high-affinity
and low-affinity uptake patways. High-affinity Zn uptake predominates at low $[Zn^{2+}]$ and

is governed by the first term, following classical Michaelis-Menten kinetics dependant on the maximal uptake rate (V_{max}) and the Michaelis-Menten constant (K_M). At high Zn concentrations, low-affinity transport dominates with an uptake rate related to $[Zn^{2+}]$ concentration by a constant (A). The decreasing contribution of high-affinity uptake at higher $[Zn^{2+}]$ can result either from saturation or down-regulation of the high-affinity transporters.

These high-affinity and low-affinity transport systems for Zn have been identified in many organisms, including fish (Glover et al., 2003; Qiu and Hogstrand, 2005), yeast (Zhao and Eide, 1996), and many phytoplankton (Sunda and Huntsman, 1992; Sunda and Huntsman, 1998). ZIP-family proteins, many of which are specific Zn transporters, have been found in bacteria, archaea, and many eukaryotes, and putative ZIP homologues have been identified in the genome of the diatom *T. pseudonana*. Several other eukaryotic phytoplankton have similar Zn transporter affinities and exhibit a similar switch between high-affinity and low-affinity transport systems, including three species of diatoms, the coccolithophore *E. huxleyii*, and the alga *Chlamydomonas* (Sunda and Huntsman, 1992; Sunda and Huntsman, 1998). Similar Zn transport kinetics suggests analogous Zn isotope fractionations by these different species.

4.2 Methods

4.2.1 Culture growth

The diatom *T. oceanica* (CCMP 1005) was maintained in acid-cleaned polycarbonate bottles at 20°C under 85 µEinsteins m^{-2} s^{-1} constant light. Media was prepared from
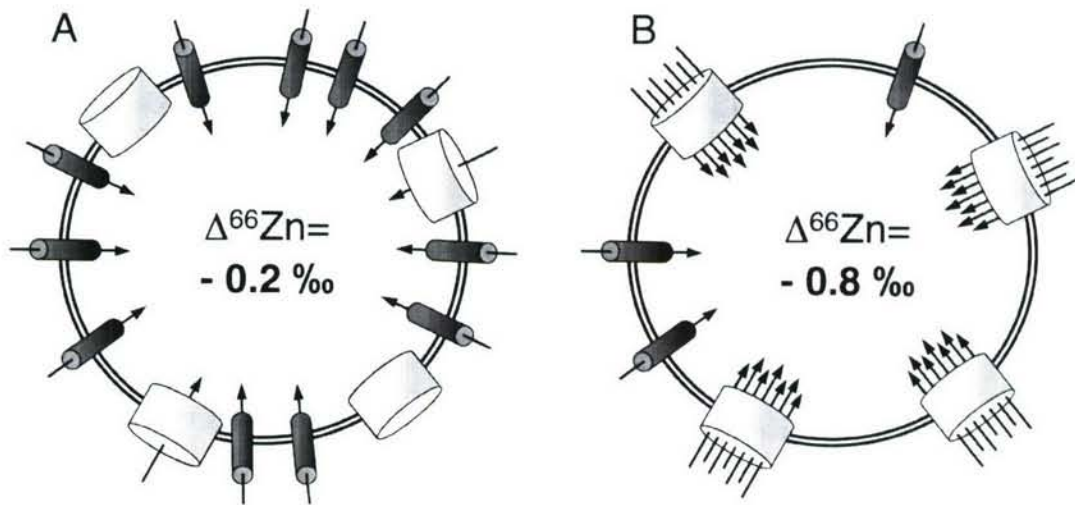
Figure 4.1. The biological isotope effect during Zn uptake is different for high-affinity and low-affinity transport. Suggested Zn transport by high-affinity (dark grey) and low-affinity (light grey) transporters under low-Zn (A) and high-Zn (B) conditions. When Zn concentrations are low (e.g. central oceans), high-affinity transporters are upregulated and account for most Zn transport with an isotope effect of $\Delta^{66}Zn = -0.2‰$. Under high-Zn concentrations, Zn uptake occurs primarily through a low-affinity transport pathway with an isotope effect of $\Delta^{66}Zn = -0.8‰$.

filtered Sargasso surface seawater collected with a towed trace-element clean Fish modified with a rigid rubber tube in place of the PVC pipe used for support (Vink et al., 2000) amended with major and trace element nutrients and vitamins (Sunda and Huntsman, 1995) with 10 μM Fe, 25 nM Co, and varying amounts of Zn. Added Zn was a laboratory standard prepared with Zn from the Canadian Electrolytic Zinc (CEZ) corporation. This Zn has a similar isotopic composition to natural Zn (S. John, submitted

to Chemical Geology) so small amounts of Zn contamination would not have a large effect on $\delta^{66}Zn$. Seawater was microwave sterilized and all nutrients, vitamins, and trace-elements were sterilized by syringe filtration with an acid-cleaned rubber/silicone-free syringe (NormJect, HSW) through an acid-cleaned 0.4 μm polycarbonate filter (Nuclepore) and added to the seawater after it had cooled. 0.1% inoculums by volume for experiments were taken from cultures in log-phase growth that were maintained in media with a Zn concentrations within one log unit of experimental conditions. Growth in 1L polycarbonate bottles at maintenance conditions was monitored by measuring in-vivo Chl*a* fluorescence with a Synergy HT Microplate reader (BioTek). Specific Zn uptake rate was calculated by multiplying the log-phase growth rate by the Zn:P ratio of the final cultures.

4.2.2 Processing cultures for isotopic analysis

Cultures were harvested near the end of log-phase growth and filtered onto a 1 μm polycarbonate filter (Whatman Nuclepore). Each culture was split into two equal parts, one of which was rinsed once with metal-free seawater and the other was rinsed with an oxalate-EDTA reagent to remove adsorbed extracellular metals (Tovar-Sanchez et al., 2003; Tovar-Sanchez et al., 2004) modified to pH=7 for two 5-minute rinses to ensure complete removal of extracellular ferric oxides (Tang and Morel, 2006). Cells and filters were transferred to ~5 mL quartz beakers and organics were partially oxidized be reacting for several hours with 2 mL warm HNO_3 and 200 μL H_2O_2. When the liquid had evaporated the remaining organics were oxidized by combusting samples for 8 hours at

450°C. Combusted material was dissolved in warm 6N HCl for column purification of Fe and Zn, small subsamples were diluted for measurement of Zn:P ratios.

Zn concentrations were measured by isotope dilution ICP-MS with a ^{68}Zn spike. P concentrations were performed colorimetrically according to standard procedures for measurements of P in natural seawater (Strickland and Parsons, 1972). Zn and Fe were purified by anion exchange chromatography (Maréchal et al., 1999) using small column volumes to reduce metal contamination from acids (Archer and Vance, 2004) and the Zn fraction was eluted with 0.1% HCl to avoid co-elution of other elements (Chapman et al., 2006). Samples were evaporated, then reacted overnight in 5 mL PFA capsules (Savillex) at high temperature with 200 µL HF and 100 µL H_2O_2 to drive off silicates remaining from the diatom frustules and organics that may have leached off the column. Samples were evaporated to dryness, evaporated again with 100 µL 16N HNO_3 to drive off remaining F⁻, and dissolved in 2% HNO_3 for isotopic analysis.

4.2.3 Isotope analysis

Samples were analyzed for Zn isotopes on an IsoProbe multi-collector ICP-MS (GV Instruments, formerly MicroMass) equipped with an Apex Q inlet system without the optional desolvator. Samples were prepared with 50 ppb Cu and either 25, 50, or 100 ppb Zn. Signal was monitored on masses 60, 63, 64, 65, 66, 67, and 68. Corrections for instrumental mass bias were made by monitoring the $^{65}Cu/^{63}Cu$ ratio of the Cu spike in samples and using interspersed standards to establishing a linear mass bias relationship between the natural log $^{65}Cu/^{63}Cu$ and the natural log of $^{66}Zn/^{64}Zn$ (Maréchal et al.,

1999). $^{64}Ni^+$ was subtracted from $^{64}Zn^+$ by monitoring $^{60}Ni^+$ and applying the Cu mass bias correction, although these corrections were insignificant. $\delta^{68}Zn$ values showed twice the fractionation compared to $\delta^{66}Zn$ values and indicate the absence of polyatomic interferences. Extensive error analysis based on hundreds of samples was performed in conjunction with a study of Zn isotopes in hydrothermal systems (S. John, in preparation). External reproducibility is 0.07‰ (2σ s.d.) independent of the Zn concentration in the analysis.

4.3 Results and discussion

4.3.1 Zn uptake kinetics

We have modeled our specific Zn uptake rate data as the sum of high-affinity and low-affinity uptake, assuming that nearly all of the uptake at $10^{-8.5}$ M Zn^{2+} occurs through low-affinity transport (Fig. 2). According to Eqn. 2, Zn uptake through the low-affinity transport system decreases linearly with Zn concentration. Any uptake in excess of the predicted low-affinity Zn uptake is assumed to have occurred through the high-affinity Zn transport pathway. Accordingly, nearly 100% of Zn uptake occurs though the low-affinity transport system at 10^{-9} M Zn^{2+} and above, there is a transition between the predominance of these two uptake pathways between $10^{-10.5}$ and $10^{-9.5}$ M Zn^{2+}, and low-affinity transport accounts for less than 10% of total Zn uptake when the concentration of Zn^{2+} is 10^{-11} M and below (Fig. 3).

4.3.2 Biological Zn isotope fractionation

The Zn isotope ratio in our diatoms is correlated to the switch in Zn transport systems (Fig 3). The values of $\Delta^{66}Zn$ ($\delta^{66}Zn_{diatoms}$ - $\delta^{66}Zn_{media}$) changes rapidly over the same range of Zn concentrations where the Zn uptake switches from predominantly high-affinity uptake to predominantly low-affinity uptake when Zn^{2+} is between $10^{-10.5}$ M and $10^{-9.5}$ M. $\Delta^{66}Zn$ is around -0.2‰ at the lowest Zn concentrations and around -0.8‰ at the highest Zn concentrations, with intermediate values when there is significant uptake through both the high-affinity and low-affinity transport systems. We have averaged values of $\Delta^{66}Zn$ at the three lowest Zn concentrations and the two highest Zn concentrations resulting in the first estimates of the isotopic fractionation factors for Zn transport, with $\Delta^{66}Zn$ = -0.2‰ for high-affinity transport and $\Delta^{66}Zn$ = -0.8‰ for low affinity transport.

We hypothesize that the fractionation observed during high-affinity transport probably does not occur at the transporter itself, but occurs because the $\delta^{66}Zn$ of free-Zn arriving at the transporter is lighter than Zn in the bulk media. At equilibrium, free-Zn is -0.16‰ lighter than EDTA-bound Zn in aqueous solution (Ban et al., 2002). An additional isotope effect will be conferred by the difference in diffusivity between the different Zn isotopes. $^{64}Zn^{2+}$ will diffuse towards the cell more quickly than $^{66}Zn^{2+}$, and the difference in aqueous diffusivity of free Zn is equivalent to a preference for light Zn uptake by $\Delta^{66}Zn$ = -0.06‰ (Rodushkin et al., 2004). Together, the free Zn/Zn-EDTA equilibrium isotope effect and the difference in isotope diffusivity can account for the entire -0.2‰ fractionation observed under high-affinity transport. Zn concentrations in
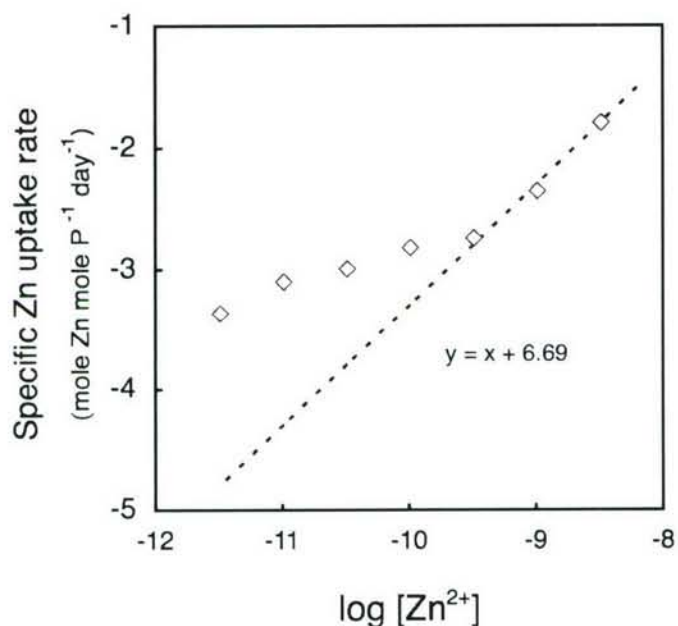
Figure 4.2. Zn uptake rates show a concentration-dependant switch in the predominance of high-affinity and low-affinity Zn transport. Specific Zn uptake rates measured for washed ($\diamond$) *T. oceanica* cells at different concentrations of Zn^{2+}, and the predicted specific Zn uptake rate by the low-affinity transport system alone (- - -).

[Zn]$_{total}$	[Zn^{2+}]	Unwashed cells		Washed cells	
		δ^{66}Zn (‰)	s.d. (2σ)	δ^{66}Zn (‰)	s.d. (2σ)
4.5	8.5	0.38	0.02	-0.79	0.03
5	9	0.29	0.08	-0.80	0.01
5.5	9.5	0.19	0.06	-0.68	0.02
6	10	0.22	0.03	-0.41	0.09
6.5	10.5	0.15	0.06	-0.16	0.10
7	11	0.03	0.12	-0.19	0.02
7.5	11.5	-0.05	0.08	-0.29	0.05

Table 4.1. δ^{66}Zn of washed and unwashed diatoms grown at a range of Zn concentrations.

the open ocean are nearly low enough to limit phytoplankton growth (Ellwood and Van den Berg, 2000; Lohan et al., 2002), so it stands to reason that high-affinity transporters efficiently acquire all Zn diffusing to the transporters regardless of isotope. By contrast, the isotope effect associated with the low-affinity uptake pathway is much larger. This isotope effect could result from preferential retention of the heavier Zn isotopes to low-affinity transport binding site, or a more rapid translocation of light Zn isotopes across the cell membrane such as would result from faster diffusion through an ion channel.

When cells are not washed to remove extracellular metals, external Zn can have a major impact on the total cellular Δ^{66}Zn. In this experiment, the Δ^{66}Zn of unwashed cells ranged from -0.05‰ at the lowest Zn concentration to +0.38‰ at the highest Zn concentration. The contribution of internal Zn isotopes can be subtracted to calculate values of Δ^{66}Zn for the external Zn pool alone. We have found that external Δ^{66}Zn increases almost linearly from +0.09‰ at $10^{-11.5}$ Zn^{2+} to +0.52‰ at $10^{-8.5}$M Zn^{2+}. These results are consistent with other studies showing that heavy Zn isotopes are preferentially adsorbed or precipitated onto diatom exteriors (Gélabert et al., 2006). In previous experiments (unpublished data) we have found the amount of externally bound Zn and the consequent values of cell total Δ^{66}Zn are be highly variable between different experiments. Cell-surface precipitation may be a major contribution to total Zn when cells are grown in EDTA-buffered seawater media because of high concentrations of total Zn and high rates of Fe-oxide precipitation (Tang and Morel, 2006). In fact, simply reducing the concentration of free Fe in the media can reduce the levels of extracellular Zn to a fraction of the intracellular concentration (Tang and Morel, 2006). Laboratory
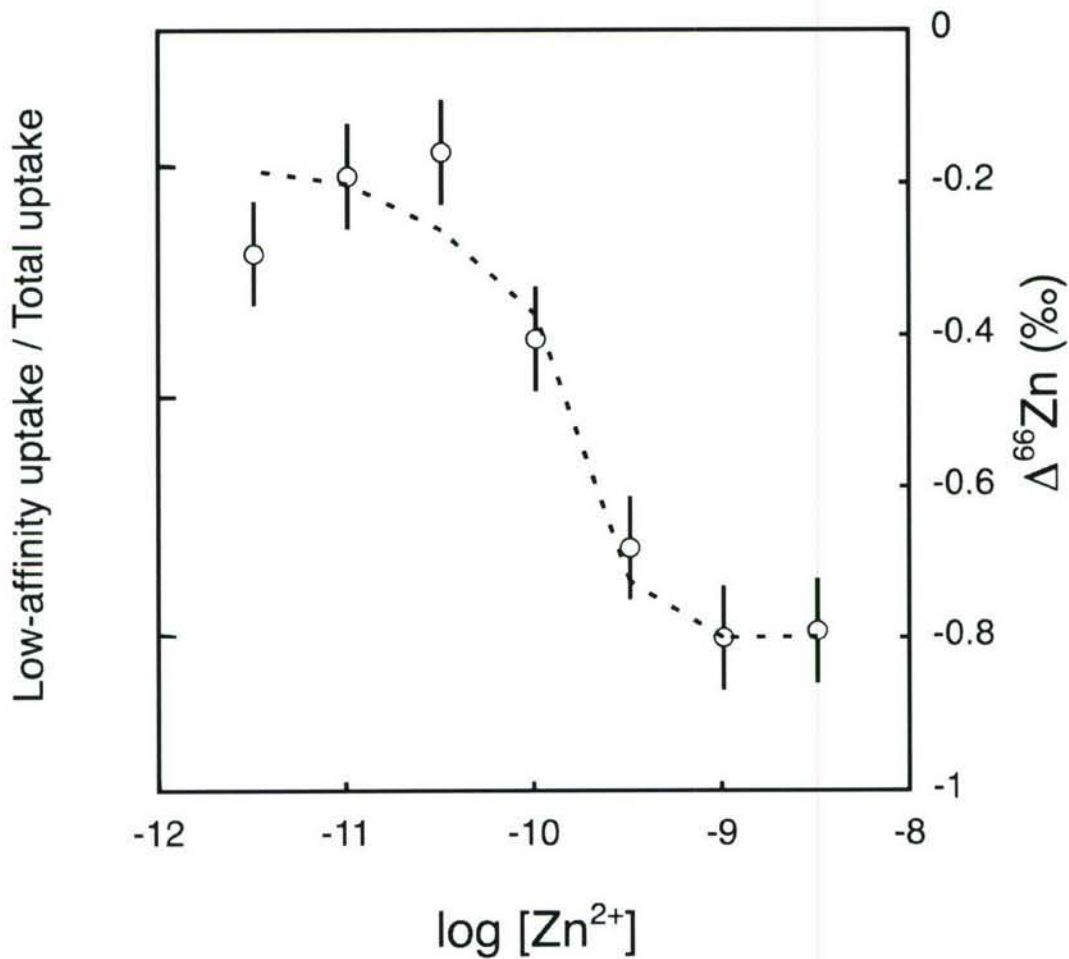
Figure 4.3. The transition between high-affinity and low-affinity transport is conincident with a change in the biological isotope effect. Predicted specific Zn uptake through the low-affinity transport system as a percentage of the total specific Zn uptake rate (- - -) and the offset between δ^{66}Zn of *T. oceanica* cells and the δ^{66}Zn of the seawater media they were grown in (Δ^{66}Zn) at different concentrations of free Zn^{2+} (O). The shift in Δ^{66}Zn occurs within a similar range of Zn concentrations to the shift between the predominance of high-affinity and low-affinity uptake indicating that each transport pathway has a unique isotope effect. Error bars represent external reproducibility (2σ s.d.).
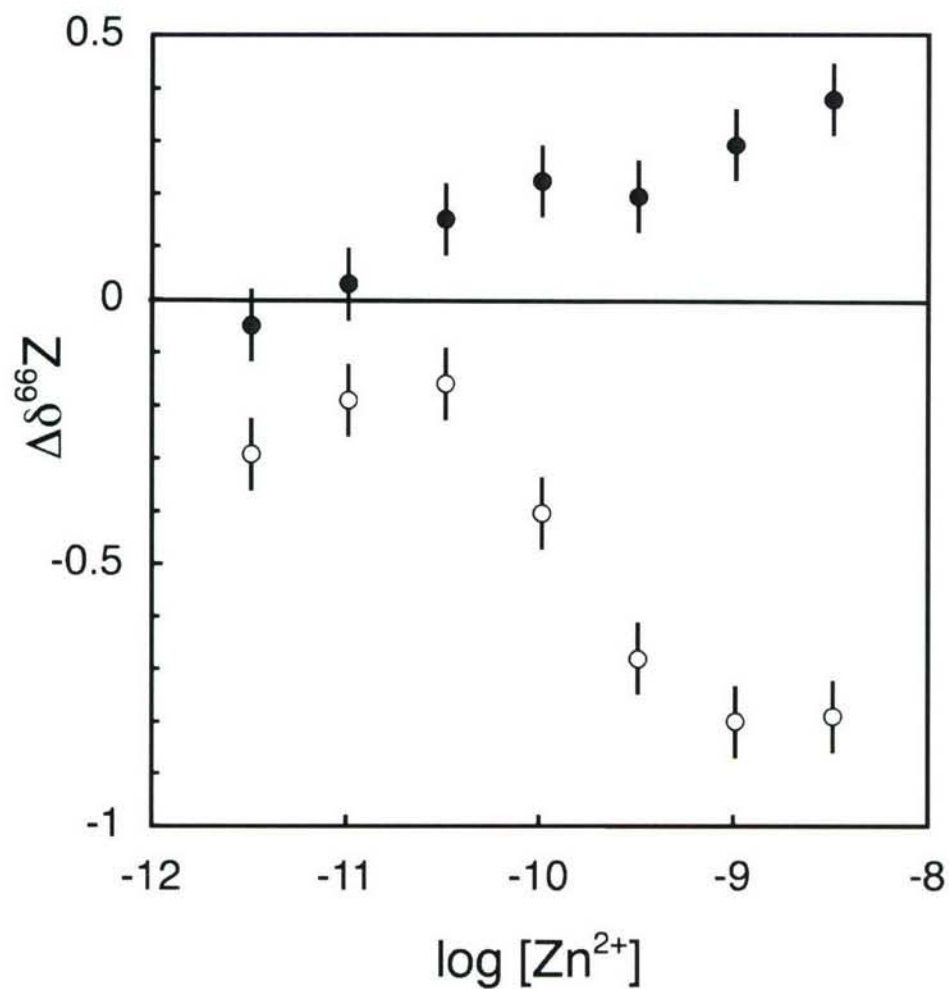
Figure 4.4. Unwashed cells are isotopically heavier than washed cells. A comparison cells washed to remove extracellular precipitates (O) with unwashed cells (●) shows that extracellular precipitates are isotopically heavy and can greatly influence the total cell isotope ratio if not removed.

studies are potentially fraught with errors associated with extracellular precipitation, a phenomenon that is not likely to be important in all but the most polluted or concentrated marine environments.

4.4 Conclusions

Our experiments distinguish between several distinct processes that may contribute to the total observed signal for "biological fractionation" in the oceans. Cell-surface precipitation may not always be a significant contribution to cellular Zn, but when precipitation does occur we expect a preference for heavy Zn to adsorb onto the cell surfaces. An isotopic fractionation between free Zn and Zn bound to organic ligands, as we have observed with Zn binding to EDTA, may also be important in the oceans where most of the dissolved Zn is organically complexed (Bruland, 1989; Ellwood and Van den Berg, 2000). Finally, we expect the isotopic composition of phytoplankton's internal Zn pool to be set by the isotope effects of high-affinity and/or low-affinity uptake depending on the ambient concentrations of free Zn.

As more data becomes available on Zn isotopes in the oceans, understanding how phytoplankton fractionate Zn isotopes will be crucial to interpreting natural signals. Dissolved δ^{66}Zn variations of 0.2‰ have been measured between surface and deeper NE Pacific seawaters (Bermin et al., 2006), attributed to a biological drawdown of Zn. With a knowledge of the molecular mechanisms responsible for isotopic fractionation, Zn isotopes may eventually be used to trace nutrient supply, dust deposition, Zn/N utilization, metal speciation, and other important biogeochemical processes in the oceans.

References for chapter 4:

Archer, C. and Vance, D., 2004. Mass discrimination correction in multiple-collector plasma source mass spectrometry: an example using Cu and Zn isotopes. Journal of Analytical Atomic Spectrometry, 19: 656-665.

Ban, Y., Aida, M., Nomura, M. and Fujii, Y., 2002. Zinc isotope separation by ligand exchange chromatography using cation exchange resin. Journal of Ion Exchange, 13(2): 8-14.

Bermin, J., Vance, D., Archer, C. and Statham, P.J., 2006. The determination of the isotopic composition of Cu and Zn in seawater. Chemical Geology, 226(3-4): 280-297.

Bruland, K.W., 1989. Complexation of Zinc by Natural Organic-Ligands in the Central North Pacific. Limnology and Oceanography, 34(2): 269-285.

Bruland, K.W. and Lohan, M.C., 2003. Controls of Trace Metals in Seawater. Treatise on Geochemistry, 6. Elsevier, 7800 pp.

Chapman, J.B., Mason, T.F.D., Weiss, D.J., Coles, B.J. and Wilkinson, J.J., 2006. Chemical separation and isotopic variations of Cu and Zn from five geological reference materials. Geostandards and Geoanalytical Research, 30(1): 5-16.

Ellwood, M.J. and Van den Berg, C.M.G., 2000. Zinc speciation in the Northeast Atlantic Ocean. Marine Chemistry, 68(4): 295-306.

Gélabert, A. et al., 2006. Interaction between zinc and freshwater and marine diatom species: Surface complexation and Zn isotope fractionation. Geochimica et Cosmochimica Acta, 70(4): 839-857.

Glover, C.N., Bury, N.R. and Hogstrand, C., 2003. Zinc uptake across the apical membrane of freshwater rainbow trout intestine is mediated by high affinity, low affinity, and histidine-facilitated pathways. Biochimica et Biophysica Acta-Biomembranes, 1614(2): 211-219.

Kozelka, P.B. and Bruland, K.W., 1998. Chemical speciation of dissolved Cu, Zn, Cd, Pb in Narragansett Bay, Rhode Island. Marine Chemistry, 60(3-4): 267-282.

Lohan, M.C., Statham, P.J. and Crawford, D.W., 2002. Total dissolved zinc in the upper water column of the subarctic North East Pacific. Deep-Sea Research Part II-Topical Studies in Oceanography, 49(24-25): 5793-5808.

Maréchal, C.N., Nicolas, E., Douchet, C. and Albarède, F., 2000. Abundance of zinc isotopes as a marine biogeochemical tracer. Geochemistry Geophysics and Geosystems, 1: 1999GC000029.

Maréchal, C.N., Telouk, P. and Albarède, F., 1999. Precise analysis of copper and zinc isotopic compositions by plasma-source mass spectrometry. Chemical Geology, 156(1-4): 251-273.

Pichat, S., Douchet, C. and Albarède, F., 2003. Zinc isotope variations in deep-sea carbonates from the eastern equatorial Pacific over the last 175 ka. Earth and Planetary Science Letters, 210(1-2): 167-178.

Qiu, A.D. and Hogstrand, C., 2005. Functional expression of a low-affinity zinc uptake transporter (FrZIP2) from pufferfish (Takifugu rubripes) in MDCK cells. Biochemical Journal, 390: 777-786.

Rodushkin, I., Stenberg, A., Andren, H., Malinovsky, D. and Baxter, D.C., 2004. Isotopic Fractionation during diffusion of transition metal ions in solution. Analytical Chemistry, 76(7): 2148-2151.

Strickland, J.D.H. and Parsons, T.R., 1972. A practical handbook of seawater analysis. Fisheries Research Board of Canada, Ottowa.

Sunda, W.G. and Huntsman, S.A., 1992. Feedback Interactions between Zinc and Phytoplankton in Seawater. Limnology and Oceanography, 37(1): 25-40.

Sunda, W.G. and Huntsman, S.A., 1995. Cobalt and zinc interreplacement in marine phytoplankton: Biological and geochemical implications. Limnology and Oceanography, 40(8): 1404-1417.

Sunda, W.G. and Huntsman, S.A., 1998. Interactions among Cu2+, Zn2+, and Mn2+ in controlling cellular Mn, Zn, and growth rate in the coastal alga Chlamydomonas. Limnology and Oceanography, 43(6): 1055-1064.

Tang, D.G. and Morel, F.M.M., 2006. Distinguishing between cellular and Fe-oxide-associated trace elements in phytoplankton. Marine Chemistry, 98(1): 18-30.

Tovar-Sanchez, A. et al., 2003. A trace metal clean reagent to remove surface-bound iron from marine phytoplankton. Marine Chemistry, 82(1-2): 91-99.

Tovar-Sanchez, A. et al., 2004. Corrigendum to "A trace metal clean reagent to remove surface-bound iron from marine phytoplankton (vol 82, pg 91, 2003)". Marine Chemistry, 85(3-4): 191-191.

Vink, S., Boyle, E.A., Measures, C.I. and Yuan, J., 2000. Automated high resolution determination of the trace elements iron and aluminium in the surface ocean using a towed Fish coupled to flow injection analysis. Deep-Sea Research Part I-Oceanographic Research Papers, 47(6): 1141-1156.

Weiss, D.J. et al., 2005. Isotopic discrimination of zinc in higher plants. New Phytologist, 165(3): 703-710.

Wilkinson, J.J., Weiss, D.J., Mason, T.F.D. and Coles, B.J., 2005. Zinc isotope variation in hydrothermal systems: Preliminary evidence from the Irish Midlands ore field. Economic Geology, 100(3): 583-590.

Zhao, H. and Eide, D., 1996. The yeast ZRT1 gene encodes the zinc transporter protein of a high-affinity uptake system induced by zinc limitation. Proceedings of the National Academy of Sciences of the United States of America, 93(6): 2454-2458.

Chapter 5

Zinc isotopes in seawater and natural marine plankton

The zinc distribution in the oceans is largely controlled by biological uptake and remineralization. Phytoplankton in culture fractionate Zn isotopes, so measurements of Zn isotope ratios may be a valuable tool for tracing biological processes in the oceans. Here, I report data on Zn isotopes in seawater and natural phytoplankton samples in order to better understand the marine distribution of Zn isotopes and to better understand how natural biological processes fractionate Zn isotopes. A new isotope dilution method for the measurement of Zn isotope concentrations in seawater has been developed that is compatible with high-precision isotope ratio measurements. Methods have also been developed for the separation and purification of Zn from large volumes of seawater for isotopic analysis. Zn isotope ratios were measured in samples from five depths in the

north Pacific, and in deep waters from the north Atlantic (0.4 – 0.5 ‰). There appears to be a trend towards lighter values of $\delta^{66}Zn$ in surface waters that correlates well with Zn concentrations. Based on this isotopic evidence, we suggest that much of the Zn transported to the deep ocean is not isotopically light "primary" biological Zn, but instead results from the adsorption of isotopically heavy Zn^{2+} onto falling biological material. Phytoplankton samples from the Peru Upwelling Region, as well as several other locations across the globe, show that most natural phytoplankton have $\delta^{66}Zn$ between 0‰ and +0.6‰. There is no significant change in the $\delta^{66}Zn$ of natural plankton over large changes in nutrient concentrations in the Peru Upwelling Region. This suggests either that the isotope effect for Zn uptake in this region is very small, or that nutrient supply is predominantly vertical, rather than horizontal.

5.1 Introduction

5.1.1 Zinc concentration distribution in the oceans

Zn has a "nutrient-like" vertical concentration profile in the oceans (Fig. 1). The shape of this profile is similar to Si, with a deeper regeneration maximum than N and P. As with other nutrients, the concentration of Zn increases from the Atlantic to the Southern Ocean to the Pacific. The Zn maximum increases from around 2 nM in the North Atlantic to 6 nM in the Southern Ocean to 9 nM in the North Pacific (Bruland et al., 1978; Coale et al., 2005; Ellwood and Van den Berg, 2000; Fitzwater et al., 2000). In the surface ocean, concentrations of Zn can be depleted by several orders of magnitude with reported concentrations as low as 0.04 nM (Lohan et al., 2002) in the surface North
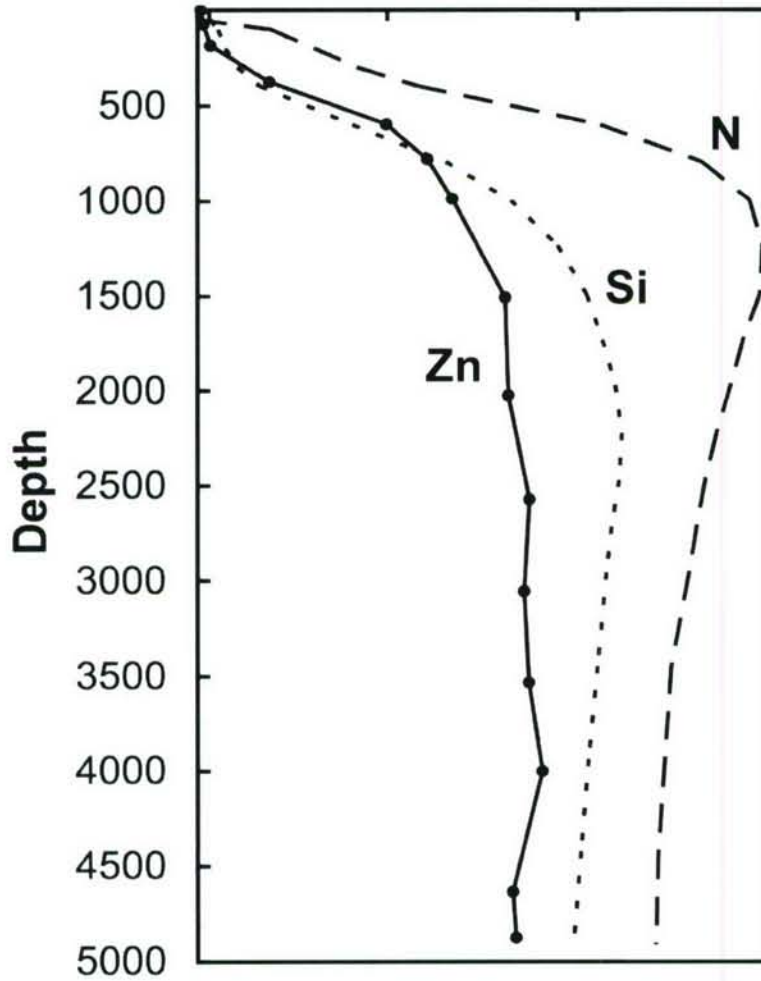
Figure 5.1. The vertical concentration profiles of Zn (——), Si (- - -), and N (– –) in the North Pacific Ocean. Zn data from (Bruland, 1980), N and Si data from GEOSECS (GEOSECS Operations Group, 1987).

Pacific and 0.06 nM in the surface North Atlantic (Bruland and Franks, 1983). Throughout much of the oceans, Zn is mostly present complexed to organic ligands rather than as inorganic "free-Zn" (Bruland and Lohan, 2003).

5.1.2 Zinc isotope analysis in seawater

Zinc isotopes have been measured in seawater by several different methods. Zn has been extracted from seawater by adsorption onto Chelex-100 (Bermin et al., 2004a; Bermin et al., 2004b) and co-precipitation with $Mg(OH)_2$ (Bermin et al., 2006; John et al., 2005). The possible effects of isotope fractionation during Zn extraction can be compensated for by quantitative recovery of the Zn, or by adding a Zn double spike to the sample before concentration. Instrumental mass bias has been evaluated by either a Zn double spike or an internal Cu spike. Different methods of isotope analysis have different strengths. A Zn double-spike method does not require that Zn recovery be quantitative and allows for the mass bias correction to be done using Zn, rather than Cu which may have a slightly different instrumental mass bias. By avoiding a double spike, it is possible to compare $^{66}Zn/^{64}Zn$ values with $^{68}Zn/^{64}Zn$ in order to evaluate the presense of isobaric interferences.

Using Chelex extraction, the $\delta^{66}Zn$ of English Channel water was measured to be +0.46‰ using a Cu-correction and +0.38‰ using a double-spike approach (Bermin et al., 2004a). $Mg(OH)_2$ co-precipitation and a Cu correction was used to measure a $\delta^{66}Zn = $ +0.46‰ for deep North Pacific waters (John et al., 2005). A profile of Zn isotopes from the North Pacific using a Zn double-spike method includes lighter $\delta^{66}Zn$ values ranging

92

from -0.1‰ to +0.2‰. This study expands the range of seawater samples in which Zn

isotopes have been measured and, by employing a different analytical methodology,

provides an important check on previous measurements.

5.1.3 Zinc isotopes in marine plankton

Zinc isotopes have previously been measured in biological material such as plants

(Weiss et al., 2005), tissue from several marine species (Maréchal et al., 2000), and

cultured phytoplankton (Gélabert et al., 2006). The isotope effect of extracellular Zn

precipitation and biological transport has been determined for diatoms grown in culture

(Chapter 4). Diatoms preferentially acquired light Zn isotopes from the surrounding

media, and the magnitude of this fractionation depended on the cellular machinery used

to transport the Zn. The isotope effect for transport though a high-affinity pathway was

measured to be $\Delta^{66}Zn = -0.2‰$ and for low-affinity uptake $\Delta^{66}Zn = -0.8‰$. At the low Zn

concentrations that predominate in the open oceans, high-affinity transport will dominate

total Zn uptake. In coastal regions where Zn concentrations are much higher, low-affinity

transport may contribute. The Zn isotope ratio for natural phytoplankton will be equal to

the $\delta^{66}Zn$ of the surrounding seawater plus the biological isotope effect. By measuring Zn

isotopes in natural phytoplankton and seawater, we can better understand how Zn

isotopes may be used as a tracer for biological processes in the modern and ancient

oceans.

5.2 Methods

5.2.1 Trace-element clean laboratory practices

Class-100 clean airflow conditions were maintained during manipulation of all samples subsequent to collection. Water was distilled in a borosilicate glass still (Corning MegaPure) to remove metal contaminates, and all acids were triply or quadrupally distilled in Vycor® glass to remove contaminants.

5.2.2 Sample collection

Seawater samples from the North Pacific (47°N, 170.5°W) were collected aboard the R/V Kilo Moana in 2003. Samples from the North Atlantic (16.5°N, 59°W) were collected aboard the R/V Endeavor in 2005, and samples from the Peru Upwelling Region were collected aboard the R/V Knorr in 2006.

Seawater samples from the North Pacific were collected using Teflon-coated GO-FLO samplers (General Oceanics) attached to a Kevlar wire for all samples at 1000 m and above. GO-FLO samplers were attached to a stainless steel CTD cable to collect waters below 1000 m. Seawater samples from the North Atlantic were collected using individual MITESS samplers modified to hold 1L bottles and attached to a hydrowire with a VANE to keep the sampler upstream of the wire (Bell et al., 2002; Bergquist, 2004). Seawater samples from the Peru Upwelling Region were collected using either a MITESS/VANE sampler or Teflon-coated Niskin bottles attached to a plastic-covered frame and suspended from a Kevlar hydrowire. All seawater samples were filtered through a 0.2 μm or 0.4 μm polycarbonate filter and acidified to pH 2 immediately after collection with HCl.

Plankton tows were collected using a 50 μm mesh nylon net with no metal fittings attached to a Kevlar hydrowire with plastic rope (Sea Gear Corp.). Tows were conducted in the upper mixed layer above the chlorophyll maximum. Tows ranged in time from five minutes to thirty minutes depending on the productivity of the region. Concentrated plankton from the cod end was mixed vigorously and split into to two equal portions before filtration. Plankton were filtered onto 1 μm polycarbonate filters and washed either with clean surface seawater or a plankton wash designed to remove extracellular metals (Tang and Morel, 2006; Tovar-Sanchez et al., 2003; Tovar-Sanchez et al., 2004) followed by a seawater rinse. Filtered phytoplankton were frozen for storage. When euphausiidae (krill) were found in filtered plankton tows, they were picked out with Teflon tweezers and washed to remove extracellular metals in the same manner described for bulk plankton.

5.2.3 Zn concentration in seawater measurements

Zn concentration in seawater was determined by isotope dilution ICP-MS after coprecipitation with $Mg(OH)_2$ (Wu and Boyle, 1998) and purification by anion exchange chromatography. A known weight of each sample (approximately 15 mL) in a polypropylene centrifuge tube was spiked with an approximately equimolar amount of ^{68}Zn. After several hours of isotopic equilibration, samples were precipitated with 300 μL of Optima trace-element free ammonium hydroxide (Fisher Scientific). The precipitate was concentrated by centrifugation and fluid was poured off. The remaining precipitate was dissolved in 1 mL of 2N HCl, the Cl⁻ concentration at which Zn has the highest
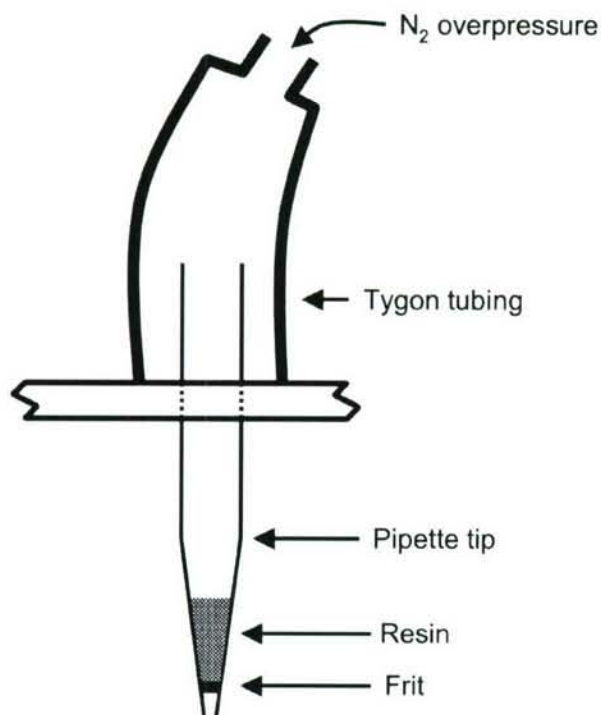
Figure 5.2. Micro-column design for purification of Zn from Mg(OH)2 precipitates, for measurement of Zn concentration in seawater by isotope dilution.
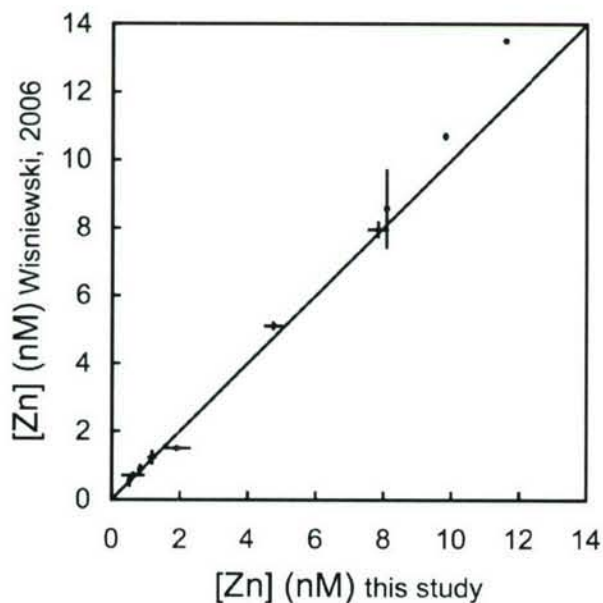
Figure 5.3. Comparison of the measured Zn concentration for this study and by R. Wisniewski (Wisniewski, 2006) for a vertical profile of samples from the North Pacific. Error bars represent the 2σ s.d. for triplicate analysis.

affinity for anion exchange resins (Kraus and Moore, 1953). Samples were purified to remove Mg and other elements in the precipitate using similar anion exchange chromatography to that used in the preparation of samples for Zn isotope analysis (Maréchal et al., 1999). 75 μL of AG MP-1 resin (Bio-Rad) was loaded into a column made by inserting a small frit into a large pipette tip. The column exterior was wrapped in Teflon tape and the column was inserted tightly into an acrylic stand so that filtered N_2 overpressure could be applied to quickly (~5 mL/min) push sample and eluent through the column (Fig. 1). Samples were loaded in 2N HCl, rinsed twice with 0.5 mL 2N HCl, and eluted with 250 μL 0.06N HCl. The column was rinsed twice in between each sample with 1-2 mL 0.06N HCl. Samples were analyzed on an IsoProbe multi-collector ICP-MS using an APEX Q inlet system (ESI) with a 75 μL min^{-1} MicroMist nebulizer (Glass Expansion) (Elemental Scientific, Inc.). Signals were monitored on masses 64 and 68 (^{64}Zn and ^{68}Zn) to calculate the concentration of Zn in the original seawater sample by isotope dilution.

Blanks were interspersed with all samples. Blanks were prepared and purified in the same manner as samples, except using was 1 mL of Sargasso Sea surface water containing 0.33 nM Zn.

5.2.4 Separation of Zn from seawater for isotopic analysis

The isotope effect of $Mg(OH)_2$ co-precipitation and the efficiency of Zn recovery by this method was tested by adding small amounts of ammonia to precipitate Zn slowly (Table 1.). Sargasso Sea surface water (1 L) was acidified to pH 2, spiked with 20 μg Zn

(20 ppb) and allowed to equilibrate overnight. Several times, the entire sample was precipitated with several mL of ammonia, the precipitate was separated by filtration. The filtrate was recovered and more precipitate was allowed to form by waiting a few minutes, or by adding additional ammonia. The precipitate from each step was dissolved separately for Zn isotope and concentration analysis.

A similar precipitation method was used for standards and natural samples. Zn was separated from seawater for isotopic analysis by coprecipitation with $Mg(OH)_2$ and filtered to remove the precipitate. Precipitate formed after the addition of 15 mL Optima ammonium hydroxide to 1 L of seawater. The precipitate was allowed to settle for 1-3 hours and the fluid was filtered through a 0.4 µm Nuclepore polycarbonate filter membrane (Whatman) in a PFA filter holder (Savillex). Approximately 30 mL of 2N HCl was used to rinse the sample bottle, dissolve the precipitate, and rinse the filter holder. The filtrate was reprecipitated with 5 mL Optima ammonium hydroxide and immediately filtered again. Another 30 mL of 2N HCl was used to dissolve the precipitate and rinse the labware. Both HCl fractions were combined for purification by anion exchange chromatography.

5.2.5 Preparation of plankton tows for isotopic analysis

Plankton samples were scraped off the filter with a clean plastic implement and placed in 8 mL quartz beakers. They were reacted at low heat overnight with 2mL 16N HNO_3 to burn off some of the organic material. When the sample was dry quartz beakers were placed in a shallow beaker covered by a watch glass and combusted overnight at

450°C in a muffle furnace to eliminate residual organic material (Bergquist, 2004).

Combusted samples were dissolved in 2N HCl.

5.2.6. Sample purification and isotopic analysis

Samples were purified by anion exchange chromatography on AG-MP1 resin

(Bio-Rad) based on previous methods (Maréchal et al., 1999). Samples were loaded onto

the column in 2N HCl, the Cl⁻ concentration at which Zn has the highest affinity for the

resin (Kraus and Moore, 1953), in order to conserve acid and maximize Zn retention on

the column. Plankton tow samples were purified once through a column containing

1.8 mL of resin. Seawater samples were purified on a larger column, and subsequently

passed through a smaller heat-shrink TFE (Tef Cap Industries) column with 400µL of

resin to further reduce the presence of contaminates (Archer and Vance, 2004). Samples

were eluted with 0.06N HCl instead of 0.05N HNO_3 to minimize the elution of

contaminates (Chapman et al., 2006). These purified solutions were evaporated to

dryness in PFA capsules, and reacted at high heat overnight with 400 µL HNO_3 and 200

µL HF to remove residual silica from the sample and residual organics that may have

leached from the column. Isotope ratios were measured on an IsoProbe according to

standard methods (Chapters 1-4).

5.3 Results and discussion

5.3.1 Zn concentration in seawater

Isotope dilution and $Mg(OH)_2$ coprecipitation followed by anion exchange purification has successfully been used to measure Zn concentrations in seawater. Process blanks contained an average of 0.22 ng Zn, corresponding to a blank of 0.23 nM for a 15mL sample. Standard deviations for triplicate processing and analysis of a single seawater sample were between 0 to 0.2 nM after discarding anomalously high data points that were assumed to result from sample contamination. Less than 10% of the replicate data points were discarded. Separate subsamples from the same GO-FLO bottles were analyzed for dissolved Zn concentration by R. Wisniewski (Wisniewski, 2006). Concentration measurements agree well with the exception of the two samples with Zn concentrations above 10 nM (Fig. 3). Both of these samples were collected using a GO-FLO bottles attached to a stainless steel hydrowire, instead of the usual Kevlar. The measured Zn concentrations are higher than previously reported for the deep North Pacific, indicating that the samples were contaminated (Wisniewski, 2006). The reason for the discrepancy between our data and that of Wisniewski is unknown, but may result from the entrainment of small metal particles from the hydrowire which caused different levels of contamination in the different subsamples.

Anion exchange purification reduced the amount of Mg in the samples by over two orders of magnitude. This reduces the possible $^{24}Mg^{40}Ar$ interference on the ^{64}Zn peak during isotope dilution analysis. On the IsoProbe, the hexapole collision cell effectively eliminates most polyatomic interferences and so even unpurified isotope-

100
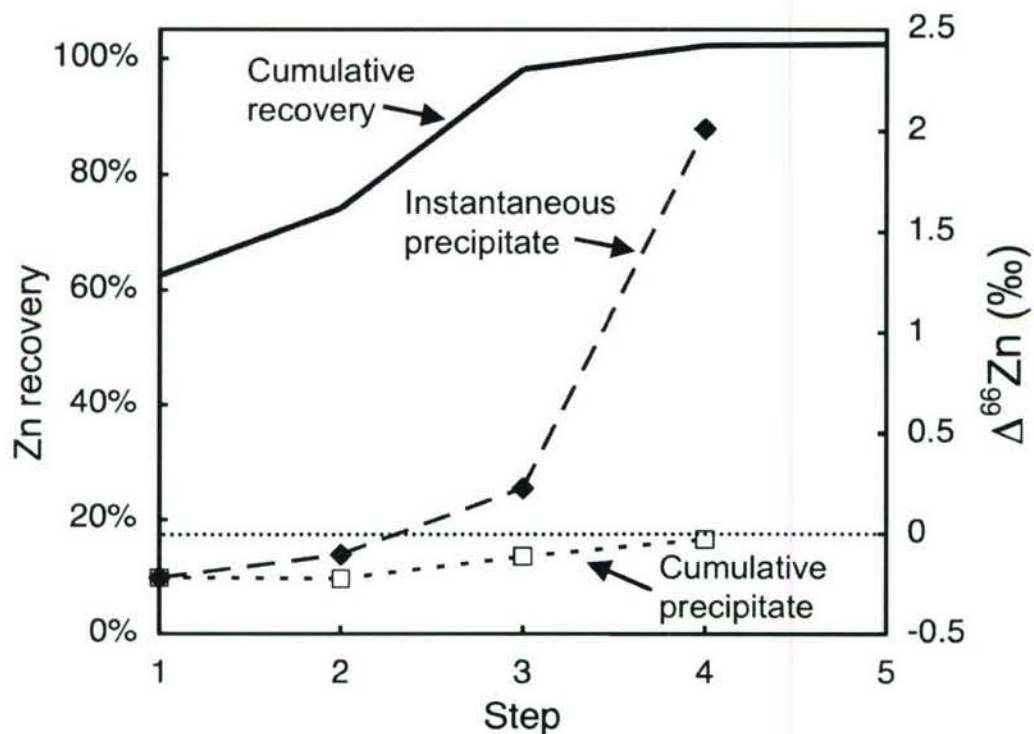
Figure 5.4. One liter of seawater spiked with 20 ppb Zn and precipitated in several steps. Instantaneous Zn recovery and $\Delta^{66}Zn$ (◆) was measured for each precipitate to calculate cumulative Zn recovery (——) and the cumulative $\Delta^{66}Zn$ (□) of the recovered product.

Step	Ammonia added (mL)	Time since last step (min)	Zn recovered (ng)	Zn recovery (cumulative)	$\Delta^{66}Zn$ of recovered Zn	$\Delta^{66}Zn$ (cumulative)
1	7.5	2	12481	62%	-0.22	**-0.22**
2	0	15	2322	74%	-0.25	**-0.22**
3	6	10	4787	98%	0.23	**-0.11**
4	10	60	816	102%	2.01	**-0.03**
5	10	60	48	102%	-	-

Table 5.1. Seawater doped with standard Zn was precipitated in several steps. For each step, both the time since the previous step and the amount of ammonia added was recorded. The amount and Zn isotope ratio of the Zn recovered at each step was used to calculate the cumulative Zn recovery and the $\Delta^{66}Zn$ of the cumulative Zn recovery.

101

dilution concentration samples can be accurately measured in low-resolution mode. On instruments without a hexapole, unpurified samples must be measured in a high-resolution mode to eliminate polyatomic interferences (Wisniewski, 2006). The sample purification described here may eliminate the need to make concentration measurements in a high-resolution mode. Decreasing the amount of Mg in the samples is also beneficial for maintenance of the ICP-MS. After analyzing a large number of samples with Mg precipitates, a white dusting of Mg can often be observed on the sampling cone and skimmer cone. This can decrease instrumental sensitivity and cause interferences (e.g. $^{24}Mg^{40}Ar$) that are large enough to interfere with isotope ratio measurements on natural samples.

5.3.2 Dissolved Zn isotopes in seawater

5.3.2.1 Zn separation from seawater by large-volume precipitation and filtration

The recovery efficiency of the large-volume precipitation method was evaluated by precipitating 1L of 20 ppb Zn-doped seawater in five steps (Table 1, Fig. 4). Complete recovery of Zn was achieved by the end of the precipitation Step 4. The simplified precipitation process used for actual samples is roughly equivalent to combining steps 1-3 in a single step, then completing a second precipitation equivalent to step 4. Calculated recoveries for real samples using this method was always within error of 100%.

The isotope effect of precipitation was determined by measuring Zn isotopes in precipitate recovered from several successive precipitations of a single seawater sample (Table 1, Fig. 4). The isotope effect of precipitation was calculated for the first
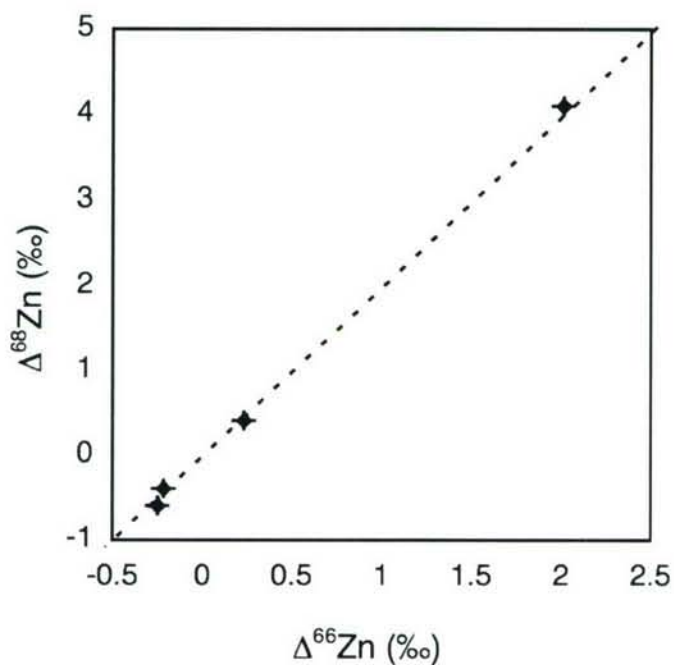
Figure 5.5. A comparison of $\delta^{68}Zn$ and $\delta^{66}Zn$ measured in precipitates from a 20 ppb seawater standard falls on the expected mass-dependent fractionation line (- - -), indicating the absence of isobaric interferences.

precipitation step using the accumulated product equation for Rayleigh distillation (Mariotti et al., 1981). We calculate an isotope effect of $\Delta^{66}Zn = -0.35‰$. The preferential incorporation of light isotopes into the precipitate suggests a kinetic isotope effect.

The quantity and isotopic composition of the Zn recovered at each step was used to calculate the cumulative $\delta^{66}Zn$ of recovered Zn. The isotopic composition of total Zn recovered was $\Delta^{66}Zn = -0.03‰$. Within our levels of analytical uncertainty, there is no isotopic offset between the Zn originally added to the seawater and the cumulative

Figure 5.6. Exponential mass-dependent fractionation will produce a linear relationship between $\delta^{68}Zn$ and $\delta^{66}Zn$ with a slope of 1.985 (- - -) and isobaric interferences will cause a point to appear off the mass-dependent line. The direction in which the measured value will deviate from the true value is shown by the arrows for an interference on mass 64, 66, and 68.

Zn recovered from the seawater. Comparison of the $\delta^{66}Zn$ and $\delta^{68}Zn$ values indicate the absence of isobaric interferences (Fig. 5).
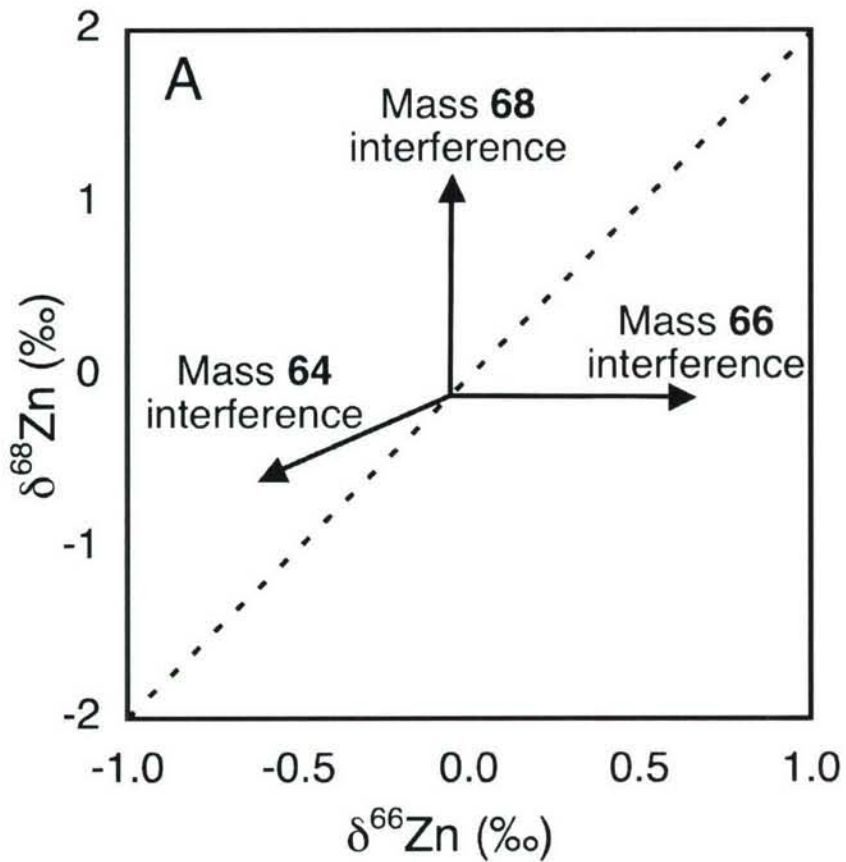
5.3.2.2 Isotopic analysis of natural seawater and standard seawater with low Zn concentrations

At the Zn concentrations found in natural seawater samples, analytical problems were discovered due to isobaric interferences on one or more of the Zn isotopes. Concentrated and purified natural seawater samples analyzed here had Zn concentrations from 0.7 to 8.6 nM, equivalent to roughly 0.05 to 0.5 ppb. Seawater standards were also processed with 0.1, 0.5, and 1.0 ppb Zn added. While isobaric interferences are rarely observed in our other studies of Zn isotopes, including the seawater experiments with 20 ppb Zn, the low concentrations of Zn in our natural samples may increase the possibility of matrix interference.

The presence of isobaric interferences was ascertained by comparing values of $\delta^{68}Zn$ and $\delta^{66}Zn$. Mass dependent fractionation should produce a linear relationship between $\delta^{68}Zn$ and $\delta^{66}Zn$ values with a slope of about two. Deviations from the mass dependent fractionation line indicate an isobaric interference with the same mass as one or more of the Zn isotopes (^{64}Zn, ^{66}Zn, and ^{68}Zn). In a two-dimensional plot of $\delta^{68}Zn$ versus $\delta^{66}Zn$, the anomalous measurement will lie off the mass-dependent line. The direction of the deviation is determined by the masses on which the interference occurs. For interferences on a single mass (64, 66, or 68), the direction of the deviation is shown

A

Zn added	$\delta^{66}Zn$ (‰)	2σ s.d.	$\delta^{68}Zn$ (‰)	2σ s.d.
0.1 μg	-0.45	0.18	-0.22	0.14
0.1 μg	-0.40	0.01	-0.27	0.11
0.5 μg	-0.09	0.08	0.42	0.55
1 μg	-0.01	0.21	0.09	0.42
1 μg	0.02	0.10	0.17	0.18

B

Location	Depth	[Zn]	$\delta^{66}Zn$ (‰)	2σ s.d.	$\delta^{68}Zn$ (‰)	2σ s.d.
N. Pac	26	25	-0.01	0.03	0.57	0.14
"	60	25	0.17	0.24	0.73	0.34
"	100	25	-0.16	0.21	0.26	0.07
"	150	50	0.06	0.08	0.18	0.33
"	150	25	0.18	0.07	0.60	0.37
"	300	50	0.53	0.06	1.47	0.13
"	300	25	0.58	0.12	1.19	0.37
"	1000	50	0.62	0.08	1.45	0.14
"	1000	50	0.52	0.06	1.35	0.19
"	1000	25	0.46	0.13	0.69	0.24
"	1000	50	0.41	0.02	0.92	0.23
"	1000	25	0.50	0.15	1.26	0.23
N. Atl.	3000	50	0.48	0.05	1.22	0.14
"	3000	25	0.45	0.03	1.14	0.35

Table 5.2. $\delta^{68}Zn$ and $\delta^{66}Zn$ values measured for seawater doped with 0.1, 0.5, or 1 ppb Zn (A) and for natural seawater samples (B). Errors are reported for triplicate analysis of a single sample.
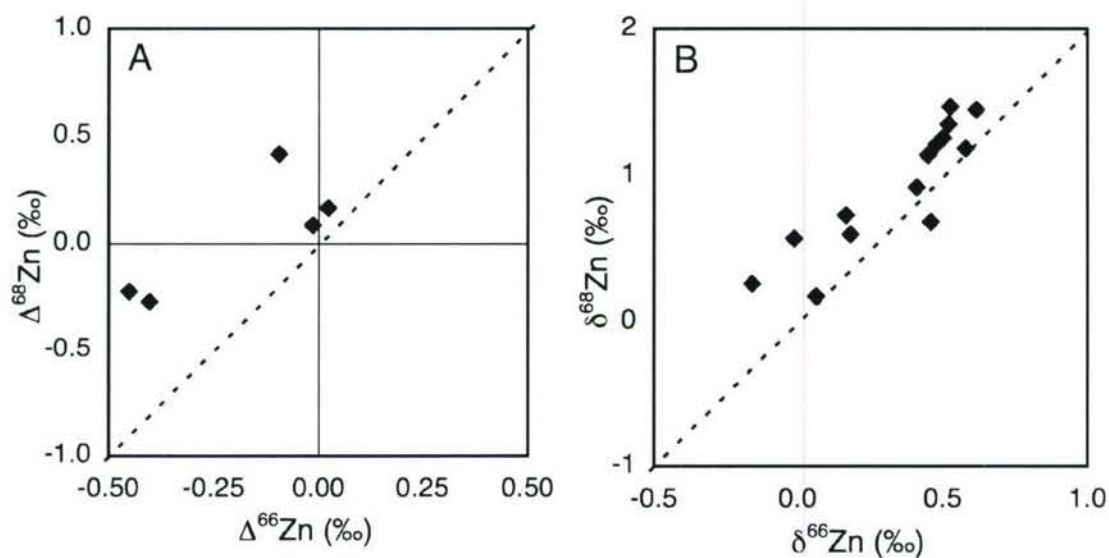
Figure 5.7. $\delta^{68}Zn$ and $\delta^{66}Zn$ values measured for seawater doped with 0.1, 0.5, or 1 ppb Zn (A) and for natural seawater samples (B). The deviation from the line of mass-dependence (- - -) indicates the presence of isobaric interferences.

in Figure 6.

We can see from a plot of $\delta^{68}Zn$ versus $\delta^{66}Zn$ measurements of five seawater standards prepared from spikes seawater that interferences are occurring on more than one mass (Fig 7A). Of the three seawater standards for which anomalous isotope ratios were measured, two appear to deviate from the expected value of $\Delta^{66}Zn = 0$ in the direction expected for an interference on mass 64, the third anomalous value is deviant in the direction consistent with an interference on mass 68. Multiple simultaneous interferences are also possible.

Mass interferences also appear in our measurements of natural seawater Zn isotopes (Fig. 7B). With these samples, too, we tested for the presence of a single-mass interference. The correction for a single-mass interference can be represented graphically by drawing a line through the observed data point with a slope shown in the arrows in Fig 6. The $\delta^{66}Zn$ value at which this line intercepts the mass-dependent fractionation line is corrected for the interference.

Seawater samples from 150 m, 300 m, and 1000 m in the north Pacific and from 3000 m in the North Atlantic were analyzed during multiple analytical sessions. Because the most common isobaric interferences occur at mass 64, each sample was corrected for the deviation from the mass-dependence line based on the assumption that the interference was on mass 64 alone. Isobaric interferences on mass 68 can be accounted for by comparing these values to the $\delta^{66}Zn$ value which takes account of only ^{66}Zn and ^{64}Zn. ^{66}Zn interferences were not examined because mass-dependent anomalies in this direction (to the right of the mass-dependence line) were not observed. Correcting our natural seawater $\delta^{66}Zn$ values for a mass 64 interference in this way does not improve the reproducibility of our data (Fig 8). Based on this result, we presume that there are multiple isobaric interferences in these measurements.

The source of these interferences is currently unknown. Only Ni has stable isotopes on the same masses as Zn, and ^{64}Ni corrections are insignificant to the ^{64}Zn measurements, so the interferences must be from polyatomic ions. These interferences may result from incomplete purification of the samples. Seawater is a complicated matrix with a total-salt/Zn ratio of 10^9-10^{11} so even a small remnant of the original contaminant
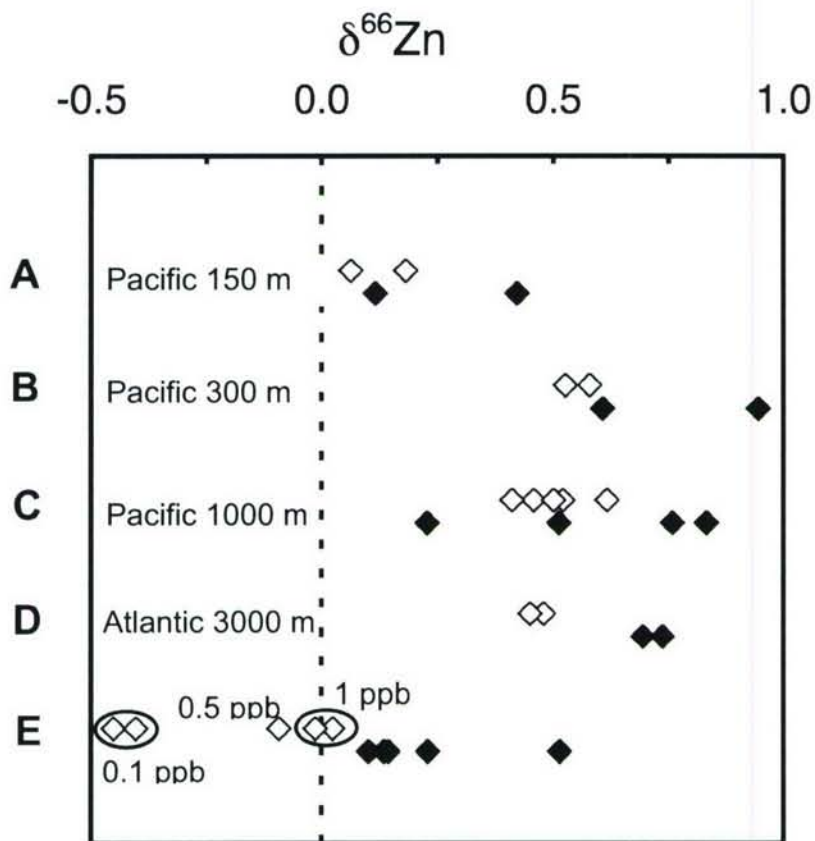
Figure 5.8. δ^{66}Zn values for seawater samples measured during different analytical sessions. Samples are from 150 m (A), 300 m (B), and 1000 m (C) in the North Pacific, from 3000 m in the Atlantic (D) and Zn-free seawater doped with varying concentrations of standard Zn (E). Shown are the δ^{66}Zn values measured with no correction for isobaric interferences ($\diamond$) and corrected for an interference on mass 64 ($\blacklozenge$). This correction does not improve the reproducibility of the measurements. Each point (per depth) represents a separate analytical session or separate sample.
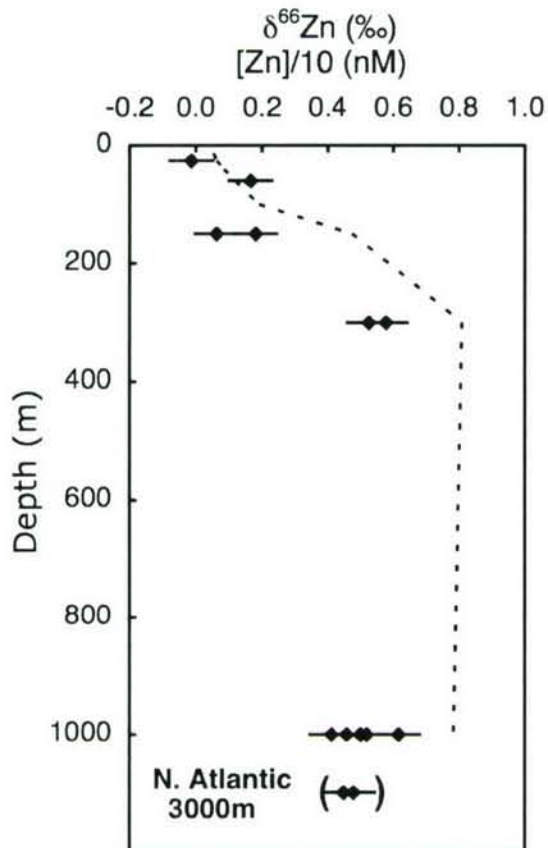
Figure 5.9. Dissolved $\delta^{66}Zn$ values at several depths in the north Pacific and north Atlantic oceans (◆). Error bars represent the minimum external analytical error (2s s.d.). A trend towards heavier $\delta^{66}Zn$ values in deeper water correlates with an increase in the concentration of Zn (- - -).
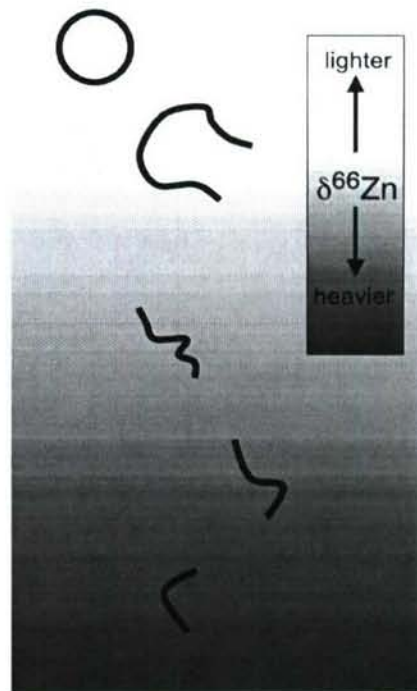
Figure 5.10. A picture of the processes that could lead to lighter dissolved $\delta^{66}Zn$ values in the surface ocean. Cells preferentially take up light Zn to the cell interior, while heavy Zn is preferentially adsorbed onto the cell surface. Cells lysis in shallow waters, and most of the internal Zn is released into the upper ocean. Isotopically heavy Zn is transported to the deep ocean adsorbed to particulate matter.
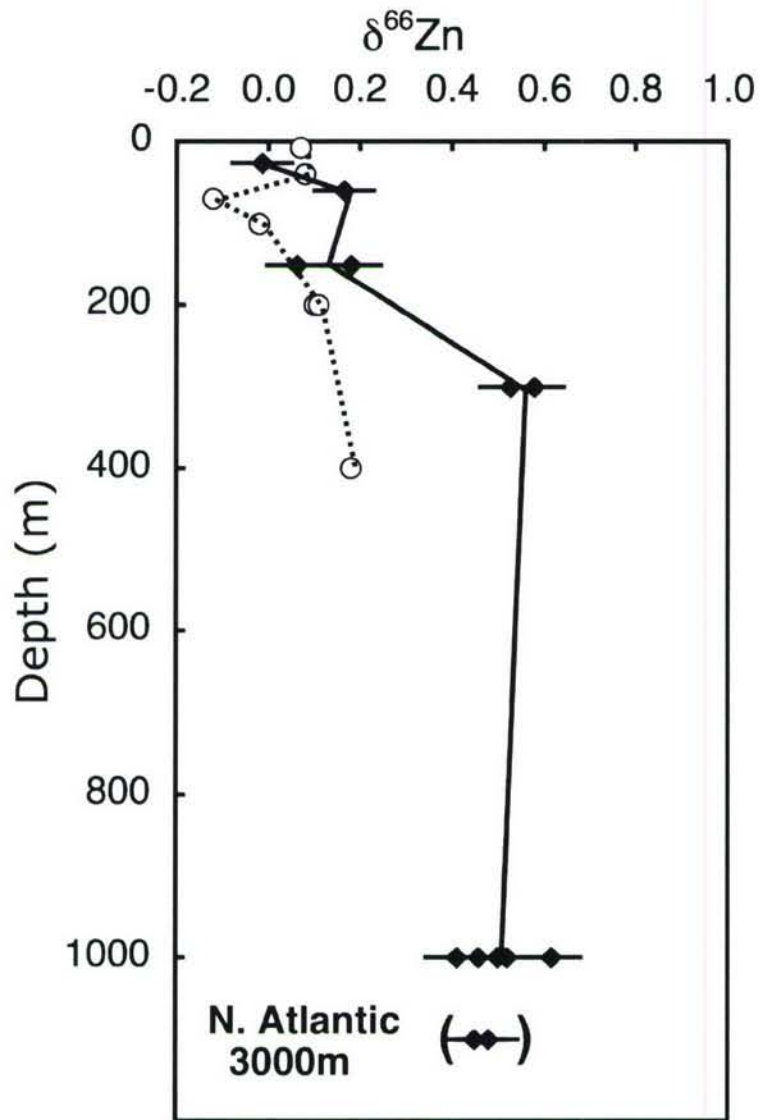
Figure 5.11. Comparison of seawater dissolved Zn isotopes from this study (♦) and reported for another station in the North Pacific (O) (Bermin et al., 2006).

elements could cause interferences. Interferences could also be ablated off of the instrument. I have observed that cleaning the sampling and skimmer cones decreased the magnitude of interferences on several occasions. $MgAr^+$ and $SiAr^+$ are considered the most likely interferences. $^{24}Mg^{40}Ar$ (79%) interferes at mass 64, $^{26}Mg^{40}Ar$ (11%) interferes at mass 66, and $^{28}Si^{40}Ar$ (92%) interferes at mass 68. The fact that single-isotope corrections do not improve the quality of the data indicates that there are multiple interferences.

5.3.2.3 Seawater dissolved Zn isotopes

A vertical trend is observed in the profile of seawater Zn isotope ratios (Fig. 9). In the North Pacific, $\delta^{66}Zn$ values are higher in deeper waters and decrease in surface waters. The Zn isotope ratio at 1000 m is the best constrained, with four separate samples having been analyzed during different analytical sessions. The average of all analyses is $\delta^{66}Zn = +0.50‰ \pm 0.08$. The two measurements presented for 300 m and 150 m are for the same sample analyzed twice during different analytical sessions. I believe the observed decrease in $\delta^{66}Zn$ at 150 m compared to deeper waters is real. Two separate measurements provided similar values of $\delta^{66}Zn$ and in one of them no isobaric interferences were observed. Unfortunately, samples at 26 m and 30 m were measured only once and strong isobaric interferences were found in both samples. Although larger analytical problems were encountered in measuring $\delta^{66}Zn$ in seawater samples from the upper water column, we believe the trend towards lighter $\delta^{66}Zn$ in the upper ocean is real. At 150m, two separate measurements confirm $\delta^{66}Zn$ of +0.06 to +0.18‰ and on one of

these measurements, no isbaric interferences were observed. The seawater sample from the deep Atlantic has a similar $\delta^{66}Zn$ to that of the Pacific samples.

The trend towards lighter seawater $\delta^{66}Zn$ in the upper ocean is unexpected based on the preference of diatoms for the uptake of lighter Zn isotopes observed in culture experiments (Chapter 4). In order to produce isotopically light surface seawater, Zn sinking out of the surface waters must be isotopically heavy compared to surface waters (Fig. 10).

Contrary to conventional wisdom, the Zn particle flux out of the surface ocean may not be "primary" biological Zn in growing phytoplankton. Perhaps most of this primary biological Zn is released during cell lysis in the upper ocean, and the downward Zn flux derives mostly from the adsorption of Zn^{2+} to sinking particles (Fig. 10). Zn adsorption to cell exteriors has repeatedly been shown to have a positive isotope effect (Chapter 4, (Gélabert et al., 2006). While experiments indicate that Zn cell-surface adsorption will be relatively unimportant compared to uptake for growing cells in the surface ocean, this may not be true of sinking particulate matter.

To illustrate the difference between Zn and N isotopes during particle degradation, we can consider the case of a single Zn-containing protein. When this protein is released from the cell into seawater during lysis, even minimal degradation of the protein may cause the Zn to be released. As the protein degrades further, numerous charged groups will be created and exposed, providing many sites onto which free Zn^{2+} atoms will re-adsorb. Thus sinking protein fragments may contain most of thier original atoms of N, while Zn atoms will have exchanged with Zn in seawater.
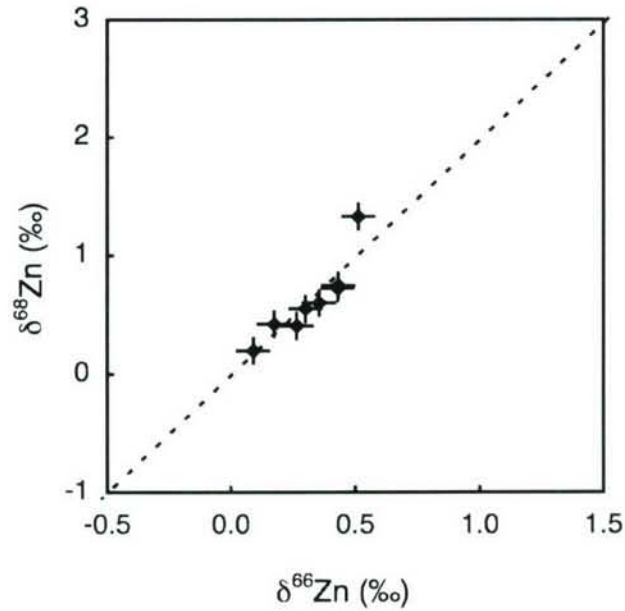
113

Figure 5.12. A comparison of $\delta^{68}Zn$ and $\delta^{66}Zn$ measured in plankton tow samples from several different sampling sites around the world. $\delta^{66}Zn$ values range from 0.08‰ to +0.57‰.
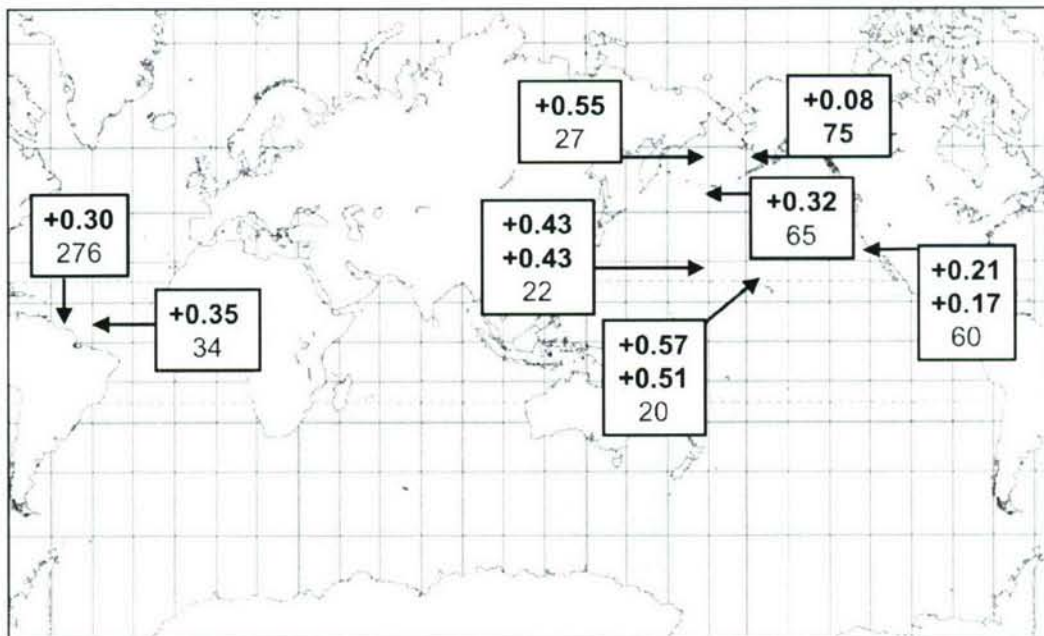
Figure 5.13. Worldwide location of plankton tows, measured $\delta^{66}Zn$, and Zn:P of the plankton (μmol/mol).

Our measurements of dissolved seawater Zn isotopes are significantly different from measurements made at another location in the North Pacific (48°39'N, 126°40'W) (Bermin et al., 2006). These differences may be attributed to real differences in seawater $\delta^{66}Zn$ at these locations, or to analytical problems.

5.3.3 Zinc isotopes in natural plankton

5.3.3.1 World-wide plankton $\delta^{66}Zn$ values

Zinc isotope ratios in plankton from around the world range from +0.09‰ to +0.51‰ (Fig. 12, Fig 13). The three heaviest $\delta^{66}Zn$ values occur in the samples that are the farthest from the shoreline of a major continent. Conversely, many of the lightest $\delta^{66}Zn$ values occur close to coastlines. Measuring plankton $\delta^{66}Zn$ values in a broader range of samples will help to determine if this is a common feature. Perhaps the isotopic similarity between open-ocean plankton and deep-water Zn, and the similarity between coastal plankton and anthropogenic/continental Zn, represents differences in the source of Zn to these plankton.

5.3.3.2 The Peru Upwelling Region

Zinc isotopes were measured in phytoplankton collected at nine stations in the Peru Upwelling Region (Table 3). Biomass in this area is dominated by fast-growing diatoms because of the rapid supply of nutrients to the surface from deeper waters. Much of the biomass here appeared to be diatoms based on the large amount of silicate frustules left after acidification and combustion of the samples.

A

Station	Unwashed cells				Washed cells			
	δ^{66}Zn (‰)	s.d. (2s)	δ^{68}Zn (‰)	s.d. (2s)	δ^{66}Zn (‰)	s.d. (2s)	δ^{68}Zn (‰)	s.d. (2s)
10	0.02	0.02	0.17	0.16	0.09	0.03	0.35	0.19
12	0.44	0.05	1.55	0.14	0.96	0.08	2.15	0.42
24	-4.26	0.02	-8.07	0.10	-0.31	0.05	-0.11	0.09
26	0.07	0.02	0.08	0.39	-1.18	0.05	-2.42	0.46
27	0.02	0.02	0.07	0.02	0.23	0.02	0.46	0.09
27	-0.14	0.06	-0.02	0.09	0.14	0.07	0.54	0.02
29	0.07	0.05	0.15	0.04	0.12	0.04	0.28	0.09
30	0.51	0.03	1.18	0.06	0.01	0.03	0.04	0.12
32	0.09	0.02	0.26	0.05	0.16	0.02	0.41	0.11
33	0.20	0.03	0.44	0.04	0.22	0.02	0.48	0.06

B

Station	Latitude	Longitude	[SiO4] (μM)	[PO4] (μM)
10	-15.6	-75.1	33.02	1.72
12	-16.3	-75.6	10.36	0.72
24	-12.3	-79.3	1.34	0.91
26	-12.0	-78.7	1.59	0.59
27	-11.8	-78.1	1.50	0.62
29	-11.8	-77.9	7.59	0.69
30	-	-	-	-
32	-11.0	-78.2	32.82	1.89
33	-8.2	-80.3	3.63	0.28

Table 5.3. (A) Zn isotope ratios of washed and unwashed phytoplankton cells collected at stations in the Peru Upwelling Region. (B) Station locations and nutrient concentrations in surface waters.

116
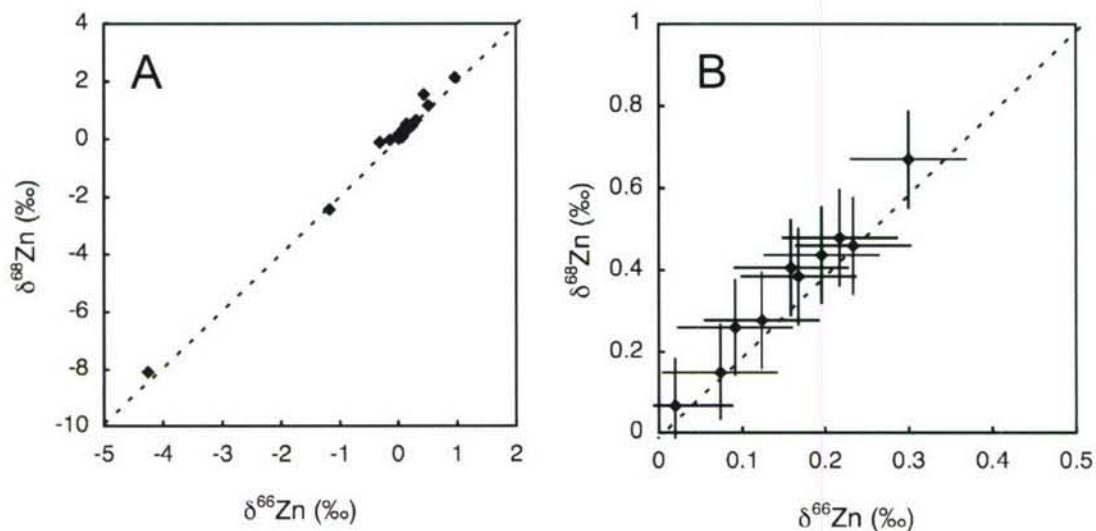
Figure 5.14. A comparison of $\delta^{68}Zn$ and $\delta^{66}Zn$ measured in plankton tow samples from the Peru Upwelling Region. When all samples that deviate from the expected relationship between $\delta^{66}Zn$ and $\delta^{68}Zn$ by more than the 2σ error are removed, the remaining samples have $\delta^{66}Zn$ between 0‰ and +0.3‰.
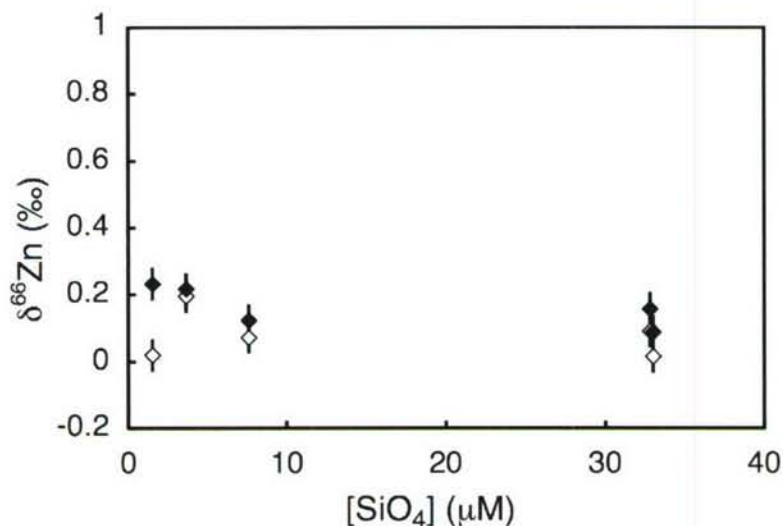
Figure 5.15. The $\delta^{66}Zn$ of washed ($\diamond$) and unwashed ($\blacklozenge$) plankton tows from the Peru Upwelling Region. Only samples which showed the expected mass-dependent fractionation relationship between $\delta^{68}Zn$ and $\delta^{66}Zn$ were included. There is no clear relationship between nutrient drawdown and dissolved Zn isotope fractionation in the Peru Upwelling region. Washed plankton tows are generally lighter than unwashed plankton tows, though the difference is small.

	Unwashed plankton	Washed plankton	Krill
Stn 27	$\delta^{66}Zn$ = +0.20‰	$\delta^{66}Zn$ = +0.19‰	$\delta^{66}Zn$ = +0.17‰
Stn 24	$\delta^{66}Zn$ = +0.22‰	$\delta^{66}Zn$ = +0.20‰	$\delta^{66}Zn$ = +0.30‰

Table 5.4. The Zn isotope ratio measured in natural samples of unwashed, and washed phytoplankton, and in krill picked out of the sample from the same tow. Krill were present an only two stations in the Peru Upwelling Region, Station 27 (upper row) and Station 33 (lower row).

Several of the samples showed extremely light values of $\delta^{66}Zn$ (Fig 14A). The stations at which we recorded these anomalously light Zn isotope ratios ($\delta^{66}Zn \ll 0$‰) were next to each other, and were both oligotrophic. Perhaps these unusual numbers result from analytical problems, although the values of $\delta^{66}Zn$ and $\delta^{68}Zn$ agree and the instrumental mass bias during these measurements was comparable to other samples. If these extremely low $\delta^{66}Zn$ values are real, perhaps they result of contamination with a highly-fractionated source of Zn such as the ship's sacrificial anode. When all samples

118

which diverged from the mass-dependant relationship between $\delta^{68}Zn$ and $\delta^{66}Zn$ were removed, $\delta^{66}Zn$ for the remaining samples ranged between 0‰ and 0.3‰.

When these samples are plotted against the concentration of silicate, no relationship is observed between nutrient depletion and Zn isotope fractionation (Fig. 15). Assuming a model where deep waters are upwelled with a full nutrient load and nutrients are slowly depleted by biological uptake, even a small isotope effect for uptake should be magnified by Rayleigh distillation. From our data, it appears that either the isotope effect for biological uptake in the Peru Upwelling Region is very small, or Rayleigh distillation is limited. If nutrient concentrations are governed by differences in vertical upwelling rates at different locations, rather than by horizontal processes, plankton would reflect the $\delta^{66}Zn$ of upwelling waters at steady state. This might explain why there is so little variation in plankton $\delta^{66}Zn$ values.

5.3.3.3 Evidence for trophic fractionation

At two stations, trophic fractionation was assessed by comparing Zn isotope ratios in krill and the diatoms on which they were grown (Table 4). At neither of these stations were the krill significantly different from the bulk plankton on which they were presumably feeding. Trophic fractionation at these sites appears to be too small for us to measure.

119

References for Chapter 5:

Archer, C. and Vance, D., 2004. Mass discrimination correction in multiple-collector plasma source mass spectrometry: an example using Cu and Zn isotopes. Journal of Analytical Atomic Spectrometry, 19: 656-665.

Bell, J., Betts, J. and Boyle, E., 2002. MITESS: a moored in situ trace element serial sampler for deep-sea moorings. Deep-Sea Research Part I-Oceanographic Research Papers, 49(11): 2103-2118.

Bergquist, B.A., 2004. The marine geochemistry of iron and iron isotopes, MIT, Cambridge, Massachusetts.

Bermin, J., Vance, D., Archer, C. and Statham, P., 2004a. The separation and isotopic analysis of seawater Cu and Zn. Eos Trans. AGU, 85(47): Fall Meet. Suppl., Abstract V51A-510.

Bermin, J., Vance, D., Archer, C. and Statham, P.J., 2006. The determination of the isotopic composition of Cu and Zn in seawater. Chemical Geology, 226(3-4): 280-297.

Bermin, J., Vance, D. and Statham, P., 2004b. A technique for the separation and isotopic analysis of Fe and Zn in seawater. Geochimica et Cosmochimica Acta, 68(11): A346-A346.

Bruland, K.W., 1980. Oceanographic distributions of cadmium, zinc, nickel, and copper in the North Pacific. Earth and Planetary Science Letters, 47(2): 176-198.

Bruland, K.W. and Franks, R.P., 1983. Mn, Ni, Cu, Zn, and Cd in the western north Atlantic., Trace metals in seawater, NATO Conf. Ser. 4.

Bruland, K.W., Knauer, G.A. and Martin, J.H., 1978. Zinc in Northeast Pacific water. Nature, 271(5647): 741-743.

Bruland, K.W. and Lohan, M.C., 2003. Controls of trace metals in seawater. Treatise on Geochemistry, 6. Elsevier, 7800 pp.

Chapman, J.B., Mason, T.F.D., Weiss, D.J., Coles, B.J. and Wilkinson, J.J., 2006. Chemical separation and isotopic variations of Cu and Zn from five geological reference materials. Geostandards and Geoanalytical Research, 30(1): 5-16.

Coale, K.H., Gordon, R.M. and Wang, X.J., 2005. The distribution and behavior of dissolved and particulate iron and zinc in the Ross Sea and Antarctic circumpolar current along 170 degrees W. Deep-Sea Research Part I-Oceanographic Research Papers, 52(2): 295-318.

Ellwood, M.J. and Van den Berg, C.M.G., 2000. Zinc speciation in the Northeast Atlantic Ocean. Marine Chemistry, 68(4): 295-306.

Fitzwater, S.E., Johnson, K.S., Gordon, R.M., Coale, K.H. and Smith, W.O., 2000. Trace metal concentrations in the Ross Sea and their relationship with nutrients and phytoplankton growth. Deep-Sea Research Part II-Topical Studies in Oceanography, 47(15-16): 3159-3179.

Gélabert, A. et al., 2006. Interaction between zinc and freshwater and marine diatom species: Surface complexation and Zn isotope fractionation. Geochimica et Cosmochimica Acta, 70(4): 839-857.

GEOSECS Operations Group, 1987. GEOSECS Atlantic, Pacific, and Indian Ocean Expeditions, 7. National Science Foundation, Washington, D.C., 200 pp.

John, S.G., Bergquist, B.A., Saito, M.A. and Boyle, E.A., 2005. Zinc isotope variations in phytoplankton and seawater. Geochimica Et Cosmochimica Acta, 69(10): A546-A546.

Kraus, K.A. and Moore, G., E., 1953. Anion exchange studies. VI. The dIvalent transition elements manganese to zinc in hydrochloric acid. Journal of the American Chemical Society, 75: 1457-60.

Lohan, M.C., Statham, P.J. and Crawford, D.W., 2002. Total dissolved zinc in the upper water column of the subarctic North East Pacific. Deep-Sea Research Part II-Topical Studies in Oceanography, 49(24-25): 5793-5808.

Maréchal, C.N., Nicolas, E., Douchet, C. and Albarède, F., 2000. Abundance of zinc isotopes as a marine biogeochemical tracer. Geochemistry Geophysics and Geosystems, 1: 1999GC000029.

Maréchal, C.N., Telouk, P. and Albarède, F., 1999. Precise analysis of copper and zinc isotopic compositions by plasma-source mass spectrometry. Chemical Geology, 156(1-4): 251-273.

Mariotti, A. et al., 1981. Experimental-determination of nitrogen kinetic isotope fractionation - Some principles - Illustration for the denitrification and nitrification processes. Plant and Soil, 62(3): 413-430.

Tang, D.G. and Morel, F.M.M., 2006. Distinguishing between cellular and Fe-oxide-associated trace elements in phytoplankton. Marine Chemistry, 98(1): 18-30.

Tovar-Sanchez, A. et al., 2003. A trace metal clean reagent to remove surface-bound iron from marine phytoplankton. Marine Chemistry, 82(1-2): 91-99.

Tovar-Sanchez, A. et al., 2004. Corrigendum to "A trace metal clean reagent to remove surface-bound iron from marine phytoplankton (vol 82, pg 91, 2003)". Marine Chemistry, 85(3-4): 191-191.

Weiss, D.J. et al., 2005. Isotopic discrimination of zinc in higher plants. New Phytologist, 165(3): 703-710.

Wisniewski, R.J., 2006. Relating the biogeochemistries of zinc, cobalt, and phosphorus to phytoplankton activities in the sea.

Wu, J.F. and Boyle, E.A., 1998. Determination of iron in seawater by high-resolution isotope dilution inductively coupled plasma mass spectrometry after Mg(OH)(2) coprecipitation. Analytica Chimica Acta, 367(1-3): 183-191.

Chapter 6

Conclusions

I have reported measurable isotopic fractionations in hydrothermal systems, cultured marine phytoplankton, natural marine plankton, and seawater. As more data on Zn isotopes in the marine environment becomes available, the potential for using Zn isotopes to trace marine biogeochemical processes will grow. In order to better interpret this data, it is worth considering how well we understand the most basic matters of Zn biogeochemical cycling in the oceans. I present here some speculations on the origin of the vertical concentration profile of Zn in the oceans, the relationship between the nutritional importance of trace elements and "nutrient-like" concentration profiles, a reconsideration of the factors responsible for the seasonal signal in sediment trap δ^{66}Zn values observed by Maréchal et. al. (2000), and some final thoughts on the factors responsible for setting the δ^{66}Zn of seawater.

6.1 Origin of the marine vertical concentration profile of Zn

The classic explaination for the concentration profile of nutrients in the ocean is based on the vertical transport of nutrients (Redfield et al., 1963). As high-nutrient waters are upwelled to the surface, nutrients are depleted by biological uptake into phytoplankton. Nutrients are transported back to deeper waters by the settling of biological material that remineralizes to regenerate the dissolved nutrients. According to such a one-dimensional model, the similarities in the Zn and Si profiles should arise from similar rates of particulate remineralization. However, Zn and Si do not occur in the same phases within a cell. Chemical dissolution of diatoms, the predominant siliceous marine plankton, show that very little of the cellular Zn is incorporated into the silicate frustule (Collier and Edmond, 1984; Ellwood and Hunter, 2000). X-ray spectroscopy has confirmed this finding by showing that Zn is contained mostly in the cell protoplasm and nucleus, the same parts of the cell where P occurs (Twining et al., 2003). It is possible that Zn is contained in a more refractory organic phase than N and P, so that Zn fortuitously dissolves at a similar rate to silicate. Or, a one-dimensional model may not be a good representation of the processes that give rise to the marine Zn profile.

An alternative explanation, based on ideas passed to me from John Edmond through Ed Boyle, invokes two-dimensional mixing to account for the similarity between marine Zn and Si profiles. Vertical features in the central ocean basins outcrop along isopycnals as horizontal features in the polar oceans (Sarmiento et al., 2004) (Fig. 1).
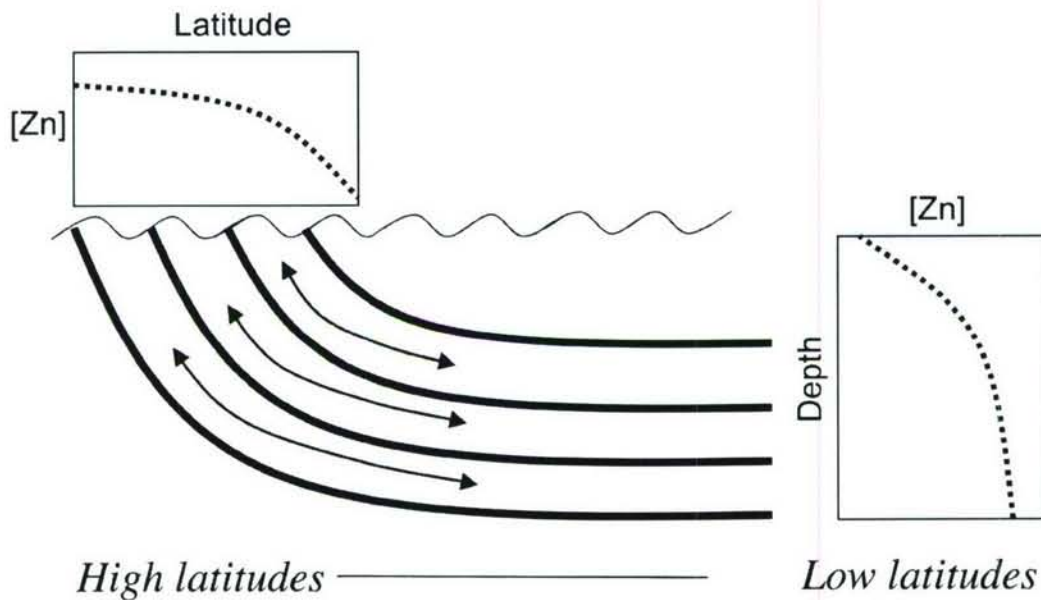
Figure 6.1. A pictoral representation of the proccess by which the biological depletion of nutrients in high-latitude surface waters can determine the vertical nutrient concentration profiles low latitudes. Zn and Si are depleted more quickly than N in surface waters of the Southern Ocean, so the similarilty between the shape of vertical Zn and Si profiles in the North Pacific could have it's origins in the surface Southern Ocean.

Because mixing along isopycnals occurs much more quickly than vertical mixing,

horizontal processes may be important even if they occur over much larger spatial scales.

Rapid depletion of Si and Zn, compared to N and P, in upwelling Southern Ocean waters

may explain nutrient profiles in the North Pacific (Sarmiento et al., 2004; Sunda and

Huntsman, 1992). According to this explanation, the similarity in the Zn and Si vertical

concentration profiles may result from similar uptake rates by diatoms, instead of a similarity in particulate remineralization rates.

The isotopic consequences of Zn biological uptake into phytoplankton and Zn remineralization are likely to be quite different, lending hope that Zn isotopes may help to clarify the relative importance of these two processes. Remineralization is unlikely to have a large isotopic signal because at steady state the dissolving Zn will have the same isotope ratio as the particulate Zn. Biological uptake by diatoms in culture has a demonstrated isotope effect of -0.2 to -0.8 ‰ (Chapter 4) and the isotope effect may be magnified during Zn depletion in surface waters by Rayleigh distillation.

6.2 What causes some trace elements to have nutrient-type profiles
6.2.1 What is a "nutrient-type" profile

Zn is regarded to have a "nutrient-type profile simply because the shape of the conentration profile is similar to that of Si, a well-studied nutrient. Whether the vertical concentration profile of Zn is controlled by vertical processes alone or horizontal process at high latitudes, it's nutrient-type profile is often implied to result from the role of Zn as a cellular nutrient and it's depletion to very low levels in oligotrphic surface waters. But, there may be other causes for a nutrient-type profile.

6.2.2 Cadmium, intracellular nutrient or extracellular toxin?

The discovery that dissolved Cd in the oceans has a similar vertical concentration profile to N and P (Boyle, Nature, 1976) has led to much subsequent speculation about a

126

biological role for Cd. In fact, Cd has been shown to act as a nutrient to Zn-stressed diatoms (Price and Morel, 1990), and Cd-containing enzymes have been isolated from two marine species (Lane and Morel, 2000; Lane et al., 2005). Kinetic data showing increased Cd and Co uptake rates under conditions of low Zn is similarly ascribed to the nutritional effects of these metals (Sunda and Huntsman, 2000).

In fact, a nutrient-type profile may just as easily derive from the *extracellular toxicity* of Cd. Cd ions appear to interact with the same transporters used for uptake of other metals such as Zn and Mn, and high Cd concentrations can retard cell growth by interfering with transport of these other metals (Sunda and Huntsman, 1996; Sunda and Huntsman, 1998; Tortell and Price, 1996). In this case, Cd is toxic only when it is outside the cell! Perhaps Cd uptake is simply a mechanism to "detoxify" Cd by removing it from the cells diffusive boundary layer where it interferes with other cellular machinery.

It may not be geochemically important in the modern oceans whether Cd uptake is the result of Cd's role as an intracellular nutrient or as an extracellular toxin. It is, however, a question that should be addressed in seeking to understand the evolutionary pressures that lead cells to acquire metals.

6.2.3 Is Zn uptake in the ocean governed by it's role as a nutrient?

There is no doubt that Zn can play an important role as a nutrient. At low Zn concentrations, the growth of phytoplankton can become severly limited (Sunda and Huntsman, 1992). Still, it is not known whether the uptake of Zn in the ocean is driven by a physiological Zn requirement. The Zn:P ratios of cultured phytoplankton increase with

increasing Zn in the culture medium. This may represent an increase in the production of Zn-containing proteins, but at some point Zn uptake surely exceeds the biological need. Diatoms grown in high-Zn media have been observed to take up Zn at mole ratios of nearly than 1:1 compared to P (Sunda and Huntsman, 1992). It is not known at what point Zn uptake by marine phytoplankton exceeds physiological use of Zn. It is also unknown whether uptake of Zn beyond immediate physiological needs represents (1) "luxury uptake" with no harmful effects of excess Zn uptake and potential benefits under future conditions of Zn starvation, (2) "accidental" Zn uptake which harms the cell but which the cell is incapapable of turning off, or (3) "de-toxifying" uptake where the cell gains a benefit from reducing the extracellular concentration of Zn in the diffusive boundary layer.

6.3 What is responsible for the seasonal $\delta^{66}Zn$ cycle observed sediment trap material

A data set with great potential to help us understand Zn isotope cycling in the oceans is a year-long record of $\delta^{66}Zn$ in sediment trap material from off the west coast of North Africa (Maréchal et al., 2000) (Fig. 2). Biological uptake of Zn in the surface ocean was suggested to be the underlying cause of the seasonal cycle in $\delta^{66}Zn$ values in this sediment trap material. Depletion of light isotopes from surface waters by biological uptake early in the spring could lead to an increase in surface water $\delta^{66}Zn$ later in the spring and summer. The $\delta^{66}Zn$ values in sediment trap material was thought to mirror trends in surface waters.
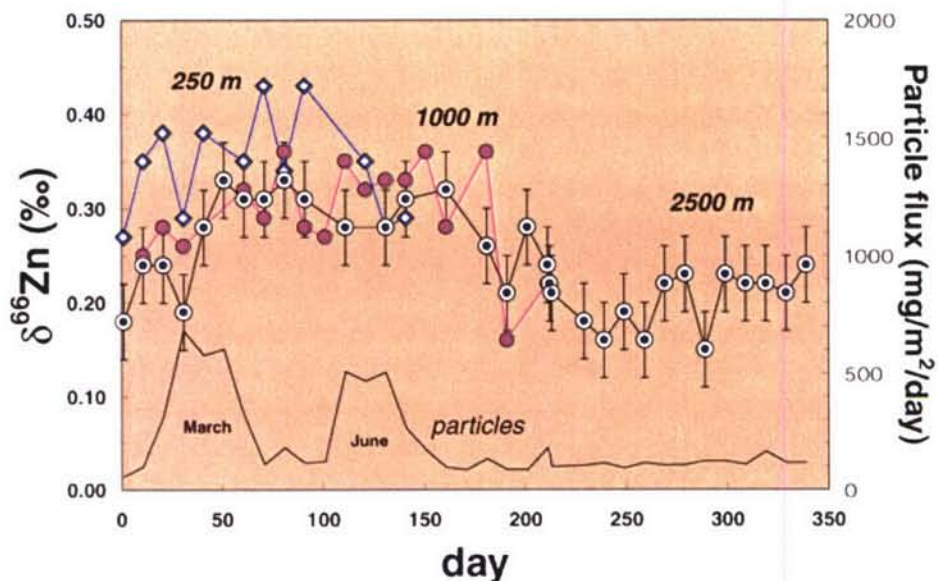
Figure 6.2. The Zn isotope composition of sediment trap materials collected off the western coast of North Africa at the EUMELI site (18°30'N 21°06'W). From (Maréchal et al., 2000).
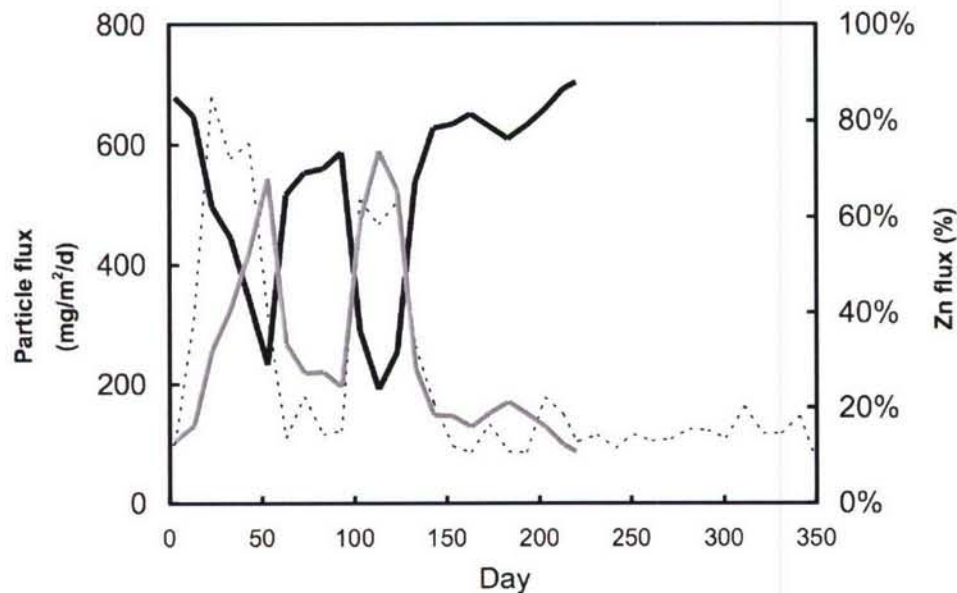
Figure 6.3. Calculated zinc flux with organic carbon (——) and continental dust (——) over the course of the year. Total particulate matter flux is also plotted (- - -). Data are from the EUMELI project (Morel, 1996), with Zn:Corg estimated from plankton tow data (Collier and Edmond, 1984), and Zn:Al estimated from measurements of African dust (Reid et al., 2003).

129

Interpretation of this data, however, may not be as straightforward as originally proposed. After estimating the amounts of Zn arriving in the sediment traps with different phases, we found that changes in the source of Zn provide an alternative explaination of the observed seasonal trends. Sediment trap material recovered from the EUMELI program is a mix of different phases (Morel, 1996) which may contain Zn. The relative amounts of different phases changes with the seasons. During the spring and summer, there is a greatly increased flux of biological carbon into the sediment traps, while dust flux (as measured by Al) is much less variable. We estimated the amount of Zn delivered to the sediment traps with these two important Zn-bearing phases. The Zn delivery with organic carbon was estimated based on a $Zn:C_{org}$ ratio of $1.8 \cdot 10^{-6}$ (mol/mg) in planton tows from the Central Tropical Pacific (Collier and Edmond, 1984). The Zn flux with continental dust (as measured by Al) was estimated based a $Zn:Al$ ratio of $1.8 \cdot 10^{-5}$ for African dust (Reid et al., 2003). According to our calculations, there is a dramatic increase in the flux of Zn with organic carbon during the spring and summer, at the same time as there is a marked increase in the $\delta^{66}Zn$ of sediment trap particles (Fig 3).

Based on this new interpretation of the data, we can infer values of $\delta^{66}Zn$ for dust-borne and organic-born Zn. The $\delta^{66}Zn$ of sediment trap material collected during the winter appears to be influenced mainly by continental dust alone, with $\delta^{66}Zn = +0.2\text{‰}$. This value is remarkably consistent with the isotope value measured for Nigerian dust of $\delta^{66}Zn = +0.19\text{‰}$ (Maréchal et al., 2000). Our calculations suggest that both dust and organic carbon are responsible for transporting Zn to the sediment traps during spring and

summer. Based on this, we suggest that the spring/summer δ^{66}Zn of between +0.3‰ and +0.4‰ represents a minimum δ^{66}Zn for the Zn flux associated with organic carbon.

The region where this sediment trap was located, just to the west of the Saharan desert, has some of the highest dust fluxes in the world (Jickells et al., 2005). Sediment trap samples from elsewhere might provide a better record of the biological flux of Zn isotopes into the deep ocean.

6.4 What controls the Zn isotope ratio in the deep ocean?

I propose that the Zn isotopic composition of crustal material is δ^{66}Zn = +0.2‰ ± 0.1‰. This is similar to the isotopic composition of basalt Zn (see Chapter 3). Most anthropogenic Zn samples have δ^{66}Zn = +0.1‰ to +0.3‰, also similar to this proposed crustal isotope ratio (Chapter 2). The isotope composition of the deep ocean, however, is about δ^{66}Zn = +0.5‰. There must be a large marine sink for light Zn.

Based on the limited data available, many sinks for Zn in the ocean will preferentially sequester heavier isotopes. We suggest that the flux of Zn out of the surface ocean is isotopically heavy compared to surface waters (Chapter 5). Sediment trap data support this assumption by showing that biogenic particles are at least δ^{66}Zn = +0.3‰ to +0.4‰. Adsorption onto sediments or other solid phases is likely to sequester heavy Zn. Zn adsorption onto cell cultures (Chapter 4)(Gélabert et al., 2006) and manganese nodules (Maréchal et al., 2000) are associated with a positive isotope effect.

The only process we have discovered that might create a sink for light Zn in the ocean is the hydrothermal precipitation of Zn sulfides. Further research may establish
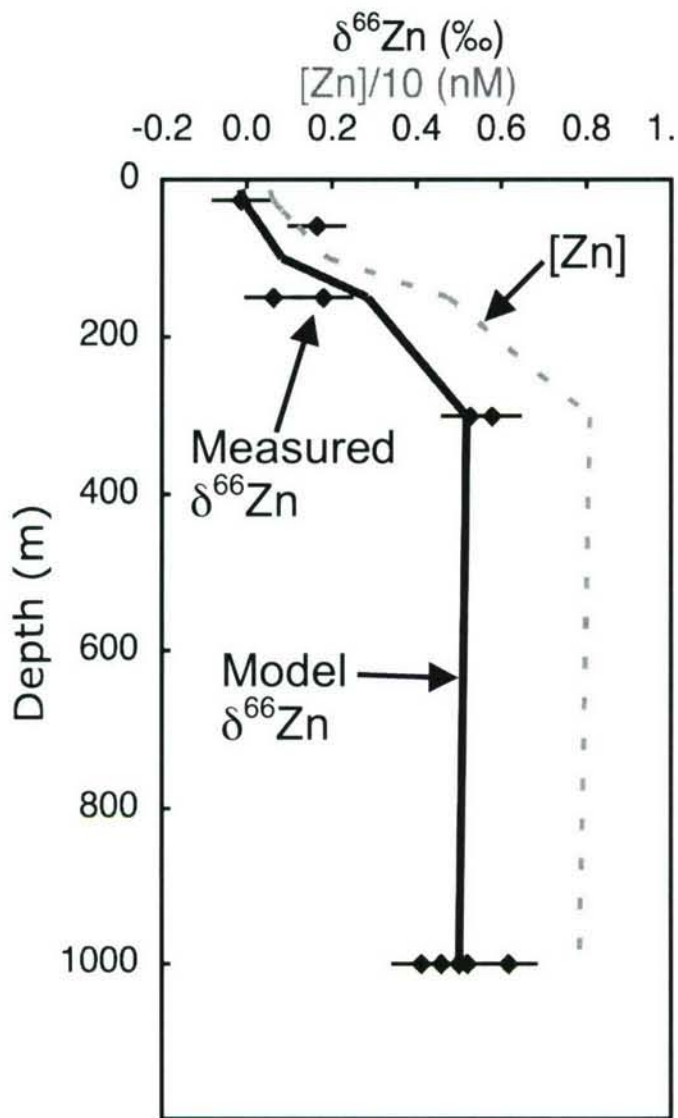
Figure 6.4. Comparison of measured seawater $\delta^{66}Zn$ (♦) with the $\delta^{66}Zn$ predicted by our model (——) based on isotope mixing and measured Zn concentrations (- - -).

whether this is the process responsible for setting the $\delta^{66}Zn$ of the deep oceans, or we may discover new processes that control zinc isotope concentrations in the oceans.

6.5. Modeling the seawater Zn isotope profile

6.5.1. Isotope mixing model

Based on the hypothesis developed in Chapter 5, that Zn transport to deeper waters occurs primary as Zn^{2+} adsorbed on sinking particles, a simple model can be constructed to explain the observed North Pacific Zn isotope profile in terms of isotope mixing between surface and deep waters plus dissolution of particulate Zn. In this model, we specify Zn fluxes and $\delta^{66}Zn$ for the surface ocean and the deep ocean in order to calculate $\delta^{66}Zn$ at intermediate Zn concentrations as an isotope mixture of surface and deep waters. We assume that the Zn flux from deep waters to surface waters occurs by advection-diffusion, and that Zn transport from surface waters to deeper waters occurs via adsorption to sinking particles. The deep water $\delta^{66}Zn$ is set at $\delta^{66}Zn = +0.50$ ‰, the average of five measurements at 1000 m. Because we assume that Zn flux downwards from the surface ocean is entirely due to particle flux (rather than mixing), the $\delta^{66}Zn$ of the particle flux must also be $\delta^{66}Zn = +0.50$ ‰. At intermediate depths between the surface and deep ocean, any Zn in excess of the surface Zn concentration is assumed to result either from mixing with deep water ($\delta^{66}Zn = +0.50$ ‰) or dissolution of sinking particles ($\delta^{66}Zn = +0.50$ ‰). Because both of these have the same isotope composition, the dissolved seawater $\delta^{66}Zn$ can be calculated as:

$$\delta^{66}Zn_{seawater} = \delta^{66}Zn_{surface} \cdot f_{surface} + \delta^{66}Zn_{deep\,/\,particulate} \cdot f_{deep\,/\,particulate}$$

where $f_{surface}$ is the fraction of Zn at that depth from surface water and $f_{deep/particulate}$ is the fraction coming from mixing of deep waters or particle dissolution. f is calculated using Zn concentration measurements from Chapter 5. Though this model is quite simple and the data are sparse, isotope mixing modeled values of δ^{66}Zn fit the observations adequately (Fig. 4). The observed δ^{66}Zn for surface waters in the North Pacific (at 26 m) is -0.01 ‰, so adsorptive isotope effect for this simple model would be:

$$\Delta^{66}Zn_{adsorption} = \delta^{66}Zn_{particles} - \delta^{66}Zn_{surface} = +0.51 \; permil$$

6.5.1. Box model

A five-box model of the upper ocean was constructed in order to explore in more detail the processes that may lead to the Zn isotope profile observed in the North Pacific. This model specifies a flux of dissolved Zn between each of the boxes dependant on the water flux, a flux of "primary" biological Zn formed in the surface ocean, and a flux of "secondary" Zn that adsorbs to the surface of particles (Fig. 5A). Dissolved and particulate fluxes of Zn between the boxes were specified by the equations:

Box1 (surface mixed layer):
$$\frac{V\Delta Zn}{\Delta T} = -Q \cdot Zn_1 + Q \cdot Zn_2 - Fp \cdot K \cdot a - Fp'_{12} \cdot K' \cdot Zn_1 \cdot a$$

Box 2:
$$\frac{V\Delta Zn}{\Delta T} = -2 \cdot Q \cdot Zn_2 + Q \cdot Zn_1 + Q \cdot Zn_3 + Fp \cdot K \cdot a + Fp'_{12} \cdot K' \cdot Zn_1 \cdot a - Fp'_{23} \cdot K' \cdot Zn_2 \cdot a$$

Box 3:
$$\frac{V\Delta Zn}{\Delta T} = -2 \cdot Q \cdot Zn_3 + Q \cdot Zn_2 + Q \cdot Zn_4 + Fp'_{23} \cdot K' \cdot Zn_2 \cdot a - Fp'_{34} \cdot K' \cdot Zn_3 \cdot a$$
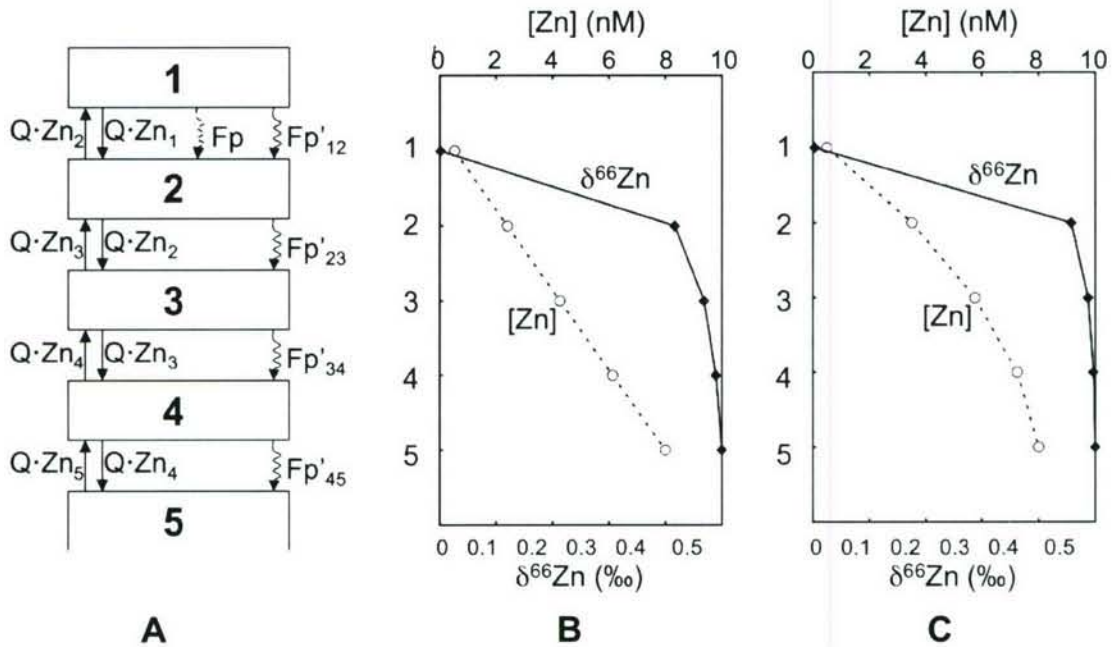
Figure 6.5. (**A**) A schematic of the 5-box model showing water fluxes carrying dissolved Zn (Q·Zn), the flux of primary biological Zn out of the surface ocean (Fp), and the fluxes of particulate-adsorbed secondary Zn (Fp'). (**B**) The results of a run of the box model where Fp = 0, and Fp'$_{12}$ draws Zn directly to the deep ocean (box 5) instead of box 2. This represents a water column in which particles formed in the surface ocean are refractory and don't remineralize before they reach the deep ocean. (**C**) Results of a model run where Fp = 0, and the flux of Zn with Fp'$_{12}$ goes is split equally between boxes 2 through 5, instead of going entirely to box 2. This is a more realistic treatment of particle remineralization, where particulate Zn is continuously dissolving as it sinks from the surface ocean to the deep ocean.

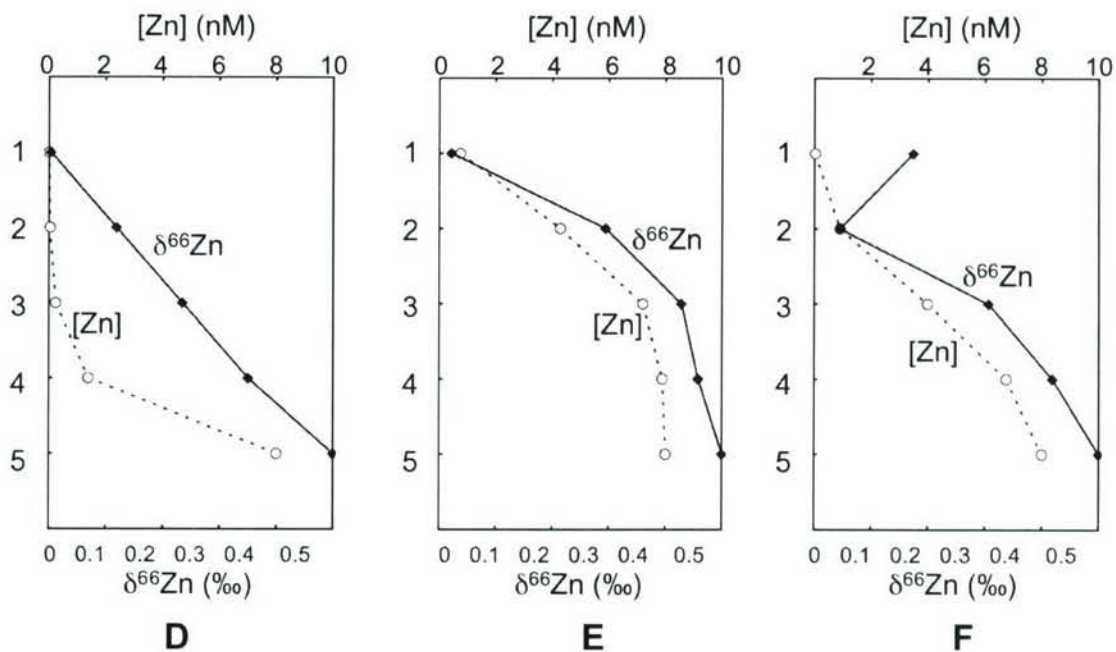Figure 6.5. (continued) (**D**) Results of a model run where Fp = 0 and Fp' is the same for all boxes. Because adsorption of Zn to falling particles decreases with Zn concentration, Zn removal is greatest from deep waters and the Zn concentration profile develops an unusual "concave" shape. (**E**) Results of a model run where Fp = 0 and Fp' decreases by a factor of five for each box deeper in the ocean. By assuming that the particle flux decreases dramatically towards the deep ocean, the model is able to adequately reproduce convex shape of both the Zn concentration profile and the Zn isotope profile that was observed in the North Pacific, even without the sinking and remineralization of primary Zn. (**F**) Results of a model run where Fp and Fp' are both non-zero, and the isotope effect for formation of primary biological Zn is negative (Δ^{66}Zn = -0.5 ‰) while the isotope effect for adsorption of secondary biological Zn is positive (Δ^{66}Zn = +0.5 ‰). This model represents the scenario described in Chapter 5, where cells release most of their isotopically light primary internal Zn in the upper water column, and particulate Zn flux deeper in the water column is isotopically heavy Zn adsorbed to particulate matter. This model produces an inversion in the upper water column Zn isotope profile similar to what has been reported in other studies of Zn isotopes in seawater (Fig 6).

Constant	Units	Run B	Run C	Run D	Run E	Run F
K	(mol/mol)	4.2E-06	6.8E-06	2.8E-05	2.8E-05	1.0E-06
K'	$(mol/m^3)^{-1}$	10	10	10	10	30
Q	(m^3/yr)	6.3	6.3	6.3	6.3	6.3
V	(m^3)	50	50	50	50	50
a	(m^2)	1	1	1	1	1
Δt	(year)	0.03	0.03	0.005	0.005	0.005
$\Delta^{66}Zn$	(‰)	-	-	-	-	-0.5
$\Delta^{66}Zn'$	(‰)	0.536	0.533	0.14	0.33	0.5
Fp	(mol C/yr)	0	0	0	0	3
$F'p_{12}$	(mol C/yr)	2.8	2.8	3	3	3
$F'p_{23}$	(mol C/yr)	0	0	3	0.6	0.6
$F'p_{34}$	(mol C/yr)	0	0	3	0.12	0.12
$F'p_{45}$	(mol C/yr)	0	0	3	0.024	0.024

Table 6.1. Variables, units, and values for five separate runs of the box model.

Figure 6. Seawater dissolved Zn isotopes measured in this thesis and by Bermin et al, (2006), as discussed in Chapter 5.
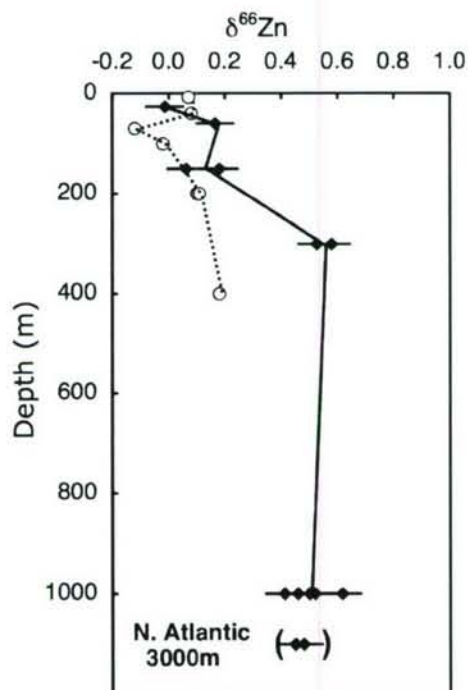
Box 4:

$$\frac{V\Delta Zn}{\Delta T} = -2 \cdot Q \cdot Zn_4 + Q \cdot Zn_3 + Q \cdot Zn_5 + Fp'_{34} \cdot K' \cdot Zn_3 \cdot a - Fp'_{45} \cdot K' \cdot Zn_4 \cdot a$$

Box 5 (deep ocean):

$$\frac{V\Delta Zn}{\Delta T} = -Q \cdot Zn_5 + Fp'_{45} \cdot K' \cdot Zn_4 \cdot a = 0$$

where Q is the flux of water between boxes, Zn_x is the concentration of Zn in box x, Fp is the particulate flux carrying primary biological Zn, K is the Redfield ration of Zn:C in those particles, Fp' is the flux of particles carrying secondary adsorbed Zn, K' is the Zn adsorptivity factor of particles, V is the volume of the box , a is the area on the top and bottom of the box, and T is time. The model was run through one thousand interactions with time step ΔT to reach steady-state.

Q was derived as a function of the vertical advective diffusivity (K) of the water column, and the water flux equations for each box:

$$\frac{V\Delta C}{\Delta T} = -2QC_{box} + QC_{top} + 2C_{bottom} \qquad (1)$$

where C_{box} is the concentration of an element in the box, C_{top} is the concentration of the element in the box above, and C_{bottom} is the concentration of the element in the box below. Equation 1 can be rewritten as:

$$\frac{V\Delta C}{\Delta T} = Q \cdot \Delta\Delta C \qquad (2)$$

Substituting a·ΔZ for V and rearranging yields:

$$\frac{\Delta C}{\Delta T} = \frac{Q \cdot \Delta\Delta C}{a\Delta Z} \qquad (3)$$

The vertical diffusivity is given by:

$$\frac{\partial C}{\partial T} = K \frac{\partial^2 C}{\partial Z^2} \tag{4}$$

and the discrete form of this equation is:

$$\frac{\Delta C}{\Delta T} = K \frac{\Delta \Delta C}{\Delta Z^2} \tag{5}$$

Combining equations 3 and 5 yields:

$$\frac{Q \cdot \Delta \Delta C}{a \Delta Z} = K \frac{\Delta \Delta C}{\Delta Z^2} \tag{6}$$

which can be simplified to:

$$Q = \frac{K \cdot a}{\Delta Z} \tag{7}$$

where ΔZ is the height of the box and a is the square area of the top and bottom.

An attempt was made to choose oceanographically-relevant values for each of the model parameters. The Zn concentration of the deep ocean was set at 8nM, and it's $\delta^{66}Zn$ was set at +0.5 ‰. A value of 10^{-5} m^2 s^{-1} was chosen for K, a typical value for the thermocline. Fp and Fp' were based on estimates of POC export in the North Pacific during the summertime using Th-234 as a tracer (Charette et al., 1999). The Zn:C Redfield ratio was based on plankton data from the North Pacific (Collier and Edmond, 1984). In some model runs, these parameters had to be adjusted to produce the expected Zn concentration and Zn isotope profiles (Table 1).

Using these values, the model consistently predicted a particle flux of Zn from surface waters that was too large to be compensated for by the vertical advective-diffusive flux of Zn from deeper waters. Profiles similar to what we observed in the

North Pacific could be obtained by increasing the vertical advective diffusivity, decreasing the particle flux, or decreasing values of K and K' (the amount of Zn transported with a given particle flux). In order to produce an isotopic offset of $\Delta^{66}Zn_{deep\text{-}surface} = +0.5$‰ between surface and deep waters, these models required adsorption isotope effects of $\Delta^{66}Zn' = +0.33$ to $+0.53$ ‰.

With this model, we were able to adequately reproduce many of the observed features of the Zn concentration profile and Zn isotope profile observed in the North Pacific (Fig. 5B-F). Experimental work on release and readsorption of Zn and Zn isotopes during particle degradation, and further measurements of the seawater dissolved Zn isotope profile, are necessary to better constrain this model.

References for chapter 6:

Bermin, J., Vance, D., Archer, C. and Statham, P.J., 2006. The determination of the isotopic composition of Cu and Zn in seawater. Chemical Geology, 226(3-4): 280-297.

Charette, M.A., Moran, S.B. and Bishop, J.K.B., 1999. Th-234 as a tracer of particulate organic carbon export in the subarctic northeast Pacific Ocean. Deep-Sea Research Part Ii-Topical Studies in Oceanography, 46(11-12): 2833-2861.

Collier, R. and Edmond, J., 1984. The trace-element geochemistry of marine biogenic particulate matter. Progress in Oceanography, 13(2): 113-199.

Ellwood, M.J. and Hunter, K.A., 2000. The incorporation of zinc and iron into the frustule of the marine diatom Thalassiosira pseudonana. Limnology and Oceanography, 45(7): 1517-1524.

Gélabert, A. et al., 2006. Interaction between zinc and freshwater and marine diatom species: Surface complexation and Zn isotope fractionation. Geochimica et Cosmochimica Acta, 70(4): 839-857.

Jickells, T.D. et al., 2005. Global iron connections between desert dust, ocean biogeochemistry, and climate. Science, 308(5718): 67-71.

Lane, T.W. and Morel, F.M.M., 2000. A biological function for cadmium in marine diatoms. Proceedings of the National Academy of Sciences of the United States of America, 97(9): 4627-4631.

Lane, T.W. et al., 2005. A cadmium enzyme from a marine diatom. Nature, 435(7038): 42-42.

Maréchal, C.N., Nicolas, E., Douchet, C. and Albarède, F., 2000. Abundance of zinc isotopes as a marine biogeochemical tracer. Geochemistry Geophysics and Geosystems, 1: 1999GC000029.

Morel, A., 1996. An ocean flux study in eutrophic, mesotrophic and oligotrophic situations: The EUMELI program. Deep-Sea Research Part I-Oceanographic Research Papers, 43(8): 1185-1190.

Price, N.M. and Morel, F.M.M., 1990. Cadmium and cobalt substitution for zinc in a marine diatom. Nature, 344(6267): 658-660.

Redfield, A.C., Ketchum, B.H. and Richards, F.A., 1963. The influence of organisms on the composition of seawater. In: M.N. Hill (Editor), The Sea. Wiley, pp. 26-77.

Reid, E.A. et al., 2003. Characterization of African dust transported to Puerto Rico by individual particle and size segregated bulk analysis. Journal of Geophysical Research-Atmospheres, 108(D19): -.

Sarmiento, J.L., Gruber, N., Brzezinski, M.A. and Dunne, J.P., 2004. High-latitude controls of thermocline nutrients and low latitude biological productivity. Nature, 427(6969): 56-60.

Sunda, W.G. and Huntsman, S.A., 1992. Feedback interactions between zinc and phytoplankton in seawater. Limnology and Oceanography, 37(1): 25-40.

Sunda, W.G. and Huntsman, S.A., 1996. Antagonisms between cadmium and zinc toxicity and manganese limitation in a coastal diatom. Limnology and Oceanography, 41(3): 373-387.

Sunda, W.G. and Huntsman, S.A., 1998. Control of Cd concentrations in a coastal diatom by interactions among free ionic Cd, Zn, and Mn in seawater. Environmental Science & Technology, 32(19): 2961-2968.

Sunda, W.G. and Huntsman, S.A., 2000. Effect of Zn, Mn, and Fe on Cd accumulation in phytoplankton: Implications for oceanic Cd cycling. Limnology and Oceanography, 45(7): 1501-1516.

Tortell, P.D. and Price, N.M., 1996. Cadmium toxicity and zinc limitation in centric diatoms of the genus Thalassiosira. Marine Ecology-Progress Series, 138(1-3): 245-254.

Twining, B.S. et al., 2003. Quantifying trace elements in individual aquatic protist cells with a synchrotron X-ray fluorescence microprobe. Analytical Chemistry, 75(15): 3806-3816.

50272-101

REPORT DOCUMENTATION PAGE	1. REPORT NO. MIT/WHOI 2007-08	2.	3. Recipient's Accession No.
4. Title and Subtitle The Marine Biogeochemistry of Zinc Isotopes			**5. Report Date** June 2007
			6.
7. Author(s) Seth G. John			**8. Performing Organization Rept. No.**
9. Performing Organization Name and Address MIT/WHOI Joint Program in Oceanography/Applied Ocean Science & Engineering			**10. Project/Task/Work Unit No.** MIT/WHOI 2007-08
			11. Contract(C) or Grant(G) No. (C) OCE-0002273 OCE-0326689 (G)
12. Sponsoring Organization Name and Address National Science Foundation Martin Family Society Fellowship for Sustainability Woods Hole Ocean Ventures Fund MIT Earth Systems Initiative Ignition Grant			**13. Type of Report & Period Covered** Ph.D. Thesis
			14.

15. Supplementary Notes

This thesis should be cited as: Seth G. John, 2007. The Marine Biogeochemistry of Zinc Isotopes. Ph.D. Thesis. MIT/WHOI, 2007-08.

16. Abstract (Limit: 200 words)

Zinc (Zn) stable isotopes record information about important oceanographic processes. This thesis presents data on Zn isotopes in anthropogenic materials, hydrothermal fluids and minerals, cultured marine phytoplankton, natural plankton, and seawater. Common forms of anthropogenic Zn have $\delta^{66}Zn$ from +0.08 ‰ to +0.32 ‰, a range similar to terrigenous materials. Hydrothermal fluids ranged in $\delta^{66}Zn$ from 0.02 ‰ to +0.93 ‰, and chimney minerals ranged from -0.09 ‰ to +1.17 ‰. Our results suggest that precipitation of isotopically light Zn sulfides is very important in hydrothermal systems. In cultured diatoms, a relationship was discovered between Zn transport by either high-affinity or low-affinity uptake pathways, and the magnitude of Zn isotope fractionation. We established isotope effects of $\delta^{66}Zn = 0.2$ ‰ for high-affinity uptake and $\delta^{66}Zn = 0.8$ ‰ for low-affinity uptake. Biological fractionation of Zn isotopes under natural conditions was investigated by measuring Zn isotopes in plankton collected in the Peru Upwelling Region and around the world. The $\delta^{66}Zn$ of deep seawater is about 0.5‰, and the dissolved $\delta^{66}Zn$ gets lighter in the upper water column. The thesis, by presenting data on several important aspects of Zn isotope cycling in the oceans, lays the groundwork for further use of Zn isotopes as a marine biogeochemical tracer.

17. Document Analysis a. Descriptors

Zinc
isotopes
marine

b. Identifiers/Open-Ended Terms

c. COSATI Field/Group

18. Availability Statement Approved for publication; distribution unlimited.	**19. Security Class (This Report)** **UNCLASSIFIED**	**21. No. of Pages** 142
	20. Security Class (This Page)	**22. Price**